Quantifying the Impact of Energy Storage as a Transmission Asset on Composite Power System Reliability

by

Josif Elias Figueroa Parra

B.Sc., University of Santiago, Chile, 2016

A Thesis Submitted in Partial Fulfillment
of the Requirements for the degree of

Master of Sciences in Engineering

in the Graduate Academic Unit of Electrical and Computer Engineering

Supervisors: Kush Bubbar, Ph.D., P.Eng
Department of Electrical and Computer Engineering

Greg Young-Morris, MSc, P.Eng, Energié NB Power

Examining Board: Shivam Saxena, Ph.D., P.Eng
Department of Electrical and Computer Engineering

Julian Cardenas Barrera, Ph.D.
Department of Electrical and Computer Engineering

Milorad Papic, Ph.D., Papic Energy Consulting

This thesis is accepted by the Dean of Graduate Studies

THE UNIVERSITY OF NEW BRUNSWICK

April, 2024

© Josif Elias Figueroa Parra, 2024

Abstract

This thesis explores the application of Composite System Reliability (CSR) assessment in power system planning, presenting an open-source evaluation tool developed in a dynamic programming language with Monte Carlo Simulation (MCS) and parallel computing capabilities. The tool addresses historical barriers by offering a transparent methodology and flexibility in incorporating various power flow methods and external solvers for large-scale projects. Energy storage, as a composite resource and transmission asset, presents both opportunities and challenges in power solutions. The thesis demonstrates the feasibility of calculating its equivalent transmission capability aligned with traditional alternatives, identifying optimal power and energy ratings for storage systems. While enhancing network adequacy, challenges such as capacity value saturation due to oversized systems are discussed. CSR assessments examine network changes' impact, emphasizing the necessity of informed decisions through security and economic analyses.

Dedication

This thesis is dedicated to my grandmother, Maria Rosa, whose unwavering support and guidance shaped the person I am today. I am deeply grateful for her love, encouragement, and sacrifices, which have propelled me towards my goals and successes. This work is a tribute to her memory and the profound impact she had on my journey.

Acknowledgements

This work was supported by MITACS through the Mitacs Accelerate program, Atlantic Canada Opportunities Agency, and Énergie NB Power, NB, Canada, under Grant IT27416. Advanced computing resources are provided by the Digital Research Alliance of Canada, the organization responsible for digital research infrastructure in Canada, and ACENET, the regional partner in Atlantic Canada. ACENET is funded by Industry Science & Economic Development, the provinces of New Brunswick, Newfoundland & Labrador, Nova Scotia and Prince Edward Island, as well as the Atlantic Canada Opportunities Agency.

Table of Contents

Abstract ii
Dedication iii
Acknowledgements iv
Table of Contents v
List of Tables vii
List of Figures ix
List of Symbols, Nomenclature, or Abbreviations xi
I. Introduction 1
I.1. Contributions 2
I.2. Thesis Structure 3
II. Literature Review 4
II.1. Power System Reliability 5
II.2. Probabilistic Transmission Planning 7
II.3. Composite System Reliability 8
II.3.1. Historical development 9
II.3.2. The objectives of CSR studies 11
II.4. Outage model of system components 14
II.5. Selection of System States 18
II.5.1. Sequential Monte Carlo Simulation 20
II.6. System State Evaluation 21
II.7. Reliability Indices 22
II.8. Effective Load-Carrying Capability 24
II.9. Adequacy Assessment Incorporating Energy Storage 26
III. Methodology 29
III.1. Composite System Reliability Assessment Tool 29
III.2. Power System Representation 30
III.2.1. Assets 31
III.2.2. SystemModel 33
III.3. Mathematical Optimization 34
III.3.1. DC-Based formulation 35
III.3.2. AC-Based formulation 40

III.4. Probabilistic Simulation 41
III.5. Probabilistic Outcomes 43
IV. Case Studies and Results 45
IV.1. Test Systems 46
IV.1.1. Roy Billinton Test System (RBTS) 47
IV.1.2. IEEE Reliability Test System (IEEE-RTS 79) 47
IV.1.3. IEEE Reliability Test System upgrades 48
IV.2. Split Network Situations 49
IV.3. Benchmarking 50
IV.4. Energy Storage Model and Dispatch 55
IV.5. Energy Storage As A Transmission Asset 56
IV.6. Application Studies 59
V. Conclusions and Future Work 70
V.1. Conclusions 70
V.2. Future Work 71
Bibliography 74
Appendix A 79
Appendix B 80
Appendix C 82
Appendix D 84
Appendix E 87
Appendix F 94
Appendix G 96
Appendix H 100
Curriculum Vitae

List of Tables

Table 1: Load curtailment benchmarking results using Gurobi solver. 50

Table 2: System EENS and EDLC Indices of RBTS: DC-based vs. AC-based Methods. 52

Table 3: System EENS and EDLC Indices of IEEE-RTS 79: DC-based vs. AC-based Methods..... 53

Table 4: System and branch results for the base system (Case 1 and Case 2) and the augmented system (with traditional transmission asset)..... 61

Table 5: Optimal energy rating at a tol=0.001 for a target metric of 38.3 min/y and ELCC of 36 MW. Augmented system, Case 1. 69

Table 6: Bus EENS and EDLC Indices of RBTS: DC-based vs. AC-based Methods. 84

Table 7: Bus EENS Index of IEEE-RTS 79: DC-based vs. AC-based Methods..... 85

Table 8: Bus EDLC Index of IEEE-RTS 79: DC-based vs. AC-based Methods. 86

Table 9: Test cases using RBTS with energy storage. 88

Table 10: Optimal Power Flow results per load bus in MW, Scenario 2. 92

Table 11: Optimal Power Flow results per load bus in MW, Scenario 3. 93

Table 12: Generator data, RBTS test system. 95

Table 13: Branch data, RBTS test system..... 95

Table 14: Bus data, RBTS test system. 95

Table 15: Generator data, IEEE-RTS 79 test system. 97

Table 16: Branch data, IEEE-RTS 79 test system. 98

Table 17: Bus data, IEEE-RTS 79 test system..... 99

Table 18: CSR assessment DC-Based results for 2000 replications. Base system, Case 1..... 100

Table 19: CSR assessment DC-Based results for 2000 replications. Augmented system, Case 1 with SATA 75MW/260 MWh. 101

Table 20: CSR assessment DC-Based results for 2000 replications. Augmented system, Case 1 and Case 2 with traditional solution. 102

Table 21: CSR assessment DC-Based results for 2000 replications. Base system, Case 2 103

Table 22: CSR assessment DC-Based results for 2000 replications. Augmented system, Case 2 with SATA 75MW/260 MWh. 104

Table 23: CSR assessment results for augmented system, Case 1 varying SATA size. 105

Table 24: CSR assessment results for augmented system, Case 2 varying SATA size. 106

Table 25: Hourly mean EENS in MWh/hr/year for Case 1 and Case 2, SATA at bus 8. 107

List of Figures

Figure 1: Programming abstraction layers of CompositeSystems. 3

Figure 2: Hierarchical levels in power system reliability studies. 6

Figure 3: Probabilistic Transmission Planning Process including CSR Assessment. ... 8

Figure 4: State-space diagram of a two-state outage model. 17

Figure 5: Energy Storage Applications in Power Systems. 27

Figure 6: Simplified flowchart of CompositeSystems. 30

Figure 7: SystemModel's structure with current (continuous line) and future (dotted line) components. 33

Figure 8: A Piecewise-Linear Approximation of Cosine using 7 inequalities. Source: [37]. 41

Figure 9: CompositeSystems' model structure. 43

Figure 10: Equivalent Transmission Capability procedure of energy storage using CSR Assessment. 60

Figure 11: Annual adequacy risk before and after decreasing transfer capability on transmission lines of the RTS 79 test system, DC-Based approach. 62

Figure 12: System EENS adding SATA at bus 8 for different power and energy ratings. Augmented system, Case 1. 64

Figure 13: System EDLC adding SATA at bus 8 for different power and energy ratings. Augmented system, Case 1. 64

Figure 14: Hourly EENS variation at bus 9, Case 1. 66

Figure 15: Hourly EENS variation at bus 9, Case 2. 66

Figure 16: ELCC for SATA at bus 8, for different power and energy ratings, for the augmented system, Case 1. 68

Figure 17: ELCC curves for different SATA energy and power ratings. Augmented system, Case 1. 68

Figure 18: JuMP's syntax (variable definition) in CompositeSystems. 83

Figure 19: JuMP's syntax (constraint definition) in CompositeSystems. 83

Figure 20: Test Scenario 1 using RBTS without storage (a), and with storage (b). 89

Figure 21: Test scenario 2 using RBTS without storage (a), and with storage (b). 90

Figure 22: Test Scenario 3 using RBTS without storage (a), and with storage (b). 91

Figure 23: Roy Billinton Test System (RBTS). Source: [54]. 94

Figure 24: Original (1979) IEEE RTS. Source: [55]. 96

Figure 25: Reliability curves at different load levels, placed at bus 8 to increase transfer capability on three transmission lines. Augmented system, Case 1. 108

Figure 26: Hourly EENS variation at bus 9, Case 2, varying SATA's energy rating.109

Figure 27: Hourly EENS variation at bus 9, Case 2, varying SATA's power rating. 109

List of Symbols, Nomenclature, or Abbreviations

AC OPF	:	Alternating Current Optimal Power Flow
BESS	:	Battery Energy Storage System
CSR	:	Composite System Reliability
CSR TF	:	Composite System Reliability Task Force
DC OPF	:	Linearized Optimal Power Flow that only considers active power flows
ESS	:	Energy Storage System
HVDC	:	High Voltage Direct Current
IEEE	:	The Institute of Electrical and Electronics Engineers
ISO	:	Independent System Operator
MCS	:	Monte Carlo Simulation
MTTF	:	Mean Time to Failure
MTTR	:	Mean Time to Repair
N-1	:	The state of a system having one element out of service (e.g. due to a contingency)
N-1-1	:	The state of a system having two elements consecutively out of service (e.g. due to a primary contingency, followed by system adjustments, followed by a secondary contingency)
PTP	:	Probabilistic Transmission Planning
p.u.	:	Per Unit
RBTS	:	6-Bus Roy Billinton Test System
RTS-79	:	Version of the IEEE Reliability Test System (RTS) of 24 buses first published in 1979
SATA	:	Storage as a Transmission Asset

NERC	:	The North American Electric Reliability Corporation
SOC	:	State of Charge of an energy storage source
SOE	:	State of Energy of an energy storage source
SOL	:	System Operating Limit
var	:	Volt-Amperes Reactive
Replication	:	In the context of sequential Monte Carlo Simulations, replication refers to the simulation of chronological power system operations over a specified timespan, which are repeated a certain number of times to ensure accurate results.

Reliability indices and metrics

ADLC	:	Average Duration of Load Curtailments in hours/failure
ELCC	:	Effective Load-Carrying Capability in MW, also known as the capacity
	:	value of a non-firm resource. When indicated as a percentage (%) it is MW of additional load supplied per MW of storage installed for a specific duration capability
EENS	:	Expected Energy Not Served in MWh/year
EFLC	:	Expected Frequency of Load Curtailments in outages/year
LOLE	:	Loss of Load Expectation in days/year
PLC	:	Probability of Load Curtailments
PRV	:	Probability of Reliability Violation
SI	:	Severity Index in system-minutes

I. Introduction

Generation and transmission outages, which individually may not have a substantial impact on the power system, can jointly affect overall power system reliability [1]. The fundamental objective of power system planning is to develop the system as economically as possible and maintain an acceptable reliability level. However, traditional planning methods have limitations when assessing reliability and while considering the stochastic nature of power systems [2], especially with the increasing use of renewable energy sources and ESS. Modern power systems experience various challenges, including unpredictable failures, market volatility, and intermittent energy sources.

ESS has been proposed as a complement to traditional transmission assets and as a competitive alternative to constructing new assets. Transmission systems can benefit from incremental capacity deployment provided by ESS to address reliability, market efficiency, and public policy needs. ESS can also help reduce renewable energy curtailment, postpone the requirement for new transmission assets, and be relocated to different locations as needs evolve. However, traditional transmission security studies or resource adequacy studies that do not model the complexity of transmission systems may not accurately represent the energy-constrained nature of ESS.

While resource reliability assessment methods were among the first to be developed [3], [4], there has been a need for new tools to assess adequacy of existing and proposed electrical configurations, as well as to quantify the reliability level at any point in a composite system, as proposed early on in [5], [6]. The evaluation of CSR, essential for assessing a system's ability to meet transmission-level load demands, is complex and

computationally intensive. However, there are currently no tools available for conducting CSR assessments with Energy Storage Systems.

Despite significant advancements in the computational landscape, including numerical solvers, efficient programming languages, and parallel computing paradigms, challenges persist in CSR analyses. Specifically, the complexity of solving AC OPF problems and the limitations of current computational tools in managing sequential MCS are noteworthy [7]. With the growing interest in energy storage in North America [8], there is a need for planning methodologies that can effectively evaluate its potential. Traditional frameworks might undervalue ESS solutions, especially near load centers. ELCC serves as a useful metric for such evaluations [9].

I.1. Contributions

This thesis presents significant contributions to the field by proposing the application of CSR assessment to evaluate energy storage as an alternative solution to transmission reliability deficiencies. The primary contribution involves developing a methodology for comparing the capacity value of energy storage against traditional solutions, leading to the identification of optimal power and energy ratings for storage systems. Objective comparisons between transmission solutions are emphasized, facilitating investments aligned with the reliability benefits of traditional assets. Additionally, an energy storage model integrated into CSR assessment determines optimal storage capacity to meet reliability needs in terms of ELCC and adequacy level. The secondary contribution is the creation of an open-source CSR Evaluation tool, addressing the lack of available software and enhancing reproducibility of results. The third contribution is proficiency in

formulating the OPF problem using both DC OPF and linearized AC OPF formulations within a unified platform, enabling efficient utilization of high-performance solvers.

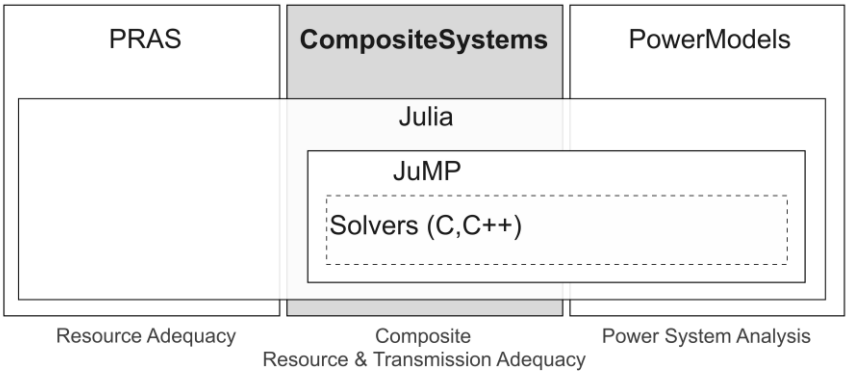

Figure 1: Programming abstraction layers of CompositeSystems.

I.2. Thesis Structure

The thesis comprises five chapters. Chapter I provides a comprehensive introduction to the thesis, covering its motivation, background, scope, and contributions. It sets the stage for the subsequent chapters by establishing the context and significance of the research. Chapter II, the literature review, describes the fundamental concepts of power system reliability (adequacy) used in the thesis, providing the context and justification for the work, and describing the current state of the art. Chapter III, methodological approach, presents an explanation of the proposed composite system assessment algorithms used for the implementation of CompositeSystems in the thesis work and highlights the unique contributions. Chapter IV, case studies and results, applies the developed tool to different test systems, including benchmark comparisons. Chapter V, conclusions and future work, summarizes the results and work in the thesis and suggests future work.

II. Literature Review

Quantitative prediction methods for assessing any component of a system's existing and future performance are informative for establishing future system design requirements. These methods help identify areas that need reinforcement, evaluate the impact of different system designs, and plan for future system behaviour. Additionally, they enable the assessment of the reliability benefits of various solutions.

Reliability is defined as the likelihood that a system will perform its intended function adequately for a specified time under given operating conditions. Probability theory provides the theoretical framework for performing numerical studies and establishing metrics for reliability assessment and system adequacy metrics. By applying probability theory to assess adequate performance, referred to as “adequacy”, it is possible to account for probabilistic or stochastic variations. The goal of quantitative predictions is to determine system requirements that will ensure adequacy above a predetermined acceptability level.

Mission-oriented systems, such as the transmission system, are expected to operate without failure, a quality measured by availability—the likelihood of the system being operational at a future point in time [7]. In planning for system expansion, both failures and normal states can occur. The emphasis, however, is on assessing the probability of the system being operational or non-operational at future moments. Future performance involves uncertainties like load growth, renewable energy variability, weather conditions, and changing system requirements. Comparing reliability metrics before and after design or operational changes helps mitigate the impact of these uncertainties.

This chapter outlines power system reliability, explores a probabilistic framework for power system planning, and underscores the importance of simulation-based Composite System Reliability (CSR) assessments.

II.1. Power System Reliability

Reliability evaluation techniques assist in the objective assessment of probabilistic risks and aid in accounting for the severity and likelihood of outages and other events. In power systems, reliability is measured by examining the frequency, duration, and magnitude of disruptions in the power supply, ensuring that electricity is delivered reliably to consumers within established standards.

Electric power systems are immensely complex and extensive. Even the most advanced computing systems do not possess the capability to analyze an extensive power system as a single entity in a comprehensive manner. Therefore, a power system is divided into three distinguished subsystems that are traditionally analyzed independently. The concept of hierarchical levels has been developed to obtain a consistent means of identifying these subsystems [8]. The hierarchical levels consist of the: 1) generation and interface assets, 2) HL1 and transmission assets, and 3) distribution assets.

Power system reliability assessment primarily focuses on two aspects: 1) adequacy and 2) operational reliability (otherwise referred to as “security”). NERC defines these two aspects as:

- **Adequacy:** The ability of the electricity system to supply the aggregate electrical demand and energy requirements of the end-use customers at all times, taking into account scheduled and reasonably expected unscheduled outages of system elements.

- **Operational Reliability** or **Security**: The ability of the Bulk-Power System to withstand sudden disturbances, such as electric short circuits or the unanticipated loss of system elements from credible contingencies, while avoiding uncontrolled cascading blackouts or damage to equipment.

CSR commonly emphasizes the adequacy perspective, given the technical complexity of integrating adequacy and security aspects into reliability assessments. Security assessments mainly employ probabilistic voltage and transient stability analyses. CSR evaluation is notably more complex than resource or substation adequacy. For instance, substation reliability deals with source-load connectivity and does not require a power flow model [2]. Distribution system reliability is the most complex evaluation assessment level due to the scale of the problem. Distribution system reliability analysis uses CSR data as an input to evaluate multiple levels and indices.

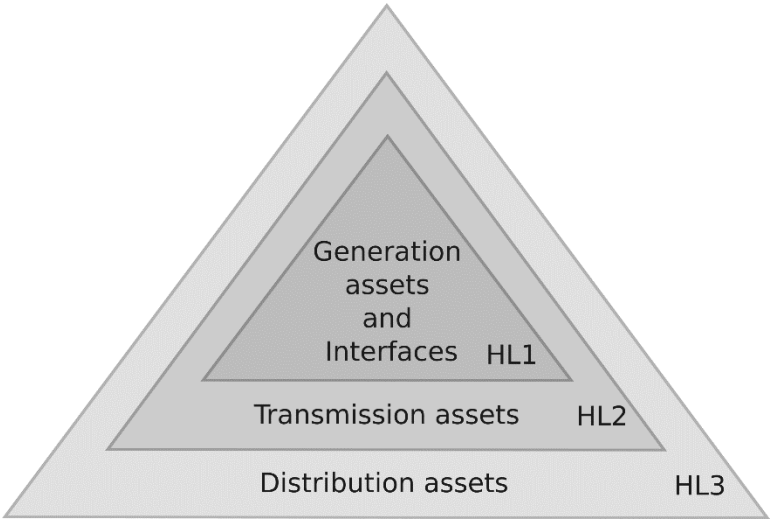

Figure 2: Hierarchical levels in power system reliability studies.

II.2. Probabilistic Transmission Planning

Probabilistic Transmission Planning emerged as a response to the limitations of conventional deterministic criteria in transmission planning [6], [7], [9]. Its evolution is effective because it combines assessing the likelihood of reliability issues along with considering economic factors, ultimately creating a comprehensive approach to power system planning. Traditional deterministic strategies rely on evaluating system performance for a fixed set of events, typically including single-element contingencies (i.e., N-1 contingencies) and some multiple-element contingencies (e.g. N-2 or N-1-1 contingencies). This provides a solid foundation for system planning but may not fully account for the complexities of modern power systems. Probabilistic planning seeks to address these gaps by developing criteria based on reliability measures and integrating these quantitative assessments with economic analyses, thus complementing one another. It uses various power system tools, from advanced load forecasts to probabilistic power flow and contingency analyses. While probabilistic criteria may seem complex compared to deterministic guidelines, they are versatile enough to work with various network sizes or specific infrastructure projects [2].

Probabilistic Transmission Planning involves evaluating different options to solve system performance deficiencies considering statistical metrics such as EENS, EFLC, EDLC, and ADLC, among others. The process includes the following steps shown in Figure 3 and described in Appendix A.

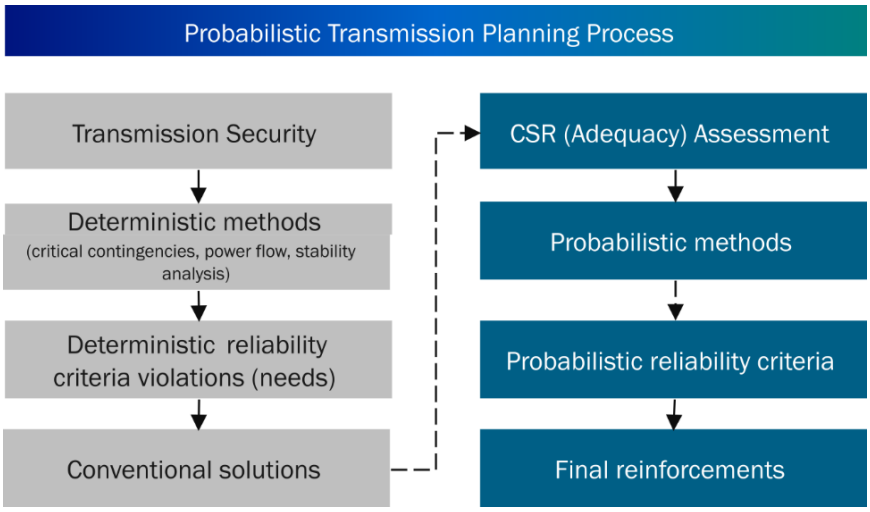

Figure 3: Probabilistic Transmission Planning Process including CSR Assessment.

II.3. Composite System Reliability

CSR analysis can provide information unavailable through other techniques used to assess the adequacy of generation and transmission facilities within a power system. It involves computing probabilistic reliability indices within an integrated generation and transmission network. This process employs various methods, including power flow analysis, optimization, contingency analysis, and remedial actions to prevent potential load reductions [8].

In CSR, relative indices take precedence over strict adherence to absolute reliability thresholds. These indices facilitate comparisons of reliability levels before and after system modifications, complementing benchmarks like LOLE. This approach emphasizes alternative solutions based on metrics such as EENS and SI. Ensuring satisfactory voltage and SOL levels at load points becomes crucial [6].

Depending on the CSR assessment's specific requirements and objectives, it falls into three categories [10]:

1. **General case:** This considers failures of both generation and transmission components.
2. **Transmission system risk evaluation:** In this case, only the failures of transmission components are considered, assuming generating units are 100% reliable. Transmission substation arrangements may also be included for specific study purposes.
3. **Resource-only risk evaluation:** This case focuses solely on the failures of generating units, assuming transmission components are 100% reliable. It is essential to note that this differs from Resource Adequacy evaluation, as it still considers constraints imposed by the transmission network.

II.3.1. Historical development

Interest in applying probabilistic methods to composite generation and transmission systems gained traction around 1968, using Markov processes to address transmission system issues [11]. However, it was not until 1969 that a state-enumeration approach, essentially enumerating the failure modes and their effects, was directly applied to composite systems by Roy Billinton [6], [12]. In the past, the adequacy of major transmission planning was typically evaluated using a single criterion: continuity of supply – which states that, if all the components in a transmission system are fully redundant, then reliability is only a matter of continuity with success and failure easily defined. An additional criterion known as the "service quality" standard was introduced. According to

this standard, if bounds are placed upon desirable voltage levels at each point in the system, any departures from these ranges can be classified as a breach of service continuity. If various permutations of facility outages result in a reliability index for a given load point that falls below an acceptable minimum, then additional facilities are needed to meet reliability standards.

The first digital computer program to address this issue was developed in 1970 [12]. Using conditional probability, it applied AC power flow analysis at multiple load buses under possible system component outages. A failure system state met any of the following conditions: a) the voltage at a load bus fell below a specified minimum value, b) line and transformer overloading occurred, or c) the available generating capacity was insufficient to meet the total load.

Authors in [13] have compiled an extensive bibliography covering CSR assessment from 2000 to 2020. This body of work includes significant contributions related to methodologies for system state selection, the development of a probabilistic transmission planning framework, and the integration of renewable energies, energy storage, demand-side management, and various technologies into probabilistic reliability assessments. These studies have also explored the impact of factors such as load forecast uncertainty, aging characteristics, and weather patterns on the CSR landscape.

The recent review of computational tools for CSR analysis by the IEEE CSR Task Force (CSR TF) [14] documented most of the CSR tools developed over the years, starting with the first tool. This task force has addressed many concerns related to the use of CSR tools by the industry. They also compiled best practices from published literature and feedback from users of probabilistic tools in the electric power industry. In their review, twenty-one

CSR tools were analyzed. While these tools utilize varying models and probabilistic methods, all can quantify risks using reliability indices. These indices convey risks in probability, frequency, and the volume of lost load, offering valuable insights for planning and operations. Nine of the twenty-one tools are incorporated into planning or operational decision systems. However, others are not fully integrated. Complete integration would simplify the process for planners and operators when factoring in risks during decision-making, promoting more extensive use of CSR tools. Notably, among the 21 tools discussed, *no open-source option is available*, and *no commercial tool can perform sequential MCS for energy-limited resources* [15]. The work presented in this thesis seeks to address both identified gaps.

There are two popular methods for CSR evaluation: 1) MCS, and 2) state enumeration. While the core system analysis remains consistent, the key difference lies in the selection of system states. MCS is particularly effective in handling complex systems due to its ability to accommodate a larger number of equations, making it well-suited for evaluating systems with numerous components. On the other hand, state enumeration is more efficient when dealing with a smaller number of states or components and accounts for most of the state space's probability [16]. Both methodologies yield similar reliability indices, with MCS offering the additional capability of providing probability distributions, although it requires increased computational capacity.

II.3.2. The objectives of CSR studies

The objective of assessing the reliability of the power system at the bulk transmission level is to gauge the system's capability to deliver power and energy from generating sources to

load buses. Reliability indices can be determined for specific points or for the entire system, and these indices are valuable for planning studies. A key metric of reliability is the expected load curtailment needed to keep power flows and voltages within SOLs. Consequently, these indices are defined based on failure events, which may include the following such as below [15]:

a. Insufficient generation to meet the load demand
b. Overloading of transmission system components
c. Bus voltages that deviate from acceptable ranges
d. Frequency deviations beyond set limits
e. Deficiencies in real power
f. Reactive power or voltage-support deficiencies
g. Power system interruptions leading to load losses
h. Network issues causing non-convergence
i. Disruptions in power supply continuity to a delivery point
j. Split situations
k. System instability
l. Risks of cascading failures
m. Voltage collapse

The evaluation of CSR is structured around five key aspects:

1. **Determination of Component Failures and Load Curve Models:** This step involves creating a multi-step load model, free from chronological constraints, for nonsequential MCS or state enumeration methods. Alternatively, chronological

load curves are employed in sequential MCS. If available, the inclusion of failure probability distributions can improve evaluation accuracy.

2. **Selection of System States:** System states at various load levels are chosen using MCS. It encompasses generating unit states, transmission component states, and weather-related considerations.
3. **System Analysis:** Each selected system state undergoes a comprehensive analysis, often involving power flow analysis.
4. **Load Curtailment Minimization:** An OPF model is used to address limit violations, either by correcting them or minimizing their impacts.
5. **Calculation of Reliability Indices:** Reliability indices are derived based on the probabilities and outcomes of all sampled system states.

A generic OPF integrates the economic dispatch calculation, which minimizes generating costs, with a power flow calculation, allowing both problems to be addressed simultaneously. This optimization is constrained to adhere to system limits, such as current flow limits on transmission components and bus voltage limits. The total losses of the power system are also incorporated into the power flow calculation. The transmission constraints can be represented using a DC or AC power flow formulation depending on the level of detail or speed required. Other constraints and features, such as those related to renewable resources, ESS, and load curtailment priority, can also be incorporated into the OPF formulation.

Consequently, outages resulting in system constraint violations can be mitigated using corrective remedial actions within the OPF problem. These actions, which might utilize

various resources, should align with actual control schemes and operating practices. Typical remedial actions are [15]:

a. Real power generation adjustment
b. Reactive power generation adjustment
c. Area interchange adjustment
d. Generation-controlled voltage adjustment
e. Transformer phase shift adjustment
f. Switchable capacitor/reactor adjustment
g. Transformer tap adjustment
h. Generator tripping
i. Circuit switching
j. Shedding interruptible load/load curtailment
k. HVDC flow adjustment

After applying all necessary and possible corrective actions, only the two most severe outcomes may persist: 1) loss of load and 2) system collapse, as determined by step 4 (OPF). As noted in [15], switching lines might alleviate violations resulting from contingencies, but this method is infrequently used in practice.

II.4. Outage model of system components

A power system comprises various components, including generators, lines, cables, feeders, transformers, breakers, switches, reactors, and capacitors. Component outages are typically categorized as independent or dependent and can be further classified in various ways. Based on their nature, they may be classified as forced, semi-forced, and planned

outages in terms of outage nature, or as full and partial failures in terms of component or system state [10]. Forced failures are often categorized as repairable or non-repairable, with repairable failures being more common but non-repairable failures occurring in real-life scenarios.

These equipment failures happen randomly, exhibiting a consistent statistical pattern. The likelihood of a component being offline at a given future point is termed its "unavailability U" (refer to eq. 2.1). Random variables often fit certain standard distributions. Despite having the same specifications, components do not fail simultaneously. Instead, their failures span different times, which follow a particular probability distribution. This distribution reflects the chance of a component failing within a defined period. Most often, this distribution is derived from operational data or sample tests. Typical standard continuous distributions include normal (Gaussian), lognormal, exponential, Weibull, gamma, and Rayleigh [7].

$$U = \frac{time\ on\ outage}{time\ on\ outage + operating\ time} \tag{2.1}$$

The exponential distribution is widely applied to repairable systems, where components alternate between operational and failure states. An important statistical property of an exponential distribution is the expected value and standard deviation are equal to the inverse of the failure rate λ, which is considered constant and only applicable to the useful life period (does not consider failures due to component wearout). the Mean Time to Failure (MTTF). A repair rate μ is analogous to λ, and its reciprocal is the Mean Time to Repair (MTTR). Its popularity comes from two primary reasons [7]:

i. For large systems, analytic techniques can be intricate. Adopting constant failure rates and exponential distributions can greatly simplify such problems. However, it may be inappropriate since it is a memory-less distribution.

ii. Often, available data is scarce and does not conclusively identify a specific distribution, prompting the use of more straightforward methods over more elaborate ones.

The probability density function of the exponential distribution is:

$$f(x) = \lambda \cdot e^{-\lambda x} \quad (x \geq 0) \tag{2.2}$$

The cumulative probability distribution function is:

$$F(x) = 1 - e^{-\lambda x} \quad (x \geq 0) \tag{2.3}$$

The failure or repair probability within a fixed time interval, associated with exponential distributions, can be characterized as a stationary Markov process. It is a sequence of potential events where the likelihood of each event relies solely on the preceding event's state, making it independent of prior occurrences. Thus, forced repairable failures of system components can be represented using a two-state model, as illustrated in Figure 4. The model's parameters (refer to eqs. 2.4 to 2.6) are interrelated as follows: U denotes forced unavailability, λ represents the failure rate (failures/year), μ stands for the repair rate (repairs/year), MTTR is the mean time to repair (hours/repair), and MTTF indicates the mean time to failure (hours/failure). The parameters λ and μ are also referred to as state transition rates since they represent the rate at which the system transits from one state of the system to another.

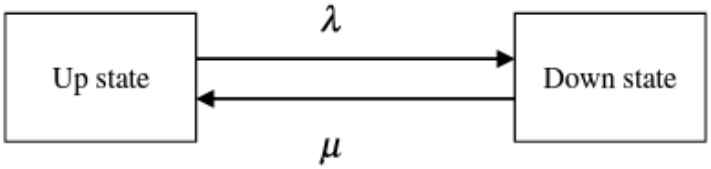

Figure 4: State-space diagram of a two-state outage model.

$$U = \frac{\lambda}{\lambda + \mu} = \frac{MTTR}{MTTF + MTTR} \tag{2.4}$$

Where:

$$MTTF = \frac{1}{\lambda} \tag{2.5}$$

$$MTTR = \frac{1}{\mu} \tag{2.6}$$

The inverse transform method is applied to the cumulative probability distribution function $F(x)$ (2.3) to obtain times to failure or repair on time, where the $F(x)$ is replaced by a uniformly distributed random number sequence as follows:

$$X = F^{-1}\{F(x)\} = -\frac{1}{\lambda}\ln\big(1 - F(x)\big) = -\frac{1}{\lambda}\ln\big(F(x)\big) \tag{2.7}$$

$$X = -\frac{1}{\lambda}\ln(R) \tag{2.8}$$

Where R is a random number sequence from a uniform distribution in the interval [0,1], and 1- R is distributed similarly. An operating cycle for any component is constructed by sampling the duration spent in each state using (2.8).

A planned outage of a system component can be either depicted using a similar two-state model, with all parameters corresponding to the scheduled outage, or scheduled to be out of service for maintenance during a specified period. Separately modelling forced and planned outages does not introduce significant errors. Similarly, a common-cause outage can be represented using an independent two-state model, where the down state encompasses simultaneous multiple component outages, and the failure and repair rates pertain to a group of components involved in the common-cause outage.

Generating units and HVDC lines can be represented using a two-state (up and down) or multiple-state model, considering derated states. Transmission components, such as overhead lines, cables, transformers, capacitors, and reactors, are generally represented using a two-state (up and down) model. A common-cause outage model is employed for overhead lines sharing the same right of way or a group of components controlled by the same protection device. Tap-connection structures in transmission lines are represented using a group outage model. Other dependent outages such as: environmental-dependent outages, cascading failures, and station-originated outages can be also modeled, where the common characteristic is that outages of more than one component are included in the outage state.

II.5. Selection of System States

System reliability or risk is evaluated to estimate the overall risk arising from individual component failures and their combined effects. Various methods for reliability evaluation are available, including probability convolution, minimum cut sets, Markov equations, frequency-duration methods, MCS, and other related approaches. The recommendation for

a particular method often depends on factors such as the desired efficiency, the size and complexity of the system, and the nature of operating conditions. It is important to note that there is no universally applicable method. The selection of a specific method should be based on its relevance to a particular system issue, the required data, and the complexity of evaluating a numerical solution.

The distinction between the analytical and simulation (i.e. MCS) approaches lies in the method of determining reliability indices. Analytical techniques use a mathematical model of the system, often simplified, to evaluate reliability indices through direct mathematical solutions. In contrast, simulation techniques approximate reliability indices by mimicking the system's operations and random behaviour. This approach treats the problem as design of experiments conducted in simulated time, estimating probability by counting event occurrences. For a true probability value, an infinite number of trials is ideal. Practically, achieving a realistic probability measure requires a large sample size. Thus, both approaches come with pros and cons [10]:

a. Analytical techniques are usually faster, whereas simulation methods can be time-consuming. However, modern computing capability is mitigating this drawback.
b. An analytical approach consistently delivers the same result for a given system, model, and data set. In contrast, simulation results can vary depending on the random number generator used and the number of simulations. This consistency in analytical methods might sometimes give users an inflated sense of confidence.
c. Often, the model used in the analytical method simplifies the system or omits time-dependencies and correlations. Meanwhile, simulation can incorporate any identifiable system characteristic.

d. While simulation can yield a broad spectrum of outputs, including complete probability density functions, analytical methods typically focus on providing just the expected values.

Stochastic simulation can be used in three primary ways: 1) state sampling (nonsequential), 2) state duration sampling (sequential), and 3) system state transition sampling (sequential). The choice between these depends on the extent to which one interval impacts the next and the significance of this effect on the reliability indices being evaluated. Like state enumeration, nonsequential MCS cannot capture the chronology of time-dependent events, i.e. sequential transitions between states, so it does not include accurate evaluation of frequency and duration indices, and the capacity to calculate statistical probability distributions of reliability indices. State duration sampling (sequential) focuses on sampling the probability distribution of component state duration. It is useful when considering the chronological behaviour of components, although it requires more computing time.

II.5.1. Sequential Monte Carlo Simulation

The basic idea of MCS is to create a series of experimental samples using random number sequence generators. According to the central limit theorem or the law of large numbers, the sample mean can be used as an unbiased estimate of the mathematical expectation of a random variable following any distribution when the number of samples is large enough. The sample mean is also a random variable, and its variance indicates estimation accuracy.

The Monte Carlo method offers flexibility and accuracy but can be computationally costly. Sequential procedures involve several steps repeated until a coefficient of variation or a

specified number of samples or replications is reached. The primary steps in using the sequential procedure are:

1. Sampling the duration of each component in its current state using probability distributions, failure rates, and repair rates. This step is repeated to produce yearly sequences or chronological component state transitions over the specified time span.
2. Applying the chronological hourly load model for each load bus and conducting system analysis for each system state based on the OPF problem and load curtailment minimization. Contingency analysis can also be performed before the minimization model.
3. Accumulating yearly adequacy indices as reliability index functions and computing the mathematical expectation of index functions per bus and system once a coefficient of variation or the total number of samples has been reached.

References [10], [17], [18], [19] provide more in-depth explanations, procedures, and applications of MCS techniques for composite power system reliability assessment.

II.6. System State Evaluation

In system state evaluation, each state is analyzed to identify its associated load curtailments. OPF analysis can be employed for evaluating the sampled states. Unlike the power flow model, the real powers and voltages at generator buses are not pre-specified. Instead, they are calculated from the model using an objective function and constraint conditions. The real power outputs and voltages of generators are often used as control variables to be optimized. The OPF model can also incorporate other control variables, such as the reactive powers of var equipment and transformer tap changer ratios.

In the case of an emergency state led by component outages, a particular OPF model is employed to reschedule generation, change transformer turn ratios, eliminate constraint violations from overloading and voltage levels, and take other actions to maintain the power balance while avoiding or minimizing load curtailment if necessary. The objective of the OPF optimization is to prevent or reduce overall load curtailment, including curtailments at individual buses. Risk indices are metrics calculated based on the load curtailments in selected system outage states and their probability of occurrence. The standard minimization model of load curtailment is described in Appendix B, where the sum of load curtailment over all buses based on a predetermined weighting factor per bus is minimized.

II.7. Reliability Indices

A parameter estimation refers to the average value derived from failure data in a component's outage model. Such a parameter can either be based on the average of the sample data or calculated over a given period, as represented by the sample mean or the mean time to failure, respectively.

In the Monte Carlo Simulation method context, a simulation yields an estimate for each of the parameters being assessed. The results of these simulations are influenced by the random numbers chosen for the process variables. Thus, if n simulations are conducted, there will be n estimations for each parameter. These estimates can be analyzed in various ways, including distribution plots such as frequency histograms or density functions and point estimates, including means, modes, minima, maxima, and percentiles.

The arithmetic average or mean estimation of sample data is presented in (2.25), where n is the number of sample data (or sampled power flows), $\bar{X}$ is the arithmetic mean, and X_i is a sample value of the output variable obtained in the i^{th} power flow sample.

$$\bar{X} = \frac{1}{n}\sum_{i=1}^{n} X_i \tag{2.25}$$

The variance measures the degree of dispersion of a random variable, and the standard deviation is derived from the variance as its square root. The sample variance is approximately calculated by (2.26).

$$s^2 = \frac{1}{n-1}\sum_{i=1}^{n}(X_i - \bar{X})^2 \tag{2.26}$$

The fundamental parameter in adequacy assessment is the mathematical expectation of a given reliability index. Some examples of this type of index are listed below and explicitly defined by equations 2.27 to 2.32:

i. Probability of Load Curtailments (PLC).

ii. Expected Demand Not Supplied (EDNS) in MW.

iii. Expected Duration of Load Curtailments (EDLC) in hours/year.

iv. Expected Energy Not Served (EENS) in MWh/year.

v. Expected Frequency of Load Curtailments (EFLC) in outages/year.

vi. Average Duration of Load Curtailments (ADLC) in hours/outage.

$$PLC_k = \sum_{k \in S} p_k \tag{2.27}$$

$$EDNS = \sum_{k \in S} p_k \cdot LC_k \tag{2.28}$$

$$EDLC = \sum_{k \in S} p_k \cdot T \tag{2.29}$$

$$EENS = \sum_{k \in S} p_k \cdot LC_k \cdot T \tag{2.30}$$

$$EFLC = \sum_{k \in S} (F_k - f_k) \tag{2.31}$$

$$ADLC = \frac{EDLC}{EFLC} \tag{2.32}$$

II.8. Effective Load-Carrying Capability

In Resource Planning, a common measure of capacity among resources with different operating characteristics and constraints, such as energy-limited resources, is called the capacity credit/value/benefit calculation. It originated as an evaluation technique for capacity expansion analysis performed in resource adequacy studies decades ago. One of the metrics used to evaluate this incremental contribution is called the Effective Load Carrying Capability (ELCC), which determines how much additional load can be served over a predefined duration by a new generation source to maintain a specific risk level [10], [20]. In other words, ELCC is the amount of load added to an augmented system with additional generation units that match the system risk of the base system under study.

The severity index (SI), a normalized EENS in MWh/year divided by the system peak load, is recommended as an appropriate risk index when comparing systems at different peak load levels [10]. SI is measured before and after adding variable generation or energy storage at the same peak load level. The resulting anticipated reduction in SI is then used

as a margin to continuously increase the augmented system's peak load until the SI converges to the pre-augmented level. Finally, the resultant ELCC will be the incremental load determined in the last step, which may be a fraction of the maximum installed capacity of the resource addition.

CSR assessment in system planning aims to compare alternative decisions and includes an option to "Do Nothing" rather than using an absolute threshold. Unlike absolute reliability and absolute indices, relative indices are measured before and after design and operating changes, thus enabling direct reliability comparisons and not against absolute specified targets such as LOLE utilized in Resource Adequacy assessment. Therefore, ranking the benefits or merits of alternatives using the ELCC metric based on relative indices provides considerable confidence [7]. ELCC aids in discerning:

1. Impacts of unit unavailability regarding extra capacity [21]
2. Effects of various unit sizes [8]
3. Influence of renewable energy and energy storage on the system [10], [20]

A pioneering methodology to estimate the downstream impacts of unit inclusions without exhaustive probability computations was proposed in [21]. This analytical method computes adequacy indices post the enhancement of peak load, as illustrated in Figure 11. A pragmatic approach for ELCC computation, presented in [22], employs the bisection method. Although necessitating an extensive iteration count, its convergence is guaranteed.

The authors in [10] define an additional metric labelled generation capacity equivalence (GCE), which indicates the equivalent generation capacity of wind power if it could be transformed into a conventional generating unit that dominates the studied system,

including its forced unavailability rate. Authors in [23] named GCE as the Equivalent Firm Power, the equivalent capacity of a 100% available power plant, which has the same ability to decrease the system adequacy level as the studied generating unit without considering ELCC.

II.9. Adequacy Assessment Incorporating Energy Storage

Unlike power-constrained conventional assets, energy storage is constrained by both: a) power, and b) energy, i.e. an energy storage device must have sufficient power output capability and energy capacity stored to supply a load over a required period. Due to the temporal nature of storing energy, the state of energy of an energy storage device is tightly linked to the network's available import capability, using existing transmission infrastructure to draw power. Thus, component outages and the magnitude and shape of load demand are highly relevant [24], [25], [26] considerations when incorporating energy storage into an existing network. Authors in [27], [28] first attempted to quantify the impacts of energy storage on reliability performance. In their work, the sequential MCS method was implemented as the only practical technique for analyzing power systems utilizing on-grid storage facilities in Resource Adequacy assessments. For distribution planning, the authors in [25] studied ESS as a transmission solution to provide local load security during an outage event.

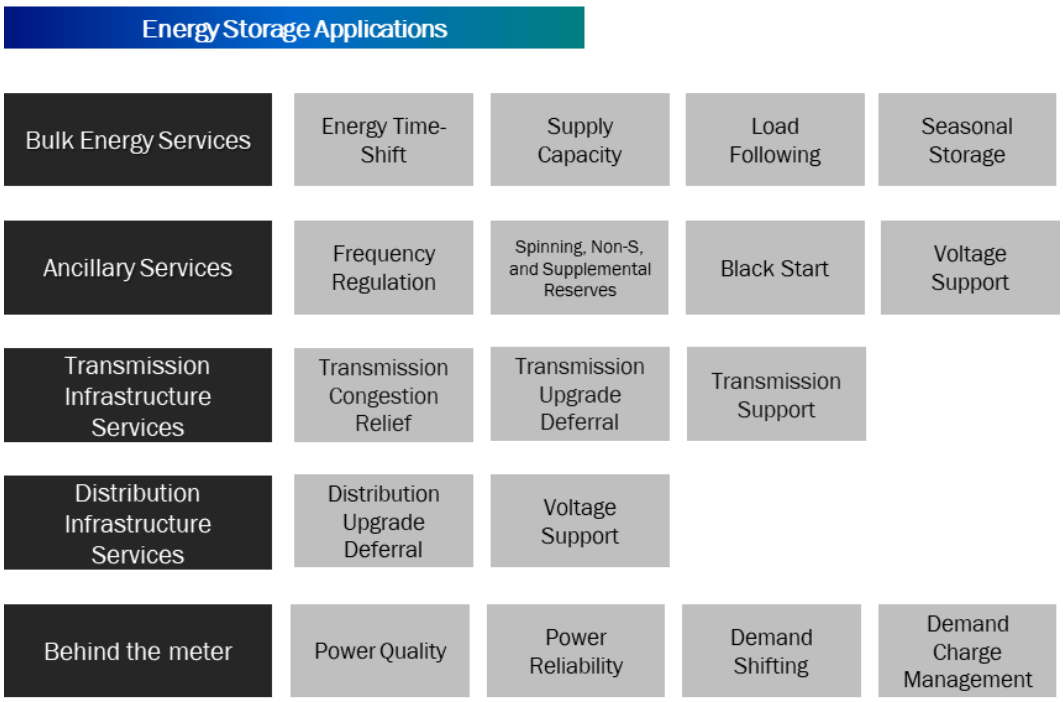

Figure 5: Energy Storage Applications in Power Systems.

The impact of energy storage integration on CSR was addressed in [29], where sequential MCS and DC OPF were implemented to accurately quantify the reliability contribution of wind energy and energy storage, studied on the IEEE-24 RTS. EENS was evaluated to find the optimal integration of storage and renewable energy generation. Storage alone, while optimally located, reduced EENS by 18%, with a nominal power rating close to 0.7% of the system peak load. Later, [30] proposed a reliability assessment framework based on CSR and AC OPF on the IEEE-24 RTS, showing the contribution of energy storage to enhance network adequacy by assuming two main applications: 1) peak load reduction in the regular daily dispatch, and 2) back up during contingencies. It must be noted that storage sizing and location were optimized to minimize total network operation costs during normal operating conditions. Recently, authors in [24] proposed a methodology for determining the optimal size of energy storage to match local peak demand for the security

of supply of customers, demand response, and a dynamic thermal rating system by applying CSR assessment with sequential MCS and DC OPF.

SATA is an electric storage resource connected to the transmission system that can be dispatched for: a) market efficiency, b) operational performance, and c) reliability improvement. FERC has previously issued a policy statement to clarify and provide guidance on the ability of storage to offer multiple services and seek to recover their CAPEX and OPEX costs [31].

The capacity value of energy storage as a solution for reliability needs identified in power system planning can be evaluated using ELCC and an equivalent capacity as compared to any conventional transmission asset with an unavailability rate can be determined. However, to the author's knowledge, storage has never been compared to transmission assets using an ELCC methodology under CSR assessment.

III. Methodology

The main objective of this thesis was to research and develop new capabilities for performing robust CSR assessments incorporating ESS as a transmission asset. The outcome of this research effort is an open-source, research-grade CSR tool (CompositeSystems) using sequential MCS. CompositeSystems allows for the simulation of power system operations under different conditions, including the integration of energy storage, to assess the risk of failing to meet load demand. Furthermore, this thesis introduces a unified framework and platform, accommodating diverse solvers and power network formulations. This platform allows comparisons, problem specifications, and variable operational conditions. The sequential MCS method was devised to characterize energy storage and its capacity contribution as an unconventional solution in transmission planning.

III.1. Composite System Reliability Assessment Tool

CompositeSystems© is a toolbox designed to evaluate the adequacy of composite resource and transmission systems. It calculates load point and system reliability indices, providing insight into the expected adequacy of service at a load point. Indices such as EDLC and EENS, which offer valuable information on transmission system performance, are implemented. However, their results depend on the load curtailment strategy applied. CompositeSystems allows users to simulate power system operations based on both DC and AC power flows, and it is written in the Julia™ programming language.

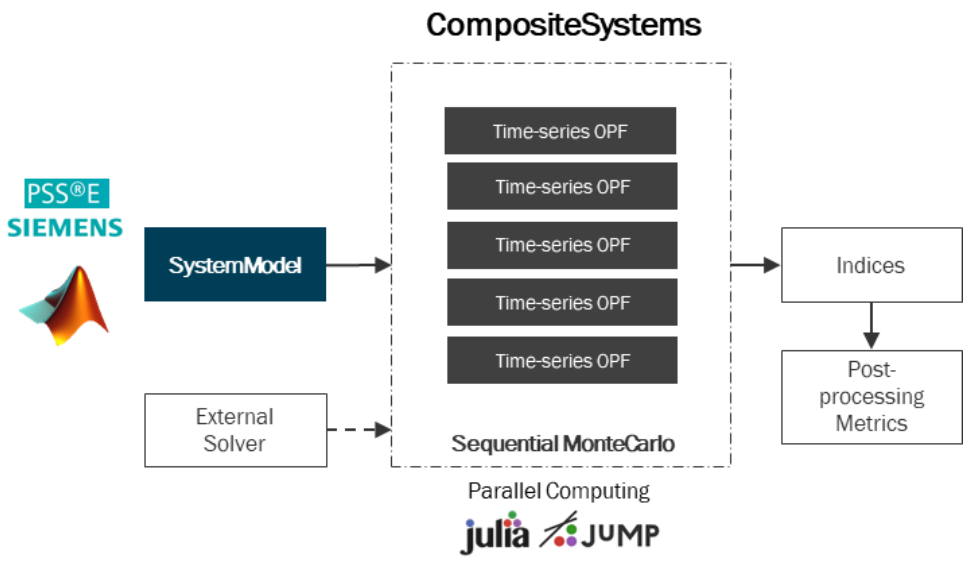

Figure 6: Simplified flowchart of CompositeSystems.

III.2. Power System Representation

CompositeSystems supports the parsing of MATPOWER™ [32] network files in .m format and PSS®E™ network files in .raw format. Once imported, these files are converted to an internal representation for MCS and power flow simulations. Components supported by CompositeSystems include buses, loads, generators, storage systems, branches, transformers, and shunts. The system model data is structured in an easily accessible format composed of properties that define organized component data and data types. Load demand and renewable energy generation data can also be imported. Reliability data is also incorporated into each system component's structure to calculate their state probabilities.

The network topology is represented using a standardized data structure that can be updated dynamically to reflect any changes in the network resulting from generation, transmission outages, or isolated components that require temporary removal. Internally, all values are expressed in per unit (p.u.) magnitudes, and the angles of complex quantities

are expressed in radians. Before the models used to solve OPF are processed, all offline components are removed. However, instead of creating new optimization problems per time step, most of the inequality, equality constraints, and objective functions are modified at runtime. This approach ensures faster simulations with efficient solvers. In some cases where the number of time steps is very small, creating new optimization problems per time step may also be a viable solution.

III.2.1. Assets

The power system components described below are defined as immutable structures in CompositeSystems© to ensure that data remains unchanged during Monte Carlo Simulation (MCS) runs for thread safety, predictability, parallel programming usage, and easy debugging. However, mutability is implemented at runtime (using recycled helper vectors and dictionaries) to propagate network changes to the optimization problem and constraints.

1. **Buses:** buses consist of complex voltage and carry the following information: keys, zone, bus type, index, magnitude ratings, base kV, voltage magnitude and angle.
2. **Generators (time-series):** generators consist of time-series, complex power injection at a specific bus, and carry the following information: keys, buses, real and reactive power, voltage magnitude, lower and upper power ratings, MW base, failure rates, repair rates, and derated rates.
3. **Loads (time-series):** power loads consist of time-series, a specified quantity of real and reactive power consumed at a bus, and carry carries the following information: keys, buses, real and reactive power, power factor and loss of load costs.

4. **Energy Storage Systems:** ESSes are modelled as a flexible storage model proposed in [33], consisting of discrete complex charging and discharging power states. They carry the following information: keys, buses, real and reactive power, energy, charge and discharge ratings, charge and discharge efficiencies, energy rating, thermal rating, reactive rating, losses, internal impedance, failure and repair rates.
5. **Branches:** Branches carry the following information: keys, buses (from and to), common mode component, real and reactive power, short and long-term ratings, complex impedance, susceptance and capacitance, angle shift and angle ratings, tap ratio, failure and repair rates. Branches (i.e., transmission lines, transformers and phase shifters) are modelled as immutable structures consisting of:
    a) An ideal phase shifting transformer at the "from side" of the branch with a fixed, complex-value voltage transformation (i.e. tap and shift).
    b) A standard π transmission line model, with series complex impedance and from and to side shunt elements.
6. **Shunt elements:** a shunt is modelled as an immutable structure consisting of a fixed impedance (complex) to ground at a bus representing a capacitor or inductor. It carries the following information: keys, buses, active and reactive power withdrawn per voltage p.u.

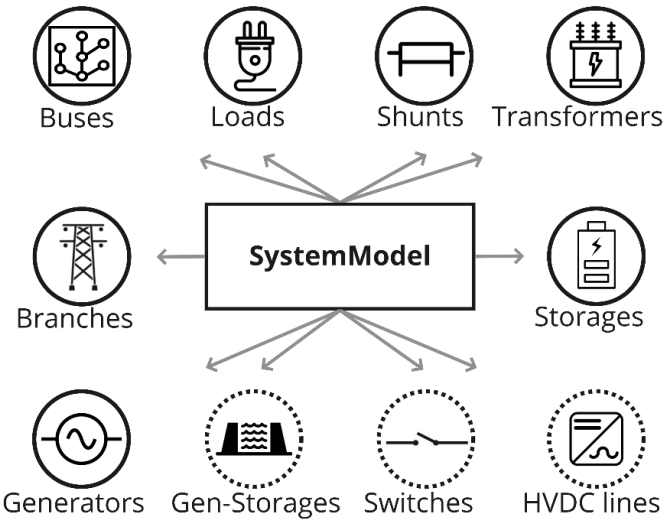

Figure 7: SystemModel's structure with current (continuous line) and future (dotted line) components.

III.2.2. SystemModel

The SystemModel structure represents a comprehensive power system model. It encompasses all the asset models in addition to system simulation parameters such as the number of time steps for each replication using sequential MCS, the duration of each time step and its associated unit, and the system's base MVA.

At the onset of each simulation, the tool facilitates the creation of a structure called **Topology,** wherein the elements, which include vectors and dictionaries, are mutable. Specifically, it includes:

1. The currently available assets (branches, generators, loads, shunts, storages, and buses).
2. Assets available in the previous time step.
3. Mapping dictionaries which connect assets to their proximate active buses for the relevant time step.

4. Interim details, including loads, power flows, stored energy, and failure states.

III.3. Mathematical Optimization

An internal structure is defined to carry all temporary information about the topology, changes, settings, and the power flow formulation as an optimization problem. The latter is characterized by a JuMP model [34]. JuMP is an algebraic modeling language for mathematical optimization embedded within the Julia programming language, which simplifies the translation between the algebraic form of the modeler, and the standard form of the external solver. For more details about JuMP modeling, see Appendix C.

CompositeSystems implements two optimization models: 1) a DC-Based model including transformer components, and 2) an AC-based (LPAC) model with no pre-defined power flow data, known as a cold start model, suitable for planning studies where no AC solution is available due to mutable network topologies.

Energy storage components in CompositeSystems, as proposed in [33] and modeled in [36], have been devised for application in various multi-period OPF problems. Specifically tailored for research purposes, the model offers the following features:

i. It captures the dynamics of an energy buffer across diverse scales, ranging from residential battery storage to grid-scale pumped hydro.
ii. It is compatible with both balanced and unbalanced formulations of the power flow equations.
iii. It is designed to be compatible with convex relaxations and linear approximations, ensuring effortless integration of the proposed model into applications where either convexity or linearity is essential.

The linearized storage model with its mathematical representation is spanned by equations (3.9) to (3.19). The mathematical model of the storage component is given by the following parameters and variables at any time:

$S_{s,i}$	:	Complex bus power injection at bus i, p.u.
S_i^{loss}	:	Complex power losses, in p.u.
PR_sc_i, PR_sd_i	:	Charge and discharge power ratings, in p.u.
sc_i, sd_i	:	Charge and discharge power of energy storage at bus i, in p.u.
ER_i	:	Energy rating of the storage system at storage bus i.
$E_{i,t}$	:	Energy content in the buffer of the storage system at storage bus i after charging or discharging at a period t.
$E_{i,t-1}$	:	Initial energy content at the beginning of the simulation t, of the storage system at bus k.
$Z_{s,i}$	:	Storage's internal injection impedance, in p.u.
η_i^c, η_i^d	:	Charge and discharge efficiencies.
s_i^u	:	Thermal injection limit, in p.u.
i_i^u	:	Current injection limit, in p.u.
$I_{s,i}, V_{s,i}$	:	Complex bus current and voltage injection, in p.u.
sqc_i	:	Reactive power slack, in p.u.
q_i^{min}, q_i^{max}	:	Reactive power injection limits, in p.u.

III.3.1. DC-Based formulation

In evaluating the reliability risk of a composite system, instances may arise where optimal power flow solutions are needed for thousands of system states. The DC OPF model,

typically employed to alleviate this computational challenge, is described in [35]. This model, a linear active-power-only approximation, uses branch susceptance values for network phase angles and incorporates transformer parameters like tap ratios and phase shifts. The same model has been implemented by PowerModels from Los Alamos Laboratory [36], yielding results consistent with MATPOWER [32]. The objective function is as follows:

$$Min \left\{ \sum_{i \in ND} w_i \cdot P_{D,i} \cdot C_i + \sum_{i \in NS} x_i \left(\frac{ER_i - E_{i,t}}{\Delta t} \right) \right\} \tag{3.1}$$

Which is subject to the following constraints:

$$\sum_{i \in NG} P_{G,i} - \sum_{i \in NS} |S_{s,i}| - \sum_{i \in ND} P_{D,i} \cdot C_i - \sum_{i \in NH} G_{Sh,i} \cdot Sh_i = \sum_{i,j \in N} \sum_{l \in NB} T_{l,ij} \tag{3.2}$$

$$P_{G,i}^{min} \leq P_{G,i} \leq P_{G,i}^{max} \quad (i = 1, \dots, NG) \tag{3.3}$$

$$T_{l,i,j}^{min} \leq T_{l,i,j} \leq T_{l,i,j}^{max} \quad (l = 1, \dots, NB)\ (i, j = 1, \dots, N) \tag{3.4}$$

$$\delta_{i,j}^{min} \leq \delta_{i,j} \leq \delta_{i,j}^{max} \quad (i, j = 1, \dots, N) \tag{3.5}$$

$$T_{l,i,j} = -\frac{\left(\delta_{i,j} - \delta_{shift,l}\right)}{\frac{-B_{i,j}}{\left(G^2{}_{i,j} + B^2{}_{i,j}\right)} \cdot tap_{ratio,l}} \quad (i, j = 1, \dots, N)\ (l = 1, \dots, NB) \tag{3.6}$$

$$0 \leq C_i \leq 1 \quad (i = 1, \dots, ND) \tag{3.7}$$

$$\delta_{slack} = 0 \tag{3.8}$$

Energy storage's constraints:

$$E_{i,t} = E_{i,t-1} + \Delta t \left(\eta_i^c \cdot sc_i - \frac{sd_i}{\eta_i^d} \right) \tag{3.9}$$

$$|S_{s,i}| \leq s_i^u \tag{3.10}$$

$$|I_{s,i}| \leq i_i^u \tag{3.11}$$

$$0 \leq E_{i,t} \leq ER_i \tag{3.12}$$

$$sc_on_i + sd_on_i = 1 \tag{3.13}$$

$$sc_on_i \cdot PR_sc_i \geq sc_i \tag{3.14}$$

$$sd_on_i \cdot PR_sd_i \geq sd_i \tag{3.15}$$

$$0 \leq sc_i \leq PR_sc_i \tag{3.16}$$

$$0 \leq sd_i \leq PR_sd_i \tag{3.17}$$

$$\left|S_{s,i}\right|^2 = \left|V_{s,i}\right|^2 \left|I_{s,i}\right|^2 \tag{3.18}$$

$$|S_{s,i}| + (sd_i - sc_i) = |S_i^{loss}| + Z_{s,i}\left|I_{s,i}\right|^2 \quad (i = 1, \dots NS) \tag{3.19}$$

Where:

w_i, x_i : Weighting factors at load bus and/or storage bus i reflecting the importance of loads and stored energy per hour, respectively, in $/p.u.

$P_{D,i}$: Real power load at bus i, in p.u.

C_i : Load curtailment (factor) control variable at load bus i, unitless.

Δt : Duration of time step t.

$P_{G,i}$: Real generation power variables at bus i, in p.u.

$G_{Sh,i}$: Real power consumed by shunt elements at shunt bus i, in p.u.

Sh_i : Binary variable representing a shunt control variable at bus i, unitless.

$T_{l,ij}$: Power flow on branch l between buses i and j, p.u.

$\delta_{i,j}, \delta_{slack}$: Angle's difference between bus i and j, and slack bus, in radians.

$P_{G,i}^{min}, P_{G,i}^{max}$: Upper and lower limits of the generating variable P_g, in p.u.

$T_{l,i,j}^{min}, T_{l,i,j}^{max}$: Upper and lower limits of the power flow variable T_l, in p.u.

$\delta_{i,j}^{min}, \delta_{i,j}^{max}$: Upper and lower limits of the corresponding variable, in radians.

$\delta_{shift,l}$: Branch phase shift angle, in radians.

$B_{i,j}, G_{i,j}$: Real and imaginary parts of a shunt element in the bus admittance matrix, in p.u.

$tap_{ratio,l}$: Branch off nominal turns ratio, in p.u.

sc_on_i, sd_on_i : Binary variables representing charge and discharge storage power at bus i, ensuring no overlaps.

$N, NG, NB, ND, NC, NT, NH, NS$ represent the number of buses (N), generators buses (NG), branches (NB), load buses (ND), buses reactive equipment (NC), transformer branches (NT), shunt device buses (NH), and storage buses (NS) in the system.

In the objective function (3.1), the first term focuses on minimizing load curtailment, while the second emphasizes minimum cost storage charging. C_i represents load curtailment control variable at load bus i, guaranteeing that the optimization model always has a solution in any outage state. Weighting factor w_i provides a load curtailment order, where a greater value represents a more important bus load.

When loss of load occurs, the storage system $i \in NS$ discharges according to the formula in (3.9), adhering to constraints (3.10) to (3.19) that set variable limits. For example, ER_i in (3.12) caps the energy content $E_{i,t}$ of the storage system at storage bus i at time t. Constraints between (3.13) and (3.17) ensure that the charge power rating, sc_i and discharge power rating, sd_i do not overlap and stay below the limits, facilitated by the binary variables sc_on_i and sd_on_i. s_i^u in (3.10) is the upper limit of $S_{s,i}$. Equation (3.18) links power $S_{s,i}$ with current $I_{s,i}$ and voltage $V_{s,i}$. (3.19) represents the single-phase nodal power (real) balance equation of the proposed energy storage model in [33]. Parameter S_i^{loss} represents power losses. Finally, the term $Z_{s,i}\left|I_{s,i}\right|^2$ denotes losses from internal impedance $Z_{s,i}$. Sh_i is an additional control variable that is switched to satisfy the power flow constraints.

The standard assumptions of the DC power flow method are applied, such as neglected transmission resistance, a small difference in voltage angle between two interconnected buses, and fixed voltage magnitudes. Although not described by the equations, other elements can be switched out using auxiliary binary variables.

The OPF problem is executed at each hour until the end of the simulation period, and the total amount of energy not served during each simulation is recorded. The model's variable bounds and constraints are updated in each system state (hourly) to reflect changes in the network due to unplanned outages and split situations.

III.3.2. AC-Based formulation

While the accuracy of DC models can vary greatly depending on the system and case, with the potential for errors in trouble spots, power flow inaccuracies are typically only a few percent compared to AC models. However, nonlinearity associated with network stress can result in significant differences between DC and AC models [35]. To address this, a novel Linear-Programming approximation of AC power flows (LPAC models) has been proposed in [37], incorporating reactive power and voltage magnitudes in a linear (piecewise) power flow approximation of the cosine terms while retaining the computational benefits of DC models. The LPAC models are based on a polyhedral relaxation of cosine terms and Taylor Series approximations of nonlinear terms, providing accurate values for active and reactive power, phase angles, and voltage magnitudes. These constraints contain quadratic terms that can be implemented by Mixed Integer Quadratically-Constrained Quadratic Programming (MIQCQP) solvers [37]. See reference [38] (CompositeSystems) for more details about the Linear Programming AC-based formulation.

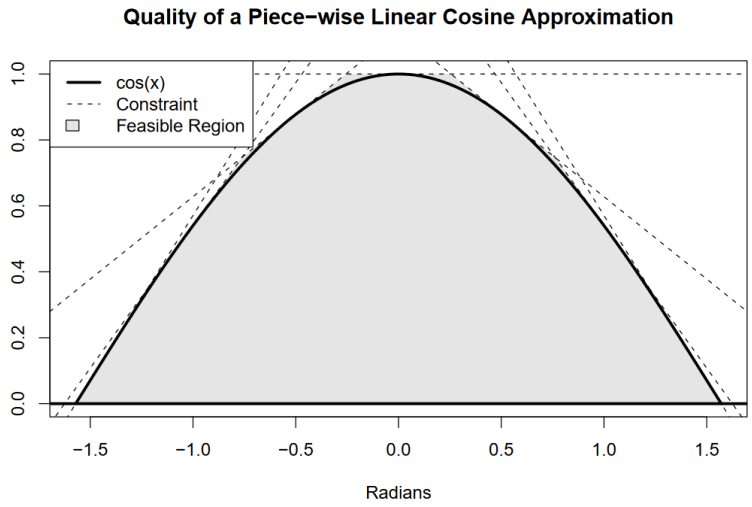

Figure 8: A Piecewise-Linear Approximation of Cosine using 7 inequalities. Source: [37].

III.4. Probabilistic Simulation

CompositeSystems has been designed to execute the sequential MCS method, allowing for simulations of unit-level outages using two- and three-state Markov models. Options such as the number of replications, the seed for random number generation, single or multi-threading simulation, power flow formulation, supported optimizer, and results can all be specified. Since multiple components can be out of service simultaneously, parts of the system may become isolated. As a result, CompositeSystems offers at least two user-specified split network treatments: 1) selecting the largest split transmission system and 2) removing single or multiple isolated PV buses.

To assess the reliability of a power system, a system state is selected and defined by the status (up and down) of its components that were sampled based on reliability data. The simulation proceeds by iteratively running steady-state power flow simulations under various scenarios, such as contingencies or changes in generation and demand. The power

flow simulations are performed using either the DC OPF or fast-decoupled AC OPF methods over one or more consecutive periods.

The performance of executing a complex numerical optimization depends on the number of constraints and variables required, the type of optimization problem, and the algorithm used to handle systems with isolated buses. The commercial optimizer Gurobi™ [39] has been found to provide high speed, parallelization, and relatively stable performance throughout sequential MC simulation using CompositeSystems, based on its ability to update parameters and constraints of the optimization problem on the fly.

The strategy implemented in this work for parallelization involves dividing the number of replications (years) by the number of available threads on each machine if multiple machines are available. This approach allows for the efficient utilization of computational resources. To support parallel execution, an abstract (JuMP) model with an attached solver is initialized and updated based on the changes in the system topology caused by random outages during the simulation. Ensuring the selected solver or optimizer is thread-safe and compatible with the specified OPF method is essential. The system model remains constant throughout the simulation, eliminating the possibility of data races and ensuring replicability of the results. In the case of nonsequential MCS, parallel computing should be applied to each load level individually rather than to the entire sample.

Julia provides a channel mechanism facilitating communication between multiple tasks, allowing for concurrent reading and writing operations. Each MCS loop produces statistical results collected concurrently using a channel in this work. The channel is closed after the last thread and replication, and the results are computed, including indices, metrics, and other statistical measures. This parallelization strategy enhances the efficiency

and scalability of the simulation, enabling faster and more robust reliability assessment of the power system.

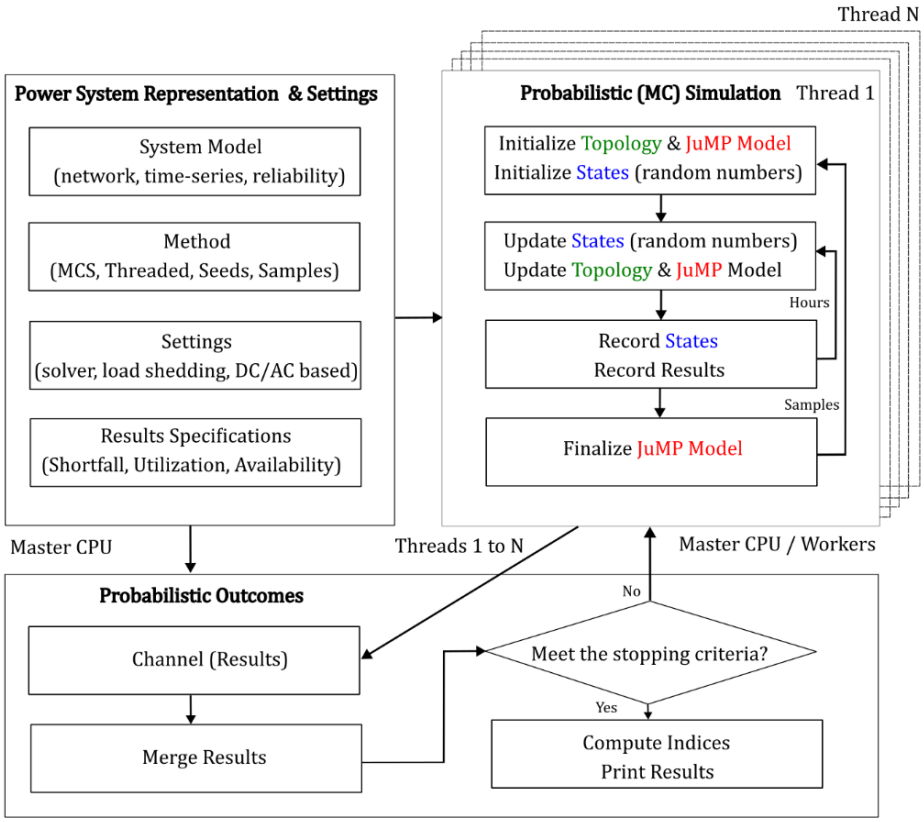

Figure 9: CompositeSystems' model structure.

III.5. Probabilistic Outcomes

Reliability indices, derived from quantified risk evaluations, indicate the risk level of the system and load buses. Through calculations of metrics like EENS and EDLC, a CSR assessment provides statistical information regarding transmission system reliability. Understanding the distribution of unserved energy across various buses and periods empowers decision-makers to effectively prioritize resources and investments in grid infrastructure. Section II.7 provides the equations to calculate reliability indices using the state duration sampling method (i.e. sequential MCS).

Bus indices compare system configurations and transmission planning alternatives, while system indices assess resource and transmission system adequacy. The justification for evaluating both system and bus reliability indices lies in the fact that the impact of single or multiple outages is not uniformly distributed across the transmission system under study. This consideration sets the stage for further exploration of probabilistic outcomes and their implications for system planning in subsequent sections of the thesis.

The application of reliability evaluation in transmission development planning involves two main aspects: 1) quantified reliability assessment (CSR assessment), and 2) overall economic analysis. Examples of CSR assessment applications in transmission planning, such as line additions, changes in local network configuration, equipment rating adjustments, and non-investment-type reinforcements, can be found in references [2], [10]. Although this work does not include the overall economic analysis, the authors in reference [10] provide technical guidance on its application.

IV. Case Studies and Results

This chapter examines the reliability value of energy storage as a transmission asset through a standard use case by determining its equivalent capacity value based on sequentially adding incremental load. In other words, how does the additional load served by a conventional transmission planning asset compare against the same load served by an energy storage alternative? While various benefits of energy storage, such as congestion reduction, transfer capability improvements, grid voltage support, and renewable energy deliverability enhancements, have been previously explored [31], [40], [41], [42], its reliability evaluation presents challenges due to its dual-use nature as both a transmission and generation asset. A composite assessment viewpoint may be necessary to fully capture its contribution.

On one hand, energy storage's role as a resource can be assessed using resource adequacy evaluation tools, which determine the adequacy level of a simplified power system to meet load growth. However, this approach often focuses solely on the balance between generation and load, neglecting the transmission network. On the other hand, energy storage offers potential as an alternative solution for alleviating thermal overloading on transmission lines, maintaining voltage levels, managing power flows, absorbing excess power, and deferring or displacing the need for new generation and transmission infrastructure. Optimal siting and sizing of these resources near load buses could reduce the need for power and energy delivery across the system.

To demonstrate the proposed methodological approaches of this thesis, CompositeSystems is developed as a CSR tool and executed on selected standardized test systems. Results

from scenarios involving curtailed load and reliability indices for system and load buses are compared to corresponding DC and AC-based results. Previous studies utilizing standard test systems [43], [44], [45], [46], [47], [48], [49], [50], [51], [52], [53] have demonstrated that reliability estimates may deviate somewhat from benchmark estimates due to the complexities of CSR assessment. Factors such as the load-shedding philosophy, contingency analysis, mathematical optimization, and the priority order of load buses can impact the results. However, similar assumptions and insignificant deviations can be considered sufficient for conducting a successful case study involving energy storage.

The implemented ESS modeling approach presented in the previous chapter has been verified. Storage as a transmission alternative, evaluated through CSR assessments, considers the modeling of the transmission system. A Newton-Raphson algorithm is implemented to compute its reliability contribution (i.e. the ELCC metric) and determine optimal storage size. Thus, some barriers preventing the identification of energy storage as a viable alternative are addressed, such as the weak link between resource and transmission planning processes and the difficulty of representing this type or resource in CSR studies.

IV.1. Test Systems

Two widely-recognized academic power system models, with specified standard parameters (e.g. generation capacity, load capacity, line capacity, failure rates and repair times of the components), were selected for adequacy assessment: 1) the Roy Billinton Test System (RBTS) [54], and 2) the IEEE-RTS 79 reliability test system [55]. These systems serve as important benchmarks in CSR evaluations, even with their inherent limitations. Specifically, both often do not fully capture the nuances of composite

(generation and transmission) issues due to their modest transmission constraints, leading to limited use of OPF analysis. Using these test systems, simulations performed by the author covered 15000, 7500 and 2000 replications, respectively. System and load point indices were determined using the state duration sampling MCS method, DC and AC-based formulations, with a consistent load profile for each bus. The simulations utilized nodes from the Narval HPC cluster, maintained by ACENET™ [56]. This cluster comprises 1145 nodes, each equipped with 64 cores powered by 2 x AMD™ Rome 7532 @ 2.40 GHz processors with a 256M cache L3, and extensive memory capacities.

IV.1.1. Roy Billinton Test System (RBTS)

The RBTS (see Figure 23, Appendix F), originating from the University of Saskatchewan, serves educational purposes. It consists of six buses, nine transmission lines, and 11 generators with an annual peak load of 185 MW. Using CompositeSystems, the accuracy and precision of results on RBTS were compared against outcomes from [43], [44], [45], [46], [47], [48].

IV.1.2. IEEE Reliability Test System (IEEE-RTS 79)

The IEEE reliability test system (IEEE-RTS 79), published in 1979, was a creation of the subcommittee on the Application of Probability Methods within the IEEE Power and Engineering Society (see Figure 24, Appendix G). The system features 24 buses, 38 lines, 32 generators, five transformers, and a reactor, supplying an annual peak load of 2850 MW with identical load profiles for each bus. CompositeSystems' performance on the IEEE-RTS 79 was compared against results from [43], [44], [49], [45], [50], [51], [47], [53], [52].

The IEEE-RTS 79 topology is frequently modified to better demonstrate reliability requirements, yet its significance in CSR research remains unchanged. Finally, the inherent differences in programming languages, machines, methods, and techniques across benchmarked papers can introduce variability in results, making benchmarking comparisons difficult.

IV.1.3. IEEE Reliability Test System upgrades

Since its publication in 1979, the IEEE-RTS has undergone three upgrades, in 1986, 1996, and 2019. The initial upgrade, known as IEEE-RTS-86, combined two identical IEEE-RTS 79 models using a single 230 kV tie line rated at 300 MW. It also introduced partial generating unit outages, load forecast uncertainty, and scheduled maintenance [57]. The subsequent upgrade, IEEE-RTS 96, significantly increased model complexity and size by incorporating operating costs and additional constraints, making it suitable for economic operation and planning of power systems [58]. The latest upgrade, IEEE-RTS GMLC, replaced some thermal units with a more representative mix of modern power generation sources, including natural gas, wind, solar photovoltaic (PV), concentrating solar power (CSP), and energy storage. This update also provided a 5-minute time-series dataset covering wind, solar, and load data, along with load forecasts, wind forecasts, utility-scale PV forecasts, rooftop PV forecasts, and CSP resources. With these enhancements, the upgraded test system offers unique opportunities to explore issues related to the reliable operation and planning of power systems, while considering both forecasted and actual time series data for wind and solar generation, as well as real power demand [59].

To adequately validate CompositeSystems, the IEEE-RTS 79 test system was chosen due to the significant number of studies published utilizing this test system. However, the IEEE-RTS GMLC offers a more comprehensive dataset for modern power systems, for which models representing variable renewable energy, energy storage, and the chronological operation of the transmission system are essential.

Table 2 and Table 3 provide a detailed view of the annual system EENS and EDLC adequacy indices. Additionally, Table 6 and Table 7 (Appendix D) offer insights into the Annual EENS and EDLC indices per bus, obtained through DC and AC-based models.

IV.2. Split Network Situations

Line and/or transformer outages can lead to situations in which the system network is divided into disconnected subnetworks. Under steady-state conditions, these subnetworks can be treated independently, allowing for the computation of reliability indices for each subnetwork. The probabilities and frequencies of these independent outages are generally quite low, and therefore, their impact on the indices is not significant. Nevertheless, their results can be compared using different tools, formulations, and models developed by various authors.

Table 1 displays load curtailment results for different test cases involving islands or network splits with multiple contingencies, employing both DC and AC-based formulations. As expected, the DC-based results are exact, while the linear programming AC-based (LPAC) results, although slightly underestimating shortfall by 0.91%, closely align with the anticipated outcomes.

Table 1: Load curtailment benchmarking results using Gurobi solver.

Test System	Split Network due to Outage of	Load Curtailment (MW)				
		Composite-Systems	**Laengen** [43]	**Difference**	**Khan** [60]	**Difference**
RBTS	**Method**	**DC OPF**	**DC OPF**	**-**	**-**	**-**
	G3, G7, G8, G9	35.00	35.00	0.0	-	-
	Lines 3, 4, 8, the largest system selected	75.00	75.00	0.0	-	-
	Lines 5, 8	40.00	40.00	0.0	-	-
	Lines 2, 7, Reduced generation	74.00	74.00	0.0	-	-
RBTS	**Method**	**LPAC**	**Full AC OPF**	**-**	**-**	**-**
	G3, G7, G8, G9	37.16	37.50	-0.34	-	-
	Lines 3, 4, 8, the largest system selected	77.03	77.50	-0.47	-	-
	Lines 5, 8	40.00	40.00	0.00	-	-
	Lines 2, 7, Reduced generation	97.92	100.10	-2.18	-	-
IEEE RTS 79	**Method**	**DC OPF**	**-**	**-**	**DC OPF**	**-**
	Lines 12, 13	0.00	-	-	0.00	0.0
	Lines 1, 4, 10	41.00	-	-	41.00	0.0
	Lines 1, 8, 10	115.00	-	-	115.00	0.0
	Lines 7, 19, 29	0.00	-	-	0.00	0.0
	Lines 7, 23, 29	165.00	-	-	165.00	0.0
	Lines 25, 26, 28	212.00	-	-	212.00	0.0
	Lines 29, 36, 37	309.00	-	-	309.00	0.0

IV.3. Benchmarking

This thesis utilizes the test systems defined in IV.1 with specified standard parameters (e.g. generation capacity, load capacity, line capacity, failure rates and repair times of the components) to perform power system reliability assessment. Metrics such as EENS and

EDL, their standard deviation and coefficient of variation establish the precision and accuracy of the MCS. While not the primary focus of this investigation, metrics related to parallel computing performance, like execution time, relative speedup, and efficiency, offer important insights into scalability. These measures can be influenced by the size of the problem and the number of CPUs employed. Still, this study refrains from using simulation time as a benchmark due to inconsistent simulation conditions across different comparative studies. More broadly, past benchmarks have used a variety of programming languages, hardware, methodologies, solvers, and computational strategies. It is common for these benchmarks to include custom code, unique starting conditions, and deliberate contingency screening to optimize the number of OPF simulations.

For RBTS, the results from CompositeSystems were validated against DC and AC-based models from references [43], [44], [45], [46], [47], [48] (see Table 2). Throughout various computing scenarios, the adequacy indices were consistent. Specifically, the DC-Based model displayed minor discrepancies of 0.2% for EENS and 0.3% for EDLC when compared to benchmarks using the same number of replications (see Table 2 and Table 6 – Appendix D). As anticipated, the LPAC model (fast decoupled AC model) yielded more optimistic adequacy indices compared to the full AC model referenced in [43], [46].

For the IEEE-RTS 79, CompositeSystems was validated using DC-based and AC-based models as referenced in [43], [44], [49], [45], [50], [51], [47], [53], [52] (see Table 3). The estimator accuracy matched benchmarks, and its standard deviation of the mean estimate and coefficient of variation were on par with other DC-based studies. Additionally, bus-specific results maintained consistent accuracy.

Table 2: System EENS and EDLC Indices of RBTS: DC-based vs. AC-based Methods.

Reference	Year	MCS	Repli-cations	EENS	$\mathbf{Diff_{EENS}}$	$\boldsymbol{SD_{error}}$	$\boldsymbol{CV_{EENS}}$	EDLC	$\mathbf{Diff_{EENS}}$	$\boldsymbol{SD_{error}}$	$\boldsymbol{CV_{EDLC}}$	CPU simulation time
				MWh/y	%	MWh/y	%	hours/y	%	hours/y	%	min
						DC-Based						
CompositeSystems	-	Seq.	15000	132.512	-	1.454	1.1%	11.116	-	0.117	1.1%	16.5
Laengen [43]	2018	Seq.	15000	132.221	0.2%	1.507	1.1%	11.081	0.3%	0.121	1.1%	20.3
CompositeSystems	-	Seq.	7500	133.655	0.9%	2.060	1.5%	11.240	1.1%	0.167	1.5%	35.6
Skjævesland [44]	2021	Seq.	7500	131.952	0.4%	2.105	1.6%	11.054	0.6%	0.169	1.5%	-
Geng [45]	2018	Seq.	-	135.240	2.0%	2.705	2.0%	11.300	1.6%	-	-	36.7
Lei [48]	2017	Seq.	300	144.901	8.9%	-	3.4%	11.562	3.9%	-	-	8.4
Skjævesland [44]	2021	Non-Seq.	1000	132.495	0.0%	1.308	1.0%	11.098	0.2%	0.103	0.9%	-
Bo Hu [47]	2023	Non-Seq.	-	134.550	1.5%	-	-	11.738	5.4%	-	-	-
						AC-Based						
CompositeSystems	-	Seq.	15000	139.555	-	1.490	1.1%	12.081	-	0.120	1.0%	476.7
Laengen [43]	2018	Seq.	15000	141.546	1.4%	1.551	1.1%	12.478	3.2%	0.125	1.0%	228.0
Hou [46]	2016	Seq.	10000	141.700	1.5%	1.899	1.3%	12.483	3.3%	-	-	10753.9
Laengen [43]	2018	Non-Seq.	500	143.409	2.7%	2.028	1.4%	12.564	3.9%	0.162	1.3%	37.3

Table 3: System EENS and EDLC Indices of IEEE-RTS 79: DC-based vs. AC-based Methods.

Source	Year	MCS	Repli-cations	EENS	$\mathbf{Diff_{EENS}}$	$\boldsymbol{SD_{error}}$	$\boldsymbol{CV_{EENS}}$	EDLC	$\mathbf{Diff_{EENS}}$	$\boldsymbol{SD_{error}}$	$\boldsymbol{CV_{EDLC}}$	CPU sim. time
				MWh/y	%	MWh/y	%	hours/y	%	hours/y	%	min
						DC-Based						
CompositeSystems	-	Seq.	15000	1416.224	-	23.910	1.7%	12.614	-	0.146	1.2%	471.9
Laengen [43]	2018	Seq.	15000	1400.112	1.1%	24.228	1.7%	12.284	2.6%	0.146	1.2%	24.2
CompositeSystems	-	Seq.	7500	1413.336	-	34.355	2.4%	12.558	-	0.207	1.6%	270.4
Skjævesland [44]	2021	Seq.	7500	1412.676	0.3%	35.710	2.5%	12.370	2.0%	0.212	1.7%	-
Magalhaes [49]	2012	Seq.	-	1370.430	3.3%	68.522	5.0%	10.733	16.1%	-	-	1050.0
Geng [45]	2018	Seq.	-	1341.160	5.4%	53.646	4.0%	10.775	15.7%	-	-	151.7
Cervan [53]	2023	Seq.	-	1349.000	4.9%	40.470	3.0%	10.696	-	-	-	180.7
Peng [50]	2019	Seq.	100	1315.290	7.4%	-	-	10.687	16.5%	-	-	-
Amarasinghe [51]	2022	Seq.	500	1490.000	5.1%	-	-	12.590	0.2%	-	-	440.2
Bo Hu [47]	2021	Non-Seq.	-	1295.980	8.9%	-	-	10.775	15.7%	-	-	-
Skjævesland [44]	2021	Non-Seq.	1000	1410.738	0.4%	17.182	1.2%	12.324	2.3%	0.111	0.9%	-
Laengen [43]	2018	Non-Seq.	500	1412.011	0.3%	24.018	1.7%	12.400	1.7%	0.149	1.2%	5.2
						AC-Based						
CompositeSystems	-	Seq.	15000	1672.639	-	26.665	1.6%	15.011	-	0.162	1.1%	5841.9
Laengen [43]	2018	Seq.	15000	1695.676	1.4%	26.146	1.5%	18.025	18.2%	0.181	1.0%	5330.2
MECORE [52]	2011	Non-Seq.	-	1593.130	4.9%	-	-	-	-	-	-	-
Laengen [43]	2018	Non-Seq.	500	1755.994	4.9%	26.550	1.5%	18.45	20.6%	0.193	1.0%	523.6

Table 7 (Appendix D) highlights a discrepancy at bus 6 for AC-Based results, linked to the shunt device. This can be attributed to differences in the implementation of contingency policies between tools. In this study, shunt devices adjust based on voltage constraints at each time step, resulting in more optimistic outcomes during emergencies compared to findings in [43]. Finally, AC-Based results show that bus 7 has a significant annual curtailed load (EENS) of 243.3 MWh/year but a brief shortfall of 4.9 hours/year. In contrast, bus 14, with an EENS of 305.4 MWh/year, has a shortfall spanning 8.1 hours/year. This information suggests strategies for mitigating energy shortfalls, such as resource deployment, load management adjustments, or investments in additional infrastructure.

The optimization framework effectively handles most network splits or islands. For instance, an outage between buses 7 and 8 could lead to isolation at bus 7, but an optimal power delivery solution can still be found. Excluding smaller islands may yield higher load losses. These discrepancies illustrate that replicating results across test systems can be complex due to diverse approaches to load curtailment, contingency methods, and interventions.

Probabilistic methods grounded in MCS techniques have emerged as effective tools for assessing the long-term adequacy of power systems. However, the computational demands and the intricate nature of CSR evaluations have made it challenging to integrate power flow-based optimizations into transmission planning. This open-source toolbox offers a foundational approach for CSR evaluations with the flexibility to integrate different perspectives on load curtailment policies, power flow methodologies, and adopt a modeling language versatile enough to accommodate various formulations and tackle a wide range

of problem classes. Furthermore, CompositeSystems provides an AC-Based formulation compatible with linear and quadratic programming solvers, such as Gurobi™.

IV.4. Energy Storage Model and Dispatch

The mathematical model of the storage component was introduced in subchapter III.2, encompassing data or parameters, variables, and equations. For simplicity, several parameters were not specified for the case studies, such as:

$S_i^{loss} = 0$: No complex power losses, in p.u.

$Z_{s,i} = 0$: No storage's internal injection impedance.

$\eta_i^c, \eta_i^d = 1$: Perfect charge and discharge efficiencies.

$q_i^{min} = 0.5 \cdot sd_i$: Reactive power injection lower limit equals 50% storage's discharging power.

$q_i^{max} = 0.5 \cdot sd_i$: Reactive power injection upper limit equals 50% storage's discharging power.

The battery energy storage model (BESS) implemented in this thesis is structured with simple charge/discharge dynamics, co-located with load and/or generation buses. The BESS model can be readily modified represent other types of energy storage and provide additional services. When not accounting for battery aging, the SOC or SOE of the component is determined by its operating efficiency and the charge/discharge level at each time step. However, estimating the State of Health (SOH) parameter leads to a more precise approximation of the SOE, as dynamic recalibration on the maximum charge/discharge level is performed. In this study, the SOH is assumed to be constant at 100%, hence degradation is not considered in the model.

Appendix E provided detailed information regarding the integration and testing of the BESS within the optimization problem discussed in Chapter III. The testing involved various scenarios on the 6-bus RBTS, including simulated transmission outages lasting four hours. The BESS data and the results for each scenario were outlined, demonstrating the effectiveness of the storage model in mitigating load curtailment, and managing system constraints under different conditions.

IV.5. Energy Storage As A Transmission Asset

In resource adequacy applications, the concept of ELCC defines the capacity value as the extra load that can be introduced to the system once the plant is integrated without compromising a chosen reliability index. This involves a probabilistically derived capacity value calculation, as it measures increments of reliability risk due to the addition of constant load in multiple steps following system changes, such as unit additions, which reduce the risk from the base system to an augmented system. The goal is to quantify the reliability value of the system changes in terms of additional constant load that the augmented system can sustain. The appropriate load amount in each step is determined using a root-finding numerical method. Furthermore, various options exist to allocate the additional load to each node, region, or bus, depending on the specific analysis goals.

This research implements an ELCC calculation using the Newton-Raphson (N-R) numerical root-finding method, which is suited for the exponential nature of reliability curves and provides fast convergence without further code development. This method aims to determine the ELCC value within a specified convergence tolerance relative to a target risk level. The initial step involves identifying endpoints and assessing the slope of the

local tangent line at these points. The x-intercept of this tangent line refines the root estimate, aligning it with the modified system's target reliability metric. Subsequent steps include increasing the load and conducting a CSR assessment, then comparing the resulting reliability metric to the initial target risk level. If the target is not met, the x-intercept is recalculated based on the revised tangent line's slope.

The algorithm requires the following inputs: maximum load capacity to be added, the tolerance level for convergence, a probability value specifying the statistical significance threshold, a vector containing pairs of load buses and their respective load values, the original system and the modified system models, and the target metric for the iterative process. The function terminates under these conditions: 1) when the gap between the upper and lower bound metrics becomes statistically insignificant, or 2) when approximations converge, indicated by only marginal differences in successive iterations.

When sizing energy storage in terms of power (PR) and energy capacity (ER) during a CSR assessment, executing multiple MCS for various capacity combinations is necessary. The ultimate objective is to identify a PR/ER combination that matches the additional load-carrying capability of a traditional solution. While there are multiple ESS sizes capable of reducing the risk of load loss to acceptable levels, these can be categorized and chosen based on maximum capacity value, EENS reduction, or unreliability costs. It is essential to determine the appropriate storage duration needed to mitigate criteria violations for single and multiple contingencies, considering a range of outage durations and loads using CSR assessment.

The process to compute an optimal storage size based on equivalent transmission capability involves the following steps:

1. **Determining Reliability Levels**: Conduct adequacy studies on both the base system, which has identified reliability needs, and the augmented system. The augmented system aims for a lower risk level and includes modifications that mitigate the reliability needs, such as a new transmission asset.
2. **Determining the ELCC Target (online process)**: Use the ELCC algorithm (N-R method) to determine the ELCC target value for the augmented system with the proposed modification. The SI value from the base system is used as the risk target.
3. **Sizing Energy Storage Systems (offline process)**: Perform adequacy studies on various SATA PR/ER combinations within the base system. The goal is to establish an ESS threshold zone where the SI value aligns with the desired SI value of the final augmented system (step 1).
4. **Identifying the Optimal Size (online process)**: Apply the N-R algorithm to determine the Equivalent Transmission Capability (ETC) of the SATA solution, using the safe PR/ER range established in the previous step. For a specific PR value and an ER range within the set tolerance, the algorithm identifies the optimal ER value. This value should equate the SI or EENS value of the base system (before SATA mitigation) with the additional load (ELCC). After finding an optimal ER value for a PR value selected, the process will continue with various PR values within the ESS threshold zone.

The resulting SATA solutions are compared using additional metrics to identify the most optimal one. Figure 10 illustrates those four steps using a base and augmented system (with a conventional solution or SATA), where step 2 is the “ELCC algorithm”, step 3 is the “ESS Threshold zone”, and step 4 is the “ETC algorithm”. The number of

iterations required depends on how closely the PR value and ER range approach the optimal solution. Storage PRs regulate the maximum charging or discharging power based on the remaining energy or capacity of the storage system, constrained by its ER. These resources are utilized to reduce load loss during the simulation, discharging when necessary and charging during periods of power surplus at their connected bus. The current model does not incorporate coordination techniques such as the 'time-to-go' priority or cross-charging avoidance strategies referenced in [22].

IV.6. Application Studies

This study uses the IEEE-RTS 79 reliability test system [58] as the augmented system (RTS-79). Notably, RTS-79's robust connectivity and high ratings result in underused transmission lines, which in combination with a uniform load profile across buses present limitations for demonstrating in-depth composite reliability studies, particularly in capturing the nuanced behavior of individual bus loads. To address the limitations of RTS 79 and provide a more dynamic and realistic analysis platform, the study introduces a modified version, termed the MRTS 79 or base system. This modification involves adjusting the transfer capabilities of specific lines, namely (7,8), (8,9), and (8,10), which are selected due to their highest average utilization in the CSR studies performed for this system. This adaptation is designed to enrich the overall system behavior, making it more reflective of real-world complexities. By reducing the ratings of these key branches, the base system (MRTS 79) amplifies their impact on essential metrics like EENS, EDLC, and SI, as shown in Table 4 and Figure 11, considering 2000 replications for each assessment.

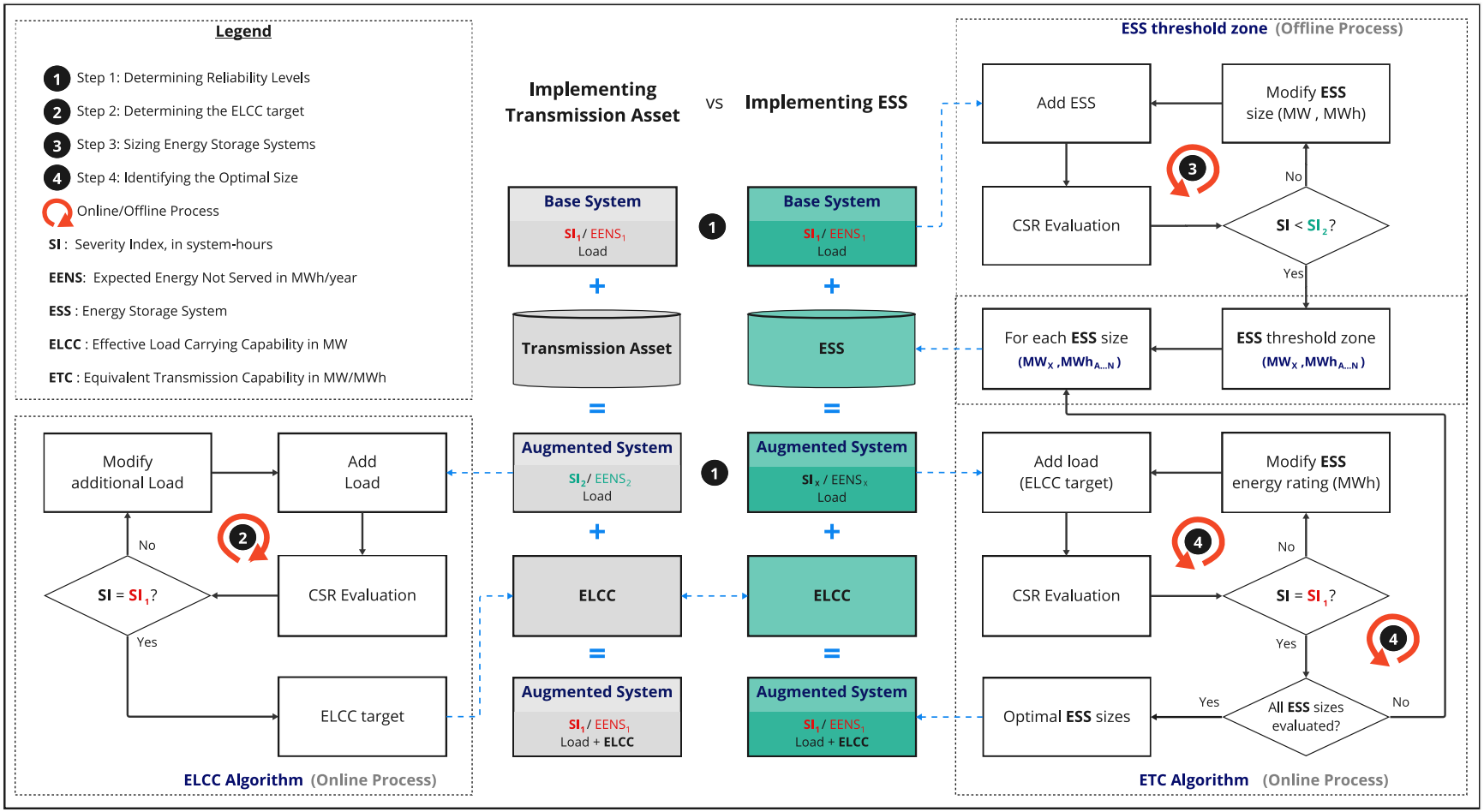

Figure 10: Equivalent Transmission Capability procedure of energy storage using CSR Assessment.

Table 4: System and branch results for the base system (Case 1 and Case 2) and the augmented system (with traditional transmission asset).

System	Index	Unit	DC-Based	AC-Based	Diff (%)
			Mean	Mean	
Base System - Case 1 (-25%)	**ELCC**	**MW**	**36.0**	**35.0**	**-2.9**
	System EENS	MWh/y	1831.9	2138.9	14.3
	System EDLC	hrs/y	15.9	18.4	13.7
	SI	Sys-hrs	38.6	45.0	14.4
	Util. L(7,8)	%	53.3	43.0	-24.0
	Util. L(8,9)	%	66.3	20.6	-221.9
	Util. L(8,10)	%	55.6	14.5	-283.2
Base System - Case 2 (-50%)	**ELCC**	**MW**	**81.0**	**79.0**	**-2.5**
	System EENS	MWh/y	2445.5	2841.2	13.9
	System EDLC	hrs/y	20.6	23.5	12.4
	SI	Sys-hrs	51.5	59.8	13.9
	Util. L(7,8)	%	57.9	49.5	-17.0
	Util. L(8,9)	%	89.8	37.3	-140.5
	Util. L(8,10)	%	74.2	28.0	-165.1
Augmented System (Trans. Asset)	System EENS	MWh/y	1442.0	1693.9	14.9
	System EDLC	hrs/y	12.8	15.0	14.4
	SI	Sys-hrs	30.4	35.7	14.9
	Util. L(7,8)	%	43.2	40.5	-6.5
	Util. L(8,9)	%	46.5	12.2	-282.1
	Util. L(8,10)	%	39.4	7.8	-405.6

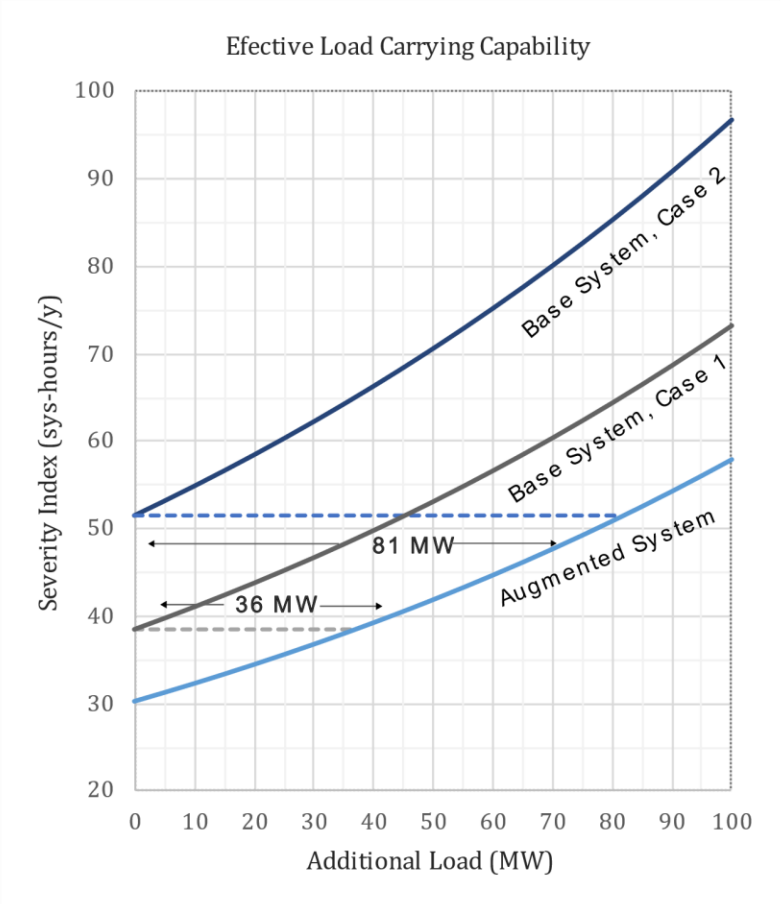

Figure 11: Annual adequacy risk before and after decreasing transfer capability on transmission lines of the RTS 79 test system, DC-Based approach.

During emergency system states, this study considers a prioritized load curtailment policy using a weighting factor, w_i, to each delivery point, prioritizing important buses. Additionally, during split network situations, certain isolated PV buses are disconnected, such as bus 7, to prevent load losses during supply-demand mismatches or thermal overloads due to inactive connecting branches. Finally, SATA's efficiency and availability are assumed to be perfect, with no consideration of ESS losses.

A. System Indices

Results from both DC and AC-based methods were analyzed for the augmented system with a traditional solution (IEEE-RTS 79) against the base system (MRTS 79). This analysis included a decrease of 25% (base system, Case 1) and 50% (base system, Case 2) in the thermal rating (transmission capacity) of the three transmission lines. The effects on carrying capability were consistent across both cases (see Figure 11, DC-Based approach), with uniform variations observed in system risk indices. However, the expected loss of load was higher when applying an AC-Based formulation (see Table 4).

The capacity benefit, defined as the additional load-carrying capability of a traditional solution that transitions the base system - Case 1 to the augmented system by adding 44 MW of transfer capability to the three most utilized transmission lines, was calculated to be 36 MW using the DC-based method and 35 MW using the AC-based method. For moving from the base system - Case 2 to the augmented system, the required capacity benefits were 81 MW and 79 MW for the DC and AC-based methods, respectively. Therefore, a slightly higher benefit is observed when transitioning from the higher-risk Case 2, which may be attributed to the congestion effect of those transmission lines (see Table 4).

Figure 12 and Figure 13 display the annual system EENS and EDLC outcomes (DC-Based approach) with SATA at bus 8, varying by power and energy storage capacities. SATA's efficiency and availability are assumed to be perfect throughout. Any ESS losses are not factored in. As detailed in [24], increasing storage capacity generally improves network adequacy. However, adding storage beyond a point sees reduced benefits, evident in the EENS reductions past the 25 MW to 75 MW power capacity. This pattern aligns with the

findings in [8], where adding large generators to a system mostly consisting of smaller units offers proportionally less added load capacity than introducing similarly-sized units in a system of the same capacity.

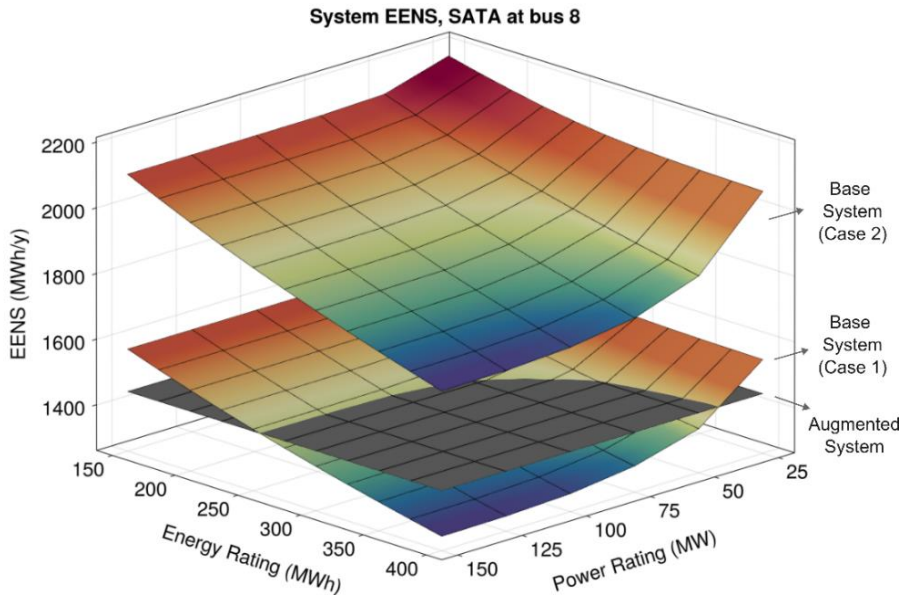

Figure 12: System EENS adding SATA at bus 8 for different power and energy ratings. Augmented system, Case 1.

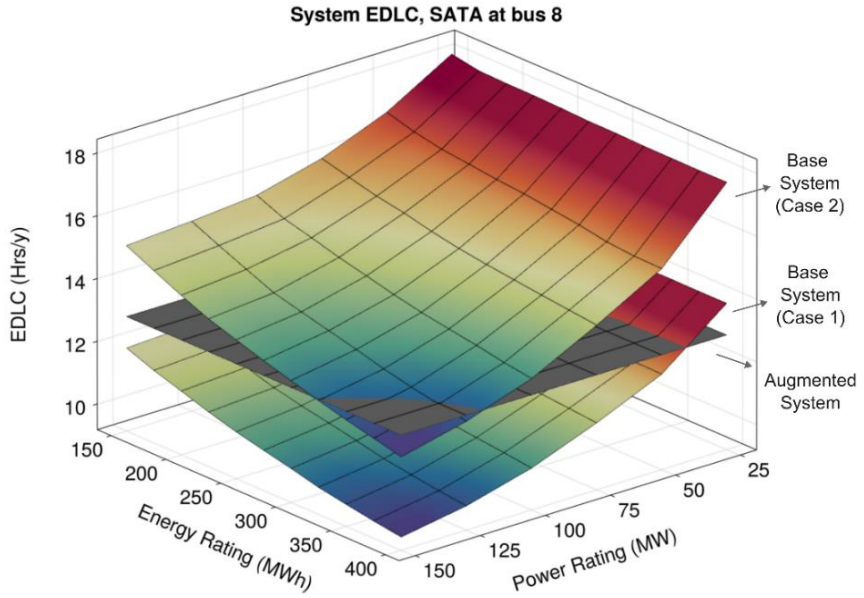

Figure 13: System EDLC adding SATA at bus 8 for different power and energy ratings. Augmented system, Case 1.

By adding (PR, ER) = (75, 275) MW/MWh or higher size storage system at bus 8 in the base system - Case 1, the annual system's EENS closely aligned with the results from the desired augmented system. However, the actual load curtailment, measured in MWh/year, was significantly higher than predicted by the EDLC index. Reducing the transfer capability of the three transmission lines by 50% (base system, Case 2) made it impossible to find a suitable storage size using the EENS index.

In Case 2, where the transfer capability was reduced by 50% in the base system, identifying a suitable storage size using the EENS index became impossible. Observations of Figure 14 and Figure 15 demonstrate that both increased transfer capability and integration of energy storage solutions tend to reduce the risk of shortfall at bus 9 (the lowest priority) during peak hours. Both the base system (Cases 1 and 2) and the augmented system (with increased transfer capability) exhibit the same profile. However, while adding SATA (PR, ER) = (75, 260) MW/MWh at bus 8 matches the reliability level of the augmented system with a traditional solution (increased transfer capability) for Case 1, there is a slightly different profile for which charging hours between 13:00 and 16:00 show higher risk. In Case 2, where the augmented system implements SATA, there is a much higher risk during charging and discharging hours (system peak hours). Consequently, the single SATA implemented at bus 8 is insufficient to mitigate the capacity deficiencies observed in the base system (Case 2). This inadequacy may stem from factors beyond the size of the storage system, possibly involving a combination of location and size. Nevertheless, employing the largest storage units effectively reduced the average failure hours (see Figure 13) bringing them in line with the augmented system levels, as indicated by the EDLC.

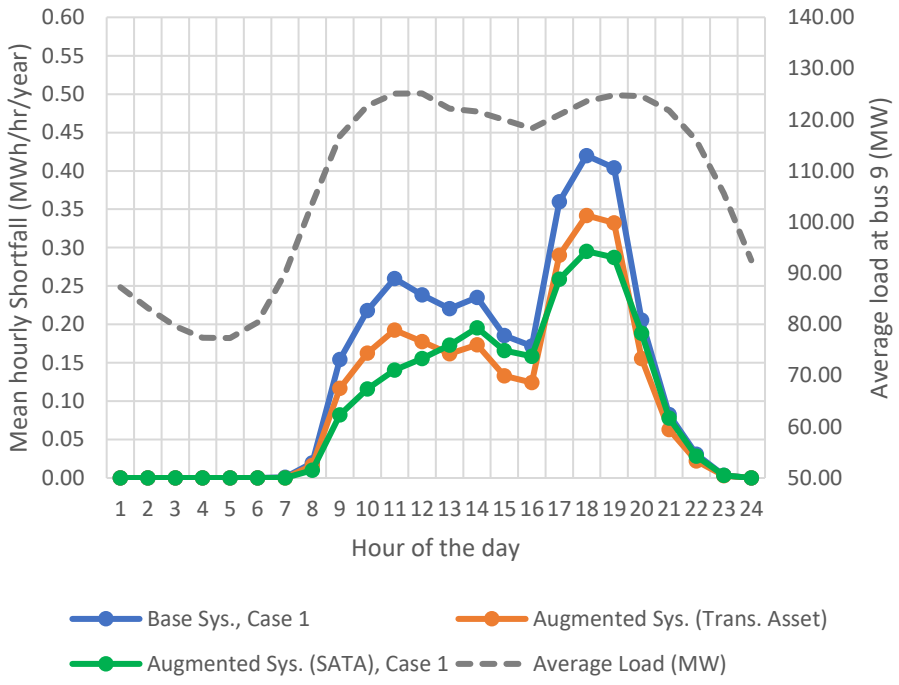

Figure 14: Hourly EENS variation at bus 9, Case 1.

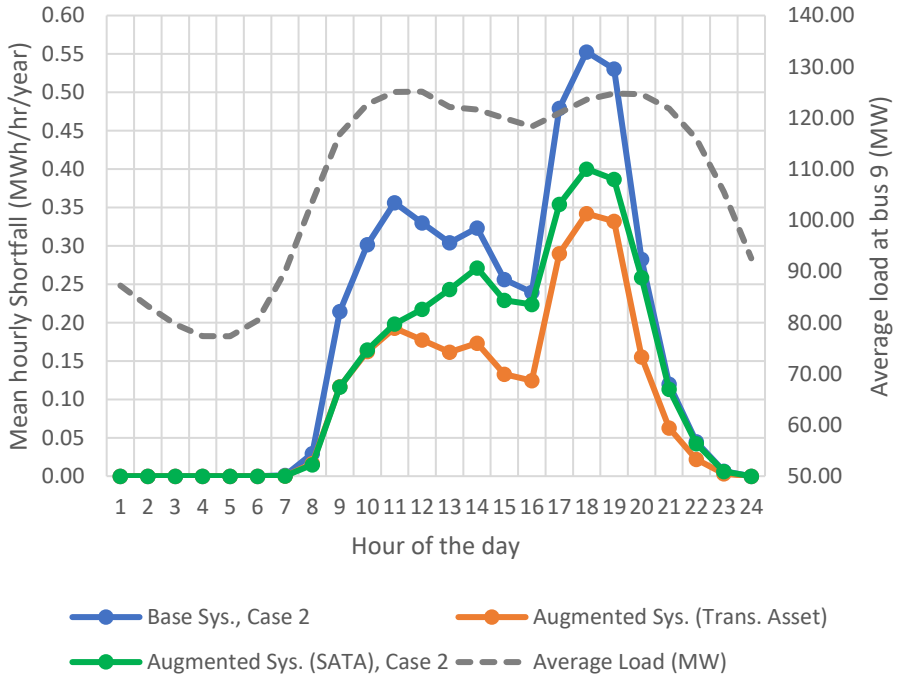

Figure 15: Hourly EENS variation at bus 9, Case 2.

B. Expected Load-Carrying Capability

The ELCC metric for the base system - Case 1 is estimated using the Newton-Raphson algorithm and the DC-based method. This estimation aims to identify the optimal size of a storage device that offers the same reliability benefits as a traditional solution, such as increasing transfer capability by 25% (from the base system – Case 1 to the augmented system). Figure 16, Figure 25 and Figure 17 illustrate the ELCC results, which are influenced by varying power and energy ratings. These results were derived using the algorithm described in the previous chapter and the CSR evaluation tool.

As seen in Figure 16, increasing the energy ratings of SATA units increases the load-carrying capability at different rates depending on the power rating, and allows them to function longer during high-load states and/or in situations with single and multiple outages, thereby avoiding potential loss of load. Any storage PR/ER combination that provides a load-carrying capability equal to or greater than 36 MW (the ELCC target) can be considered a viable alternative to traditional solutions.

Figure 25 (Appendix H) depicts the reliability curves for the base system - Case 1 + energy storage device at bus 8 (new augmented system) with a power rating of 150 MW and various energy rating values, alongside both base system - Case 1 (red curve) and augmented system with traditional solution (green curve). These curves follow an exponential trend, illustrating how the system’s risk escalates annually in response to changes in load. The system's topology and resource alterations may significantly affect the additional load capacity. Some of the values were derived using the N-R method for ELCC, with the discontinuous lines on the graph representing interpolations that provide the best fit for these data points.

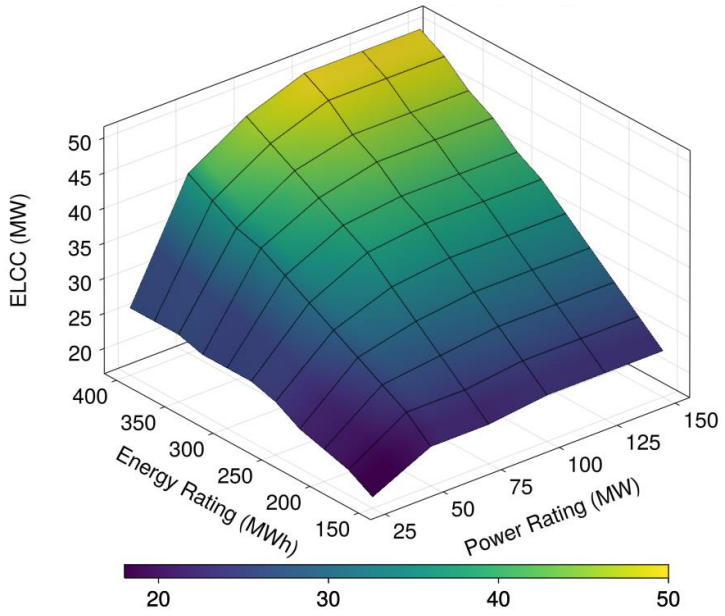

Figure 16: ELCC for SATA at bus 8, for different power and energy ratings, for the augmented system, Case 1.

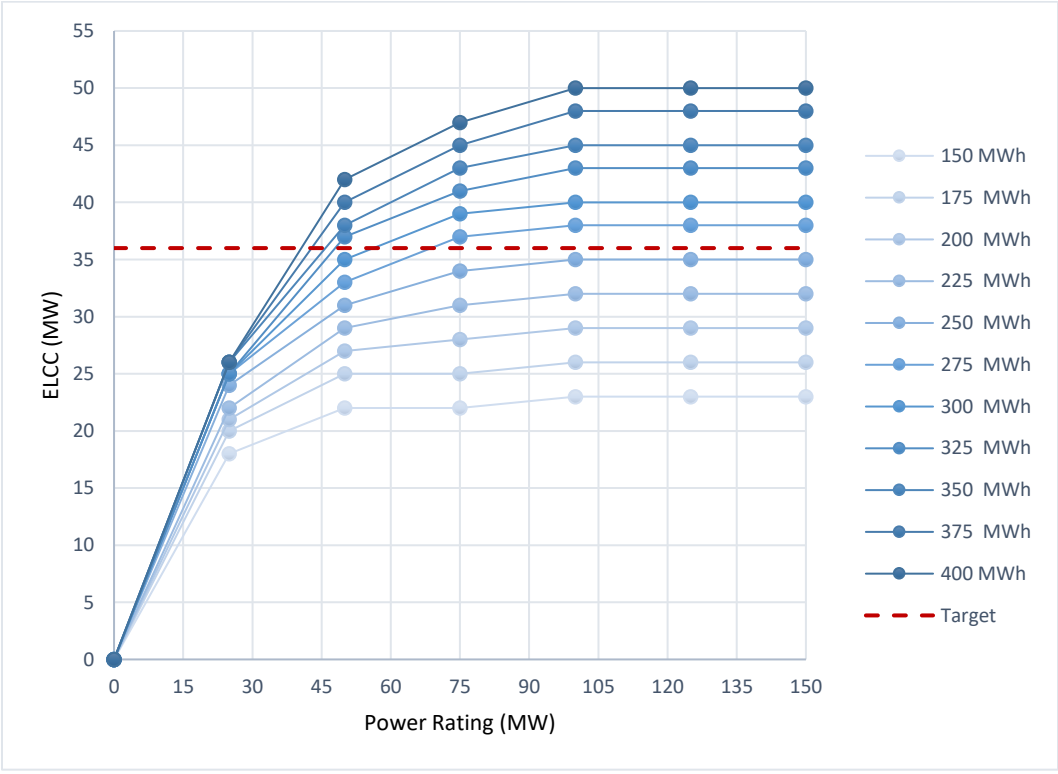

Figure 17: ELCC curves for different SATA energy and power ratings. Augmented system, Case 1.

Table 5: Optimal energy rating at a tol=0.001 for a target metric of 38.3 min/y and ELCC of 36 MW. Augmented system, Case 1.

PR	QR	DC-Based				AC-Based			
		ER	Dur	SI	EENS	ER	Dur	SI	EENS
MW	MVAR	MWh	Hrs	Sys-hrs	MWh/y	MWh	Hrs	sys-hrs	MWh/y
50	±25.0	319	6.4	38.3	1844.0	306	6.1	44.8	2154.8
75	±37.5	271	3.6	38.3	1844.5	261	3.5	44.8	2154.6
100	±50.0	260	2.6	38.4	1845.0	250	2.5	44.8	2155.5
125	±62.5	259	2.1	38.3	1844.0	249	2.0	44.8	2155.2
150	±75.0	258	1.7	38.3	1844.5	249	1.7	44.8	2154.3

Applying the N-R method to determine the ETC for specific power ratings of storage systems results in optimal energy storage sizes ranging from 319 to 258 MWh for the DC-Based technique and from 306 to 249 MWh for the AC-Based technique. These ranges correspond to power ratings between 75 MW and 150 MW, as detailed in Table 5, and were achieved after three or more iterations. This translates to storage durations between 1.7 and 6.4 hours, varying according to the power rating. Additional transmission planning security studies could identify the storage sizes capable of addressing critical contingencies in line with established security standards. The AC-Based formulation revealed no significant differences compared to the DC-Based approach, except for a minor duration reduction of 0.3 hours for a 50 MW, ±25 MVAR storage system.

For the base system - Case 2 needing 81 MW capacity, no single unit less than 400 MWh could support this capacity increase in load at the current risk level, necessitating additional unit modeling.

V. Conclusions and Future Work

V.1. Conclusions

This thesis examined the sequential MCS method using DC and linearized AC-Based mathematical optimization approaches to evaluate overall power system risk. The sequential MCS method offers greater flexibility in incorporating complex operating conditions and diverse system considerations, such as chronology, load uncertainty, renewable energy uncertainty, weather-related conditions, and energy storage operating conditions. Effort was invested to develop a complete CSR tool using a high-level, general-purpose dynamic programming language (i.e. Julia™) to overcome historical barriers in the CSR field in terms of computational capacity and replicability. To the author's knowledge, no alternative open-source, research-grade tools are available to perform these types of probabilistic studies, with the flexibility of including a powerful and high-performance external solver, and parallel programming capability to run large-scale projects on high-performance computing clusters.

Energy storage presents both opportunities and challenges as an alternative to traditional power solutions when integrated as a composite resource and transmission asset. It has been demonstrated through this thesis that it is feasible to calculate an equivalent transmission capacity of energy storage that aligns with traditional transmission alternatives, leading to the identification of various optimal power and energy ratings for SATA systems. Nevertheless, the ultimate decision to incorporate SATA should be informed by both security and economic analyses. Oversized systems may not fully exploit their capacity value, potentially resulting in the saturation of the ELCC. CSR assessments

are instrumental in assessing the impact of energy storage on generation and transmission systems.

Utilizing SATA has been proven to significantly improve network adequacy. Although increasing the capacity of energy storage typically enhances system reliability, this benefit tends to plateau beyond a certain point. The impact of changes in the energy capacity of SATA parallels the effects observed from altering the forced outage rates of generating units. Consequently, precise sizing and strategic positioning of SATA are crucial given the complex nature of the bulk transmission system.

The selection of the commercial solver Gurobi™ was based on an evaluation of various research-grade solvers such as IPOPT™, Juniper™, and Highs™. Performance issues, including those related to single-thread mode and excessive memory usage, were identified during this evaluation. Despite common performance pitfalls encountered when using external solvers with the JuMP modeling language, Gurobi™ demonstrated reliable performance when coding optimization problems according to best practices and performance tips [61].

V.2. Future Work

While this thesis has made important contributions, it is essential to acknowledge its limitations and explore various pathways for future research.

a) Enhancing the proposed methodology

Extreme weather has the potential to affect the availability of all resource types, as well as the nature of demand. To better account for the impact of these weather-related events, CSR assessment should include modeling correlated grid asset outages and utilize metrics

that highlight the outsized impact of weather events. Additionally, it is essential to verify the exponential relationship between system load increases and reliability levels in transmission systems.

The proposed methodology should also incorporate overall economic analysis based on a risk cost assessment. This approach allows for comparing investment costs with statistical results such as the EENS index. The optimal alternative should aim to minimize total costs, considering the effects of load curtailment policies due to firm and interruptible loads, if applicable.

b) Exploring Novel Case Studies

Further exploration of novel case studies can offer valuable insights into real-world applications of CSR evaluation. Although the selection of test systems in this thesis was carefully considered to address the lack of replicable results in CSR, placing BESSes on different buses yielded similar outcomes, ultimately leading to the selection of bus 8 in the IEEE RTS 79. However, a more extensive analysis of the location effects of storage systems using different transmission systems must be considered. Additionally, sensitivity analyses should be conducted to estimate the impact of power losses and battery degradation on its estimated reliability contribution during CSR assessments.

Future studies should consider incorporating the IEEE-RTS GMLC to assess CSR and the proposed framework. The IEEE-RTS GMLC provides an appropriate time-series dataset and modifications to model generation uncertainty, load uncertainty and variability, additional asset specifications, and operational constraints. The test system adequately reflects the complexity of challenges typically encountered in a modern power system.

C) Additional work

An important barrier encountered when developing CompositeSystems was the use of random number generators, which posed challenges when sampling states for a certain number of components in the 24-bus test system, leading to the decision of not sampling energy storage's forced outages. Strategies to mitigate this issue include setting random number master seeds per component type and using more stable random number generator packages.

Beyond the scope of this thesis, several factors merit further investigation. These include load variability, load uncertainty, generation uncertainty, improvements in simulation time, calculation of frequency indices, statistical probability distributions of indices, variance reduction techniques, maintenance of generating units, and more suitable constrained transmission systems as test systems. Additionally, considerations such as energy storage's power losses, derated generators, and dependent outages should be explored, among other features that could influence the results of CSR studies.

Bibliography

[1] EPRI, “Development of a Composite System Reliability Evaluation Program, Volumes 1-4: Volumes 1-4,” EPRI, Technical Report EL-6926-V1. [Online]. Available: https://www.epri.com/research/products/EL-6926-V1

[2] W. Li, *Probabilistic Transmission System Planning*. Wiley-IEEE Press, 2011. [Online]. Available: https://ieeexplore.ieee.org/book/5732783

[3] G. Calabrese, “Generating Reserve Capacity Determined by the Probability Method,” *Transactions of the American Institute of Electrical Engineers*, vol. 66, no. 1, pp. 1439–1450, Jan. 1947, doi: 10.1109/T-AIEE.1947.5059596.

[4] C. W. Watchorn, “The Determination and Allocation of the Capacity Benefits Resulting from Interconnecting Two or More Generating Systems,” *Transactions of the American Institute of Electrical Engineers*, vol. 69, no. 2, pp. 1180–1186, Jan. 1950, doi: 10.1109/T-AIEE.1950.5060277.

[5] Z. G. Todd, “A Probability Method for Transmission and Distribution Outage Calculations,” *IEEE Transactions on Power Apparatus and Systems*, vol. 83, no. 7, pp. 695–701, Jul. 1964, doi: 10.1109/TPAS.1964.4766062.

[6] R. Billinton, “Composite System Reliability Evaluation,” *IEEE Transactions on Power Apparatus and Systems*, vol. PAS-88, no. 4, pp. 276–281, Apr. 1969, doi: 10.1109/TPAS.1969.292425.

[7] R. Billinton and R. N. Allan, *Reliability Evaluation of Engineering Systems: Concepts and Techniques*, Second edition. New York, U.S.: Springer, Boston, MA, 1992.

[8] R. Billinton and R. N. Allan, *Reliability Evaluation of Power Systems*, Second edition. New York, U.S.: Springer, Boston, MA, 1996.

[9] A. D. Patton, A. K. Ayoub, and C. Singh, “Power system reliability evaluation,” *International Journal of Electrical Power & Energy Systems*, vol. 1, no. 3, pp. 139–150, Oct. 1979, doi: 10.1016/0142-0615(79)90001-2.

[10] W. Li, *Risk Assessment of Power Systems: Models, Methods, and Applications*, Second. Wiley-IEEE Press, 2014. Accessed: Nov. 12, 2021. [Online]. Available: https://ieeexplore.ieee.org/book/6774612

[11] R. Billinton and K. E. Bollinger, “Transmission System Reliability Evaluation Using Markov Processes,” *IEEE Transactions on Power Apparatus and Systems*, vol. PAS-87, no. 2, pp. 538–547, Feb. 1968, doi: 10.1109/TPAS.1968.292051.

[12] R. Billinton and M. P. Bhavaraju, “Transmission Planning Using a Reliability Criterion, Part I: A Reliability Criterion,” *IEEE Transactions on Power Apparatus and Systems*, vol. PAS-89, no. 1, pp. 28–34, Jan. 1970, doi: 10.1109/TPAS.1970.292665.

[13] M. Papic and D. Logan, “Bibliography on Composite System Reliability Assessment 2000-2020,” in *2022 17th International Conference on Probabilistic Methods Applied to Power Systems (PMAPS)*, Jun. 2022, pp. 1–8. doi: 10.1109/PMAPS53380.2022.9810643.

[14] W. Lin, Z. Yang, M. Papic, D. M. Logan, and J. Yu, “A Review of Computational Tools for Composite System Reliability Analysis,” in *2022 17th International Conference on Probabilistic Methods Applied to Power Systems (PMAPS)*, Jun. 2022, pp. 1–6. doi: 10.1109/PMAPS53380.2022.9810596.

[15] “Composite Power System Reliability (TR99) | IEEE Power & Energy Society Resource Center.” Accessed: Oct. 16, 2023. [Online]. Available: https://resourcecenter.ieee-pes.org/publications/technical-reports/pes_tp_tr99_amps_102622

[16] A. C. G. Melo, G. C. Oliveira, M. Morozowski Fo, and M. V. F. Pereira, “A hybrid algorithm for Monte Carlo/enumeration based composite reliability evaluation (power systems),” in *1991 Third International Conference on Probabilistic Methods Applied to Electric Power Systems*, Jul. 1991, pp. 70–74.

[17] Billinton and W. Li, *Reliability Assessment of Electric Power Systems Using Monte Carlo Methods*. New York, NY, U.S.: Springer, 1994. Accessed: Sep. 21, 2021. [Online]. Available: http://ebookcentral.proquest.com/lib/unb/detail.action?docID=3086450

[18] R. Billinton and A. Sankarakrishnan, “A comparison of Monte Carlo simulation techniques for composite power system reliability assessment,” in *IEEE WESCANEX 95. Communications, Power, and Computing. Conference Proceedings*, May 1995, pp. 145–150 vol.1. doi: 10.1109/WESCAN.1995.493961.

[19] C. L. T. Borges, D. M. Falcao, J. C. O. Mello, and A. C. G. Melo, “Composite reliability evaluation by sequential Monte Carlo simulation on parallel and distributed processing environments,” *IEEE Transactions on Power Systems*, vol. 16, no. 2, pp. 203–209, May 2001, doi: 10.1109/59.918287.

[20] E. Ibanez and M. Milligan, “Probabilistic Approach to Quantifying the Contribution of Variable Generation and Transmission to System Reliability: Preprint,” p. 7, Sep. 2012.

[21] L. L. Garver, “Effective Load Carrying Capability of Generating Units,” *IEEE Transactions on Power Apparatus and Systems*, vol. PAS-85, no. 8, pp. 910–919, Aug. 1966, doi: 10.1109/TPAS.1966.291652.

[22] G. Stephen, “Probabilistic Resource Adequacy Suite (PRAS) v0.6 Model Documentation,” NREL/TP--5C00-79698, 1785462, MainId:35919, May 2021. doi: 10.2172/1785462.

[23] L. Soder and M. Amelin, “A review of different methodologies used for calculation of wind power capacity credit,” in *2008 IEEE Power and Energy Society General Meeting - Conversion and Delivery of Electrical Energy in the 21st Century*, Jul. 2008, pp. 1–5. doi: 10.1109/PES.2008.4596666.

[24] M. K. Metwaly and J. Teh, “Probabilistic Peak Demand Matching by Battery Energy Storage Alongside Dynamic Thermal Ratings and Demand Response for Enhanced Network Reliability,” *IEEE Access*, vol. 8, pp. 181547–181559, 2020, doi: 10.1109/ACCESS.2020.3024846.

[25] I. Konstantelos and G. Strbac, “Capacity value of energy storage in distribution networks,” *Journal of Energy Storage*, vol. 18, pp. 389–401, Aug. 2018, doi: 10.1016/j.est.2018.06.002.

[26] R. Sioshansi *et al.*, “Energy-Storage Modeling: State-of-the-Art and Future Research Directions,” *IEEE Transactions on Power Systems*, vol. 37, no. 2, pp. 860–875, Mar. 2022, doi: 10.1109/TPWRS.2021.3104768.

[27] Bagen and R. Billinton, “Impacts of energy storage on power system reliability performance,” in *Canadian Conference on Electrical and Computer Engineering, 2005.*, May 2005, pp. 494–497. doi: 10.1109/CCECE.2005.1556978.

[28] R. Billinton and Bagen, “Reliability Considerations in the Utilization of Wind Energy, Solar Energy and Energy Storage in Electric Power Systems,” in *2006 International Conference on Probabilistic Methods Applied to Power Systems*, Jun. 2006, pp. 1–6. doi: 10.1109/PMAPS.2006.360204.

[29] G. Prashanti and C. Venkaiah, “Impact of energy storage integration on composite system reliability,” in *2016 National Power Systems Conference (NPSC)*, Dec. 2016, pp. 1–6. doi: 10.1109/NPSC.2016.7858840.

[30] M. Abogaleela and K. Kopsidas, “Reliability evaluation framework incorporating energy storage systems,” in *2017 Nineteenth International Middle East Power Systems Conference (MEPCON)*, Dec. 2017, pp. 490–495. doi: 10.1109/MEPCON.2017.8301225.

[31] U.S. Federal Energy Regulatory Commission (FERC), “Policy Statement PL17-2-000: Utilization of Electric Storage Resources for Multiple Services When Receiving Cost-Based Rate Recovery.” Jan. 19, 2017.

[32] “MATPOWER – Free, open-source tools for electric power system simulation and optimization.” Accessed: Jul. 07, 2023. [Online]. Available: https://matpower.org/

[33] F. Geth, C. Coffrin, and D. M. Fobes, “A Flexible Storage Model for Power Network Optimization.” arXiv, Apr. 29, 2020. doi: 10.48550/arXiv.2004.14768.

[34] M. Lubin, O. Dowson, J. D. Garcia, J. Huchette, B. Legat, and J. P. Vielma, “JuMP 1.0: Recent improvements to a modeling language for mathematical optimization.” arXiv, Mar. 19, 2023. doi: 10.48550/arXiv.2206.03866.

[35] B. Stott, J. Jardim, and O. Alsac, “DC Power Flow Revisited,” *IEEE Transactions on Power Systems*, vol. 24, no. 3, pp. 1290–1300, Aug. 2009, doi: 10.1109/TPWRS.2009.2021235.

[36] C. Coffrin, R. Bent, K. Sundar, Y. Ng, and M. Lubin, “PowerModels. JL: An Open-Source Framework for Exploring Power Flow Formulations,” in *2018 Power Systems Computation Conference (PSCC)*, Jun. 2018, pp. 1–8. doi: 10.23919/PSCC.2018.8442948.

[37] C. Coffrin and P. V. Hentenryck, “A Linear-Programming Approximation of AC Power Flows,” *INFORMS Journal on Computing*, May 2014, doi: 10.1287/ijoc.2014.0594.

[38] “JosifFP/CompositeSystems.jl: Probabilistic Reliability Evaluation for Composite Systems,” GitHub. Accessed: Jul. 07, 2023. [Online]. Available: https://github.com/JosifFP/CompositeSystems.jl

[39] “The Leader in Decision Intelligence Technology - Gurobi Optimization.” Accessed: Jul. 07, 2023. [Online]. Available: https://www.gurobi.com/

[40] D. P. Brown and D. E. M. Sappington, “Procuring electric storage as a transmission asset,” *The Electricity Journal*, vol. 33, no. 3, p. 106711, Apr. 2020, doi: 10.1016/j.tej.2020.106711.

[41] “Storage as Transmission Asset Market Study,” OurEnergyPolicy. Accessed: Mar. 16, 2024. [Online]. Available: https://www.ourenergypolicy.org/resources/storage-as-transmission-asset-market-study/

[42] J. Arteaga, H. Zareipour, and N. Amjady, “Energy Storage as a Service: Optimal sizing for Transmission Congestion Relief,” *Applied Energy*, vol. 298, p. 117095, Sep. 2021, doi: 10.1016/j.apenergy.2021.117095.

[43] Ø. S. Laengen, “Application of Monte Carlo Simulation to Power System Adequacy Assessment,” 2018, Accessed: Apr. 19, 2022. [Online]. Available: https://ntnuopen.ntnu.no/ntnu-xmlui/handle/11250/2564804

[44] J. S. Skjævesland and J. Horpestad, “Quantifying the Impact of Integrating Wind Power on Composite Power System Reliability,” Master thesis, NTNU, 2021. Accessed: Jan. 19, 2023. [Online]. Available: https://ntnuopen.ntnu.no/ntnu-xmlui/handle/11250/2778713

[45] L. Geng, Y. Zhao, and G. Chen, “Simplified Sequential Simulation of Bulk Power System Reliability Via Chronological Probability Model of Load Supplying Capability,” *IEEE Transactions on Power Systems*, vol. 33, no. 3, pp. 2349–2358, May 2018, doi: 10.1109/TPWRS.2017.2757033.

[46] K. Hou, H. Jia, X. Xu, Z. Liu, and Y. Jiang, “A Continuous Time Markov Chain Based Sequential Analytical Approach for Composite Power System Reliability Assessment,” *IEEE Transactions on Power Systems*, vol. 31, no. 1, pp. 738–748, Jan. 2016, doi: 10.1109/TPWRS.2015.2392103.

[47] B. Hu *et al.*, “Power system reliability assessment with quantification of demand response uncertainty based on advanced sigmoid cloud model,” *CSEE Journal of Power and Energy Systems*, pp. 1–10, 2023, doi: 10.17775/CSEEJPES.2021.01500.

[48] H. Lei and C. Singh, “Non-Sequential Monte Carlo Simulation for Cyber-Induced Dependent Failures in Composite Power System Reliability Evaluation,” *IEEE Transactions on Power Systems*, vol. 32, no. 2, pp. 1064–1072, Mar. 2017, doi: 10.1109/TPWRS.2016.2572159.

[49] L. de Magalhaes Carvalho, M. A. da Rosa, A. M. Leite da Silva, and V. Miranda, “Probabilistic Analysis for Maximizing the Grid Integration of Wind Power Generation,” *IEEE Transactions on Power Systems*, vol. 27, no. 4, pp. 2323–2331, Nov. 2012, doi: 10.1109/TPWRS.2012.2207411.

[50] L. Peng, B. Hu, K. Xie, H.-M. Tai, and K. Ashenayi, “Analytical model for fast reliability evaluation of composite generation and transmission system based on sequential Monte Carlo simulation,” *International Journal of Electrical Power & Energy Systems*, vol. 109, pp. 548–557, Jul. 2019, doi: 10.1016/j.ijepes.2019.02.039.

[51] P. A. G. M. Amarasinghe, S. K. Abeygunawardane, and C. Singh, “Adequacy Evaluation of Composite Power Systems Using an Evolutionary Swarm Algorithm,” *IEEE Access*, vol. 10, pp. 19732–19741, 2022, doi: 10.1109/ACCESS.2022.3150927.

[52] G. Anders and A. Vaccaro, Eds., *Innovations in Power Systems Reliability*. in Springer Series in Reliability Engineering. London: Springer, 2011. doi: 10.1007/978-0-85729-088-5.

[53] D. Cervan, A. M. Coronado, and J. E. Luyo, “Cluster-based stratified sampling for fast reliability evaluation of composite power systems based on sequential Monte Carlo simulation,” *International Journal of Electrical Power & Energy Systems*, vol. 147, p. 108813, May 2023, doi: 10.1016/j.ijepes.2022.108813.

[54] R. Billinton *et al.*, “A Reliability Test System for Educational Purposes-Basic Data,” *IEEE Power Engineering Review*, vol. 9, no. 8, pp. 67–68, Aug. 1989, doi: 10.1109/MPER.1989.4310918.

[55] P. M. Subcommittee, “IEEE Reliability Test System,” *IEEE Transactions on Power Apparatus and Systems*, vol. PAS-98, no. 6, pp. 2047–2054, Nov. 1979, doi: 10.1109/TPAS.1979.319398.

[56] “Welcome to the Universe of Supercomputing - Digital Resources, Expertise, Support & Training,” ACENET. Accessed: Jul. 10, 2023. [Online]. Available: https://ace-net.ca/

[57] R. N. Allan, R. Billinton, and N. M. K. Abdel-Gawad, “The IEEE Reliability Test System - Extensions to and Evaluation of the Generating System,” *IEEE Transactions on Power Systems*, vol. 1, no. 4, pp. 1–7, Nov. 1986, doi: 10.1109/TPWRS.1986.4335006.

[58] C. Grigg *et al.*, “The IEEE Reliability Test System-1996. A report prepared by the Reliability Test System Task Force of the Application of Probability Methods Subcommittee,” *IEEE Transactions on Power Systems*, vol. 14, no. 3, pp. 1010–1020, Aug. 1999, doi: 10.1109/59.780914.

[59] C. Barrows *et al.*, “The IEEE Reliability Test System: A Proposed 2019 Update,” *IEEE Transactions on Power Systems*, vol. 35, no. 1, pp. 119–127, Jan. 2020, doi: 10.1109/TPWRS.2019.2925557.

[60] M. D. E. Khan, “A Security Based Approach to Composite Power System Reliability Evaluation,” Thesis, University of Saskatchewan, 1991. Accessed: Feb. 18, 2022. [Online]. Available: https://harvest.usask.ca/handle/10388/11660

[61] “jump-dev/Gurobi.jl.” JuMP-dev, Mar. 08, 2024. Accessed: Mar. 22, 2024. [Online]. Available: https://github.com/jump-dev/Gurobi.jl

[62] “Installation Guide · JuMP.” Accessed: Mar. 12, 2024. [Online]. Available: https://jump.dev/JuMP.jl/stable/installation/#Supported-solvers

Appendix A

Probabilistic Transmission Planning involves evaluating different options to solve system performance deficiencies considering statistical metrics such as EENS, EFLC, EDLC, and ADLC, among others. The process includes the following steps [10]:

1. If adhering to the deterministic planning criteria is a requirement, choose planning alternatives that comply with those criteria through traditional power flow and contingency analyses. If meeting deterministic planning criteria is not a strict requirement, additional alternatives may be considered using PTP that solve system performance deficiencies in many or most (but not all) system conditions.
2. Use a risk assessment tool to conduct risk evaluations and assess the associated costs for the selected alternatives over the required planning horizon in composite or transmission systems.
3. Determine the cash flows and calculate the present values of capital investments, operational costs, and risk costs associated with the selected alternatives over the planning horizon.
4. Select appropriate criteria for a comprehensive probabilistic economic evaluation. For instance, considering a performance-based cost-efficiency criterion that evaluates system unreliability costs and aims to minimize the total cost, including investment, operational, and risk costs.

Appendix B

The following standard minimization model of load curtailment can be applied [2], where the sum of load curtailment over all buses based on a predetermined weighting factor per bus is minimized:

$$Min \sum_{i \in ND} w_i \cdot LC_i \tag{B.1}$$

Which is subject to the following constraints:

$$P_{G,i} - P_{D,i} + LC_i = V_i \cdot \sum_{j \in N} V_j \cdot \left(G_{i,j} \cos \delta_{i,j} + B_{i,j} \sin \delta_{i,j}\right) \quad (i = 1, \dots, N) \tag{B.2}$$

$$Q_{G,i} + Q_{C,i} - Q_{D,i} + LC_i \cdot \frac{Q_{D,i}}{P_{D,i}} = V_i \cdot \sum_{j \in N} V_j \cdot \left(G_{i,j} \sin \delta_{i,j} - B_{i,j} \cos \delta_{i,j}\right) \quad (i = 1, \dots, N) \tag{B.3}$$

$$P_{G,i}^{min} \leq P_{G,i} \leq P_{G,i}^{max} \quad (i = 1, \dots, NG) \tag{B.4}$$

$$Q_{G,i}^{min} \leq Q_{G,i} \leq Q_{G,i}^{max} \quad (i = 1, \dots, NG) \tag{B.5}$$

$$Q_{C,i}^{min} \leq Q_{C,i} \leq Q_{C,i}^{max} \quad (i = 1, \dots, NC) \tag{B.6}$$

$$K_t^{min} \leq K_t \leq K_t^{max} \ (t = 1, \dots, NT) \tag{B.7}$$

$$V_i^{min} \leq V_i \leq V_i^{max} \ (i = 1, \dots, N) \tag{B.8}$$

$$T_l^{min} \leq T_l \leq T_l^{max} \ (l = 1, \dots, NB) \tag{B.9}$$

$$0 \leq LC_i \leq P_{D,i} \ (i = 1, \dots, ND) \tag{B.10}$$

Where w_i is the weighting factor reflecting the importance of loads. LC_i is the load curtailment control variable at bus i. $P_{G,i}$ and $Q_{G,i}$ are, respectively, the real and reactive generation power variables at bus i. $P_{D,i}$ and $Q_{D,i}$ are, respectively, the real and reactive power loads at bus i. $Q_{C,i}$ is the reactive power of var source equipment at bus i. V_i and δ_i are, respectively, the magnitude and angle of the voltage at bus i. δ_{ij} is the angle's difference between bus i and j. $G_{i,j}$ and $B_{i,j}$ are, respectively, the real and imaginary parts of the element in the bus admittance matrix. K_t is the turn ratio variable of transformer t. T_l is the power flow in MVA on branch l. Equations (B.2) and (B.3) are power flow equations in polar coordinate form per bus i. Each bus has at least four variables required to solve the system of equations. V_i and δ_i of the swing bus must be specified to adjust the power balance of the system and power at load buses are known. Equations (B.4) to (B.10) are the upper and lower limits of the corresponding variables. N, NG, NB, ND, NC, NT represent the number of buses (N), generators buses (NG), branches (NB), load buses (ND), buses reactive equipment (NC) and transformer branches (NT) in the system. T_l^{max} is the rating limit of branch l.

Appendix C

JuMP supports a range of common problem classes, including linear programming, integer programming, conic optimization, semidefinite programming, and nonlinear programming. It handles the low-level details of communication with underlying solvers, and stores its own copy of the problem data, enabling problem modifications and allowing the solver to be changed at any time.

To formulate the optimization problem within a JuMP model, all variables, constraints, expressions, and objective functions must be defined using the JuMP modelling language. To translate a model specified by the user into a model that a solver understands, the following steps are required:

1. Writing the algebraic formulation of a mathematical optimization model by the user using JuMP macros
2. Translating variables and constraints into a functional form (automatic process)
3. Converting the functional form of the problem into an abstraction layer designed to provide an interface to mathematical optimization solvers (automatic process)
4. Converting the abstraction layer into a solver-specific API using a solver-specific Julia package (automatic process),

The main benefit of an algebraic modeling language like JuMP is that the solver can be changed without needing to rewrite the optimization routine. The external solver is tasked with solving the specified optimization problem as defined within the JuMP model. The number of supported solvers is specified in reference [62], as well as JuMP installation guidelines and documentation.

```
function var_storage_charge(pm::AbstractPowerModel, system::SystemModel; nw::Int=1, bounded::Bool=true)

    sc = var(pm, :sc)[nw] = @variable(pm.model, sc[assetgrouplist(topology(pm, :storages_idxs))], start = 1.0)

    if bounded
        for i in assetgrouplist(topology(pm, :storages_idxs))
            JuMP.set_lower_bound(sc[i], 0)
            JuMP.set_upper_bound(sc[i], field(system, :storages, :charge_rating)[i])
        end
    end
end
```

Figure 18: JuMP's syntax (variable definition) in CompositeSystems.

```
function _con_storage_state_initial(pm::AbstractPowerModel,
    n::Int, i::Int, energy, charge_eff, discharge_eff, time_elapsed)

    sc = var(pm, :sc, n)[i]
    sd = var(pm, :sd, n)[i]
    stored_energy = var(pm, :stored_energy, n)[i]

    con(pm, :storage_state, n)[i] = @constraint(
        pm.model, stored_energy - time_elapsed*(charge_eff*sc - sd/discharge_eff) == energy)
end
```

Figure 19: JuMP's syntax (constraint definition) in CompositeSystems.

Appendix D

Table 6: Bus EENS and EDLC Indices of RBTS: DC-based vs. AC-based Methods.

		DC-Based					**AC-Based**				
		CompositeSystems		**Laengen** [43]			**CompositeSystems**		**Laengen** [43]		
Bus	**Priority**	**EENS**	**SD_{error}**	**EENS**	**SD_{error}**	**$Diff_{Mean}$**	**EENS**	**SD_{error}**	**EENS**	**SD_{error}**	**$Diff_{Mean}$**
		MWh/y	**MWh/y**	**MWh/y**	**MWh/y**	**%**	**MWh/y**	**MWh/y**	**MWh/y**	**MWh/y**	**%**
2	1	0.015	0.008	0.024	0.014	-	0.015	0.008	0.024	0.014	-
3	5	9.763	0.417	10.027	0.450	2.67%	14.830	0.523	15.930	0.581	7.16%
4	3	0.000	0.000	0.000	0.000	-	0.000	0.000	0.000	0.000	-
5	2	0.113	0.031	0.147	0.034	-	0.113	0.031	0.148	0.034	-
6	4	122.621	1.391	122.024	1.434	0.49%	124.597	1.393	125.444	1.437	0.68%
System		132.512	1.454	132.221	1.507	0.22%	139.555	1.490	141.546	1.561	1.42%
CV_{EENS} (%)		1.10%	-	1.14%	-	-	1.07%	-	1.10%	-	-
Replications		15000	-	15000	-	-	15000	-	15000	-	-
Bus	**Priority**	**EDLC**	**SD_{error}**	**EDLC**	**SD_{error}**	**$Diff_{Mean}$**	**EDLC**	**SD_{error}**	**EDLC**	**SD_{error}**	**$Diff_{Mean}$**
		hours/y	**hours/y**	**hours/y**	**hours/y**	**%**	**hours/y**	**hours/y**	**hours/y**	**hours/y**	**%**
2	1	0.001	0.001	0.002	0.001	-	0.001	0.001	0.002	0.001	-
3	5	1.121	0.034	1.147	0.036	2.25%	1.650	0.041	1.906	0.046	14.38%
4	3	0.000	0.000	0.000	0.000	-	0.000	0.000	0.000	0.000	-
5	2	0.009	0.002	0.012	0.003	-	0.009	0.002	0.012	0.003	-
6	4	9.994	0.112	9.934	0.115	0.61%	10.485	0.113	11.360	0.120	8.01%
System		11.116	0.117	11.081	0.121	0.32%	12.081	0.120	12.478	0.125	3.23%
CV_{EDLC} (%)		1.05%	-	1.14%	-	-	1.00%	-	1.10%	-	-
Replications		15000	-	15000	-	-	15000	-	15000	-	-

Table 7: Bus EENS Index of IEEE-RTS 79: DC-based vs. AC-based Methods.

		DC-Based					**AC-Based**				
		CompositeSystems		**Laengen** [43]			**CompositeSystems**		**Laengen** [43]		
Bus	**Priority**	**EENS** MWh/y	**SD_{error}** MWh/y	**EENS** MWh/y	**SD_{error}** MWh/y	**$Diff_{Mean}$** %	**EENS** MWh/y	**SD_{error}** MWh/y	**EENS** MWh/y	**SD_{error}** MWh/y	**$Diff_{Mean}$** %
1	3	0.000	0.000	0.000	0.000	-	0.000	0.000	0.000	0.000	-
2	5	0.000	0.000	0.000	0.000	-	0.000	0.000	0.000	0.000	-
3	11	0.000	0.000	0.000	0.000	-	0.203	0.077	0.742	0.198	-
4	1	0.049	0.028	0.074	0.056	-	0.049	0.028	0.070	0.035	-
5	2	0.044	0.025	0.056	0.027	-	0.044	0.025	0.055	0.026	-
6	9	0.309	0.112	0.447	0.169	-	1.031	0.231	41.991	1.261	190.41%
7	8	231.405	4.807	226.071	4.891	2.33%	243.273	4.902	240.861	5.028	1.00%
8	4	0.000	0.000	0.420	0.203	-	0.002	0.002	0.276	0.134	-
9	17	871.873	14.515	852.296	14.376	2.27%	1049.869	16.236	1033.967	15.874	1.53%
10	14	8.189	0.863	9.222	1.113	11.87%	10.252	0.985	9.864	0.910	3.86%
13	6	0.000	0.000	0.000	0.000	-	0.000	0.000	0.000	0.000	-
14	16	253.061	7.276	257.780	7.361	1.85%	305.436	8.109	305.762	7.933	0.11%
15	10	0.000	0.000	0.000	0.000	-	0.000	0.000	0.014	0.001	-
16	7	0.000	0.000	0.000	0.000	-	0.000	0.000	0.000	0.000	-
18	13	0.865	0.280	1.122	0.401	-	1.065	0.317	0.942	0.225	-
19	15	50.427	2.667	52.621	2.881	4.26%	61.410	3.022	61.081	2.983	0.54%
20	12	0.002	0.002	0.003	0.003	-	0.003	0.003	0.052	0.025	-
System		1416.224	23.910	1400.112	24.228	1.14%	1672.639	26.665	1695.676	26.146	1.37%
CV_{EENS} (%)		1.69%	-	1.73%	-	-	1.59%	-	1.54%	-	-
Replications		15000	-	15000	-	-	15000	-	15000	-	-

Table 8: Bus EDLC Index of IEEE-RTS 79: DC-based vs. AC-based Methods.

		DC-Based					**AC-Based**				
		CompositeSystems		**Laengen** [43]			**CompositeSystems**		**Laengen** [43]		
Bus	**Priority**	**EENS** MWh/y	**SD_{error}** MWh/y	**EENS** MWh/y	**SD_{error}** MWh/y	**$Diff_{Mean}$** %	**EENS** MWh/y	**SD_{error}** MWh/y	**EENS** MWh/y	**SD_{error}** MWh/y	**$Diff_{Mean}$** %
…		…					…				
6	9	0.004	0.001	0.006	0.002	-	0.071	0.013	3.255	0.081	191.51%
7	8	3.009	0.062	2.930	0.063	2.66%	3.362	0.066	3.357	0.069	0.17%
8	4	0.000	0.000	0.004	0.002	-	0.001	0.000	0.012	0.002	-
9	17	9.609	0.133	9.351	0.131	2.73%	11.592	0.149	11.425	0.146	1.45%
…		…					…				
System		12.614	0.146	12.284	0.146	2.65%	15.011	0.162	18.025	0.181	18.25%
CV_{EENS} (%)		1.16%	-	1.19%	-	-	1.08%	-	1.00%	-	-
Replications		15000	-	15000	-	-	15000	-	15000	-	-

Appendix E

In Chapter III an energy storage model was introduced and subsequently integrated into the optimization problem. This integration was subjected to testing to confirm its suitability for deployment under normal and emergency conditions. The test scenarios encompassed 24 hours of simulation time, employing a DC-based formulation that incorporated generation costs. These tests were conducted on the 6-bus RBTS, and three distinct cases were examined, both with and without energy storage. Additionally, simulated transmission outages occurred, lasting four hours, specifically from 17:00 to 20:00 hours. The load model represented the first week of the year and was increased by 25% to amplify the consequences of load shedding. Below is the model data about the battery energy storage system (BESS).

a) Bus connected = #6

b) $ER_6 =$ 40 MWh

c) $E_{6,t=0} = 0\ MWh$

d) $\eta_i^c = \eta_i^d = 0.0$

e) $Q_{s,6}^{min} = Q_{s,6}^{max} = Z_{s,6} = S_i^{loss} = 0.0$

f) $s_i^u = 10$ MVA

g) $PR_sd_i = 10$ MW

h) $PR_sc_i = 5$ MW

The results for each case are summarized as follows:

- **Scenario 1**: The transmission system did not experience thermal overloading or voltage angle constraints either before or after the addition of BESS (see Figure 20). BESS reached full charge by hour 8.
- **Scenario 2**: The occurrence of two outages resulted in the division of the network into two subsystems (see Figure 21). Notably, the smaller subsystem lacked generation sources, necessitating load curtailment. The maximum curtailment observed was 40

MW, impacting loads at bus 5 and bus 6. The BESS was charged until hour 8 and then completely discharged during the 4-hour outage. Subsequently, the charging process recommenced. It is worth noting that while load curtailment was not entirely averted, the discharging rating of 10 MW was less than the total isolated load of 40 MW at its peak.

- **Scenario 3**: Similar to Scenario 2, buses 5 and 6 faced the risk of load loss, as their combined daily peak load reached 40 MW (refer to Figure 22). Due to load curtailment priority, the load at bus 6 was curtailed. The line between bus 3 and bus 5 operated at its maximum thermal rating, resulting in a reduced level of load loss compared to Scenario 2, where both lines to bus 5 were out of service.

Thus, the BESS model was found to perform as expected before and after outages and split situations. These scenarios demonstrate the effectiveness of the BESS in mitigating load curtailment and managing system constraints.

Table 9: Test cases using RBTS with energy storage.

Scenario	Outages	Duration	Constraints	Energy Storage included
1	None	-	Normal	Not included
	None	-	Normal	Included
2	line #5 (3,5) / line #8 (4,5)	17-20 hrs	Normal	Not included
	line #5 (3,5) / line #8 (4,5)	17-20 hrs	Normal	Included
3	line #8 (4,5)	17-20 hrs	line #5 (3,5)	Not included
	line #8 (4,5)	17-20 hrs	line #5 (3,5)	Included

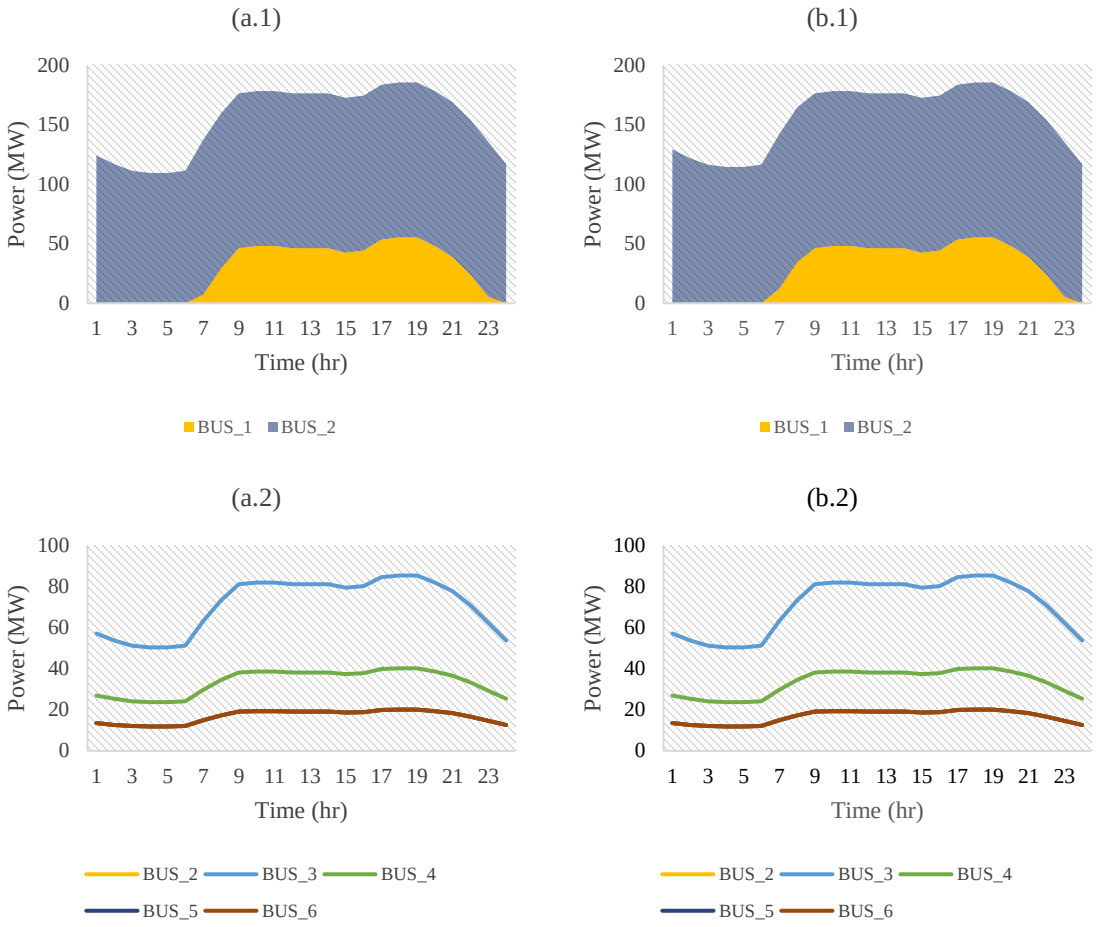

Figure 20: Test Scenario 1 using RBTS without storage (a), and with storage (b).

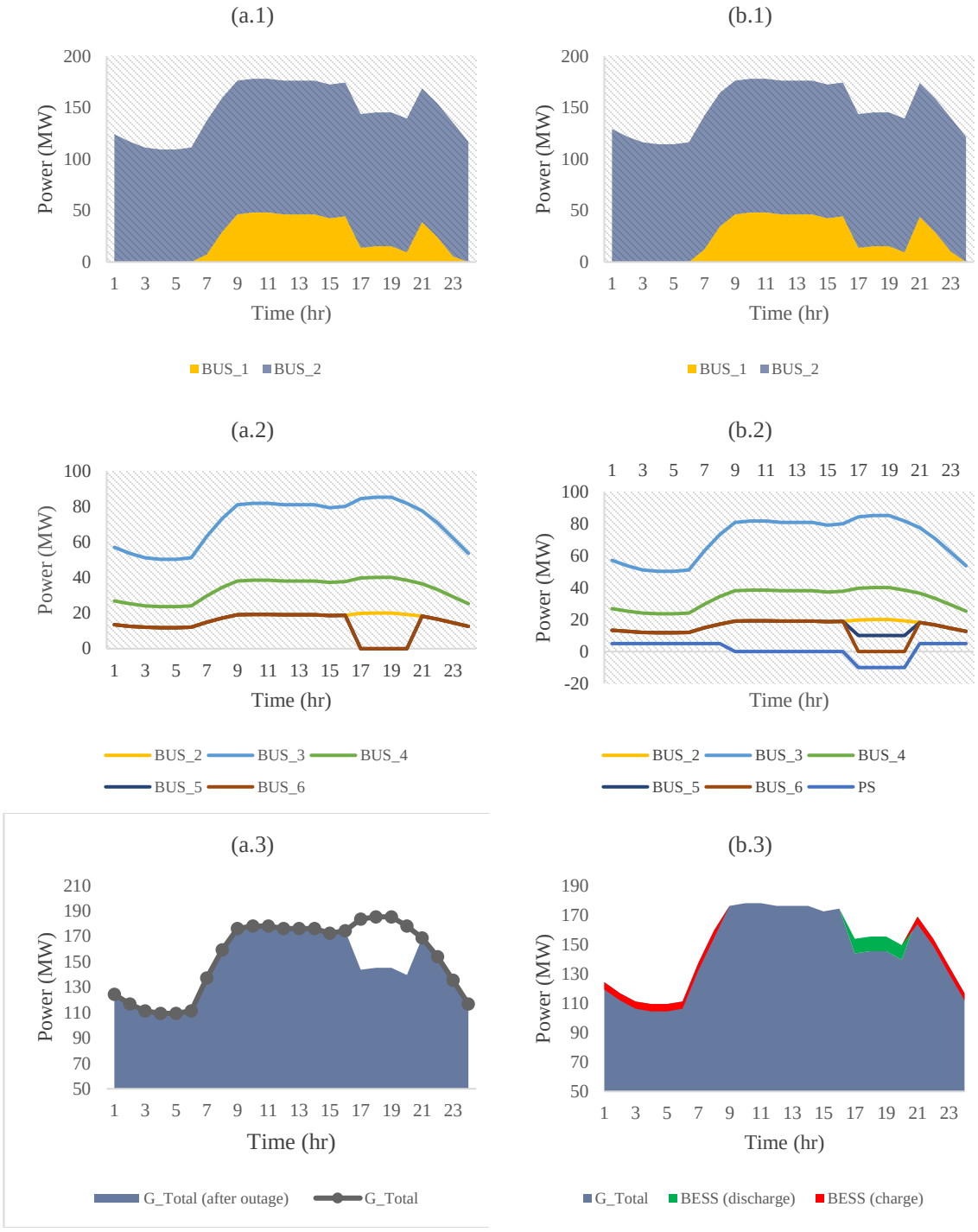

Figure 21: Test scenario 2 using RBTS without storage (a), and with storage (b).

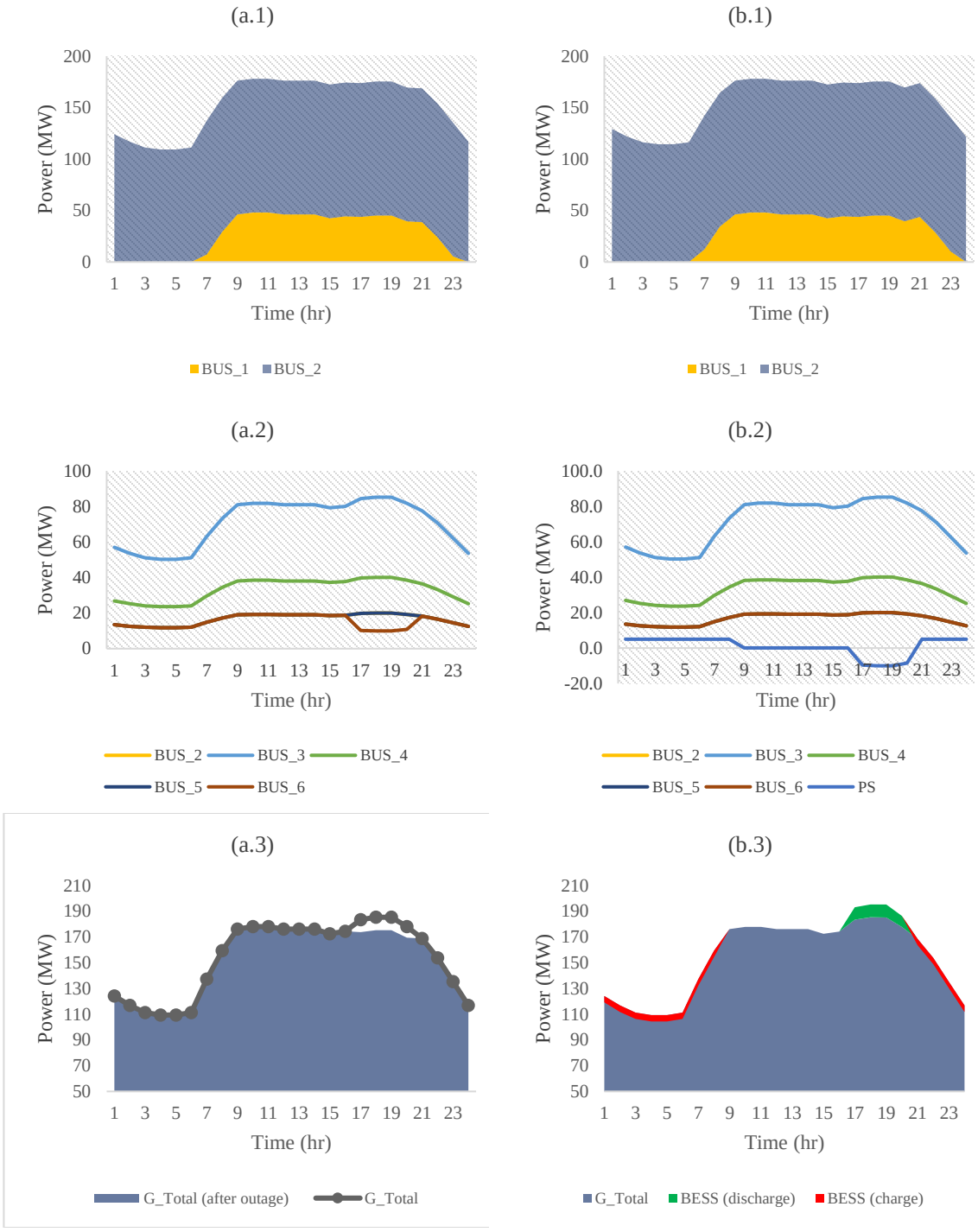

Figure 22: Test Scenario 3 using RBTS without storage (a), and with storage (b).

Table 10: Optimal Power Flow results per load bus in MW, Scenario 2.

	Connected Load (MW)						BESS		Curtailed Load (MW)				
Hr	2	3	4	5	6	Total	PS	Stored Energy (MWh)	2	3	4	5	6
1	13.4	57.1	26.9	13.4	13.4	124.2	5.0	5.0	0.0	0.0	0.0	0.0	0.0
2	12.6	53.7	25.3	12.6	12.6	116.8	5.0	10.0	0.0	0.0	0.0	0.0	0.0
3	12.0	51.1	24.0	12.0	12.0	111.2	5.0	15.0	0.0	0.0	0.0	0.0	0.0
4	11.8	50.3	23.6	11.8	11.8	109.4	5.0	20.0	0.0	0.0	0.0	0.0	0.0
5	11.8	50.3	23.6	11.8	11.8	109.4	5.0	25.0	0.0	0.0	0.0	0.0	0.0
6	12.0	51.1	24.0	12.0	12.0	111.2	5.0	30.0	0.0	0.0	0.0	0.0	0.0
7	14.8	63.0	29.7	14.8	14.8	137.2	5.0	35.0	0.0	0.0	0.0	0.0	0.0
8	17.2	73.3	34.5	17.2	17.2	159.4	5.0	40.0	0.0	0.0	0.0	0.0	0.0
9	19.0	80.9	38.1	19.0	19.0	176.1	0.0	40.0	0.0	0.0	0.0	0.0	0.0
10	19.2	81.8	38.5	19.2	19.2	178.0	0.0	40.0	0.0	0.0	0.0	0.0	0.0
11	19.2	81.8	38.5	19.2	19.2	178.0	0.0	40.0	0.0	0.0	0.0	0.0	0.0
12	19.0	80.9	38.1	19.0	19.0	176.1	0.0	40.0	0.0	0.0	0.0	0.0	0.0
13	19.0	80.9	38.1	19.0	19.0	176.1	0.0	40.0	0.0	0.0	0.0	0.0	0.0
14	19.0	80.9	38.1	19.0	19.0	176.1	0.0	40.0	0.0	0.0	0.0	0.0	0.0
15	18.6	79.2	37.3	18.6	18.6	172.4	0.0	40.0	0.0	0.0	0.0	0.0	0.0
16	18.8	80.1	37.7	18.8	18.8	174.3	0.0	40.0	0.0	0.0	0.0	0.0	0.0
17	19.8	84.3	39.7	10.0	0.0	153.9	-10.0	30.0	0.0	0.0	0.0	9.8	19.8
18	20.0	85.2	40.1	10.0	0.0	155.3	-10.0	20.0	0.0	0.0	0.0	10.0	20.0
19	20.0	85.2	40.1	10.0	0.0	155.3	-10.0	10.0	0.0	0.0	0.0	10.0	20.0
20	19.2	81.8	38.5	10.0	0.0	149.5	-10.0	0.0	0.0	0.0	0.0	9.2	19.2
21	18.2	77.5	36.5	18.2	18.2	168.7	5.0	5.0	0.0	0.0	0.0	0.0	0.0
22	16.6	70.7	33.3	16.6	16.6	153.9	5.0	10.0	0.0	0.0	0.0	0.0	0.0
23	14.6	62.2	29.3	14.6	14.6	135.3	5.0	15.0	0.0	0.0	0.0	0.0	0.0
24	12.6	53.7	25.3	12.6	12.6	116.8	5.0	20.0	0.0	0.0	0.0	0.0	0.0

Table 11: Optimal Power Flow results per load bus in MW, Scenario 3.

	Connected Load (MW)						BESS		Curtailed Load (MW)				
Hr	2	3	4	5	6	Total	Power Output (MW)	Stored Energy (MWh)	2	3	4	5	6
1	13.4	57.1	26.9	13.4	13.4	124.2	5.0	5.0	0.0	0.0	0.0	0.0	0.0
2	12.6	53.7	25.3	12.6	12.6	116.8	5.0	10.0	0.0	0.0	0.0	0.0	0.0
3	12.0	51.1	24.0	12.0	12.0	111.2	5.0	15.0	0.0	0.0	0.0	0.0	0.0
4	11.8	50.3	23.6	11.8	11.8	109.4	5.0	20.0	0.0	0.0	0.0	0.0	0.0
5	11.8	50.3	23.6	11.8	11.8	109.4	5.0	25.0	0.0	0.0	0.0	0.0	0.0
6	12.0	51.1	24.0	12.0	12.0	111.2	5.0	30.0	0.0	0.0	0.0	0.0	0.0
7	14.8	63.0	29.7	14.8	14.8	137.2	5.0	35.0	0.0	0.0	0.0	0.0	0.0
8	17.2	73.3	34.5	17.2	17.2	159.4	5.0	40.0	0.0	0.0	0.0	0.0	0.0
9	19.0	80.9	38.1	19.0	19.0	176.1	0.0	40.0	0.0	0.0	0.0	0.0	0.0
10	19.2	81.8	38.5	19.2	19.2	178.0	0.0	40.0	0.0	0.0	0.0	0.0	0.0
11	19.2	81.8	38.5	19.2	19.2	178.0	0.0	40.0	0.0	0.0	0.0	0.0	0.0
12	19.0	80.9	38.1	19.0	19.0	176.1	0.0	40.0	0.0	0.0	0.0	0.0	0.0
13	19.0	80.9	38.1	19.0	19.0	176.1	0.0	40.0	0.0	0.0	0.0	0.0	0.0
14	19.0	80.9	38.1	19.0	19.0	176.1	0.0	40.0	0.0	0.0	0.0	0.0	0.0
15	18.6	79.2	37.3	18.6	18.6	172.4	0.0	40.0	0.0	0.0	0.0	0.0	0.0
16	18.8	80.1	37.7	18.8	18.8	174.3	0.0	40.0	0.0	0.0	0.0	0.0	0.0
17	19.8	84.3	39.7	19.8	19.8	183.5	-9.7	30.3	0.0	0.0	0.0	0.0	0.0
18	20.0	85.2	40.1	20.0	20.0	185.3	-10.0	20.3	0.0	0.0	0.0	0.0	0.1
19	20.0	85.2	40.1	19.9	20.0	185.3	-10.0	10.3	0.0	0.0	0.0	0.0	0.1
20	19.2	81.8	38.5	19.2	19.2	178.0	-8.5	1.9	0.0	0.0	0.0	0.0	0.0
21	18.2	77.5	36.5	18.2	18.2	168.7	5.0	6.9	0.0	0.0	0.0	0.0	0.0
22	16.6	70.7	33.3	16.6	16.6	153.9	5.0	11.9	0.0	0.0	0.0	0.0	0.0
23	14.6	62.2	29.3	14.6	14.6	135.3	5.0	16.9	0.0	0.0	0.0	0.0	0.0
24	12.6	53.7	25.3	12.6	12.6	116.8	5.0	21.8	0.0	0.0	0.0	0.0	0.0

Appendix F

The RBTS (Reliability Test System) is a test system developed by the Power Systems Research Group at the University of Saskatchewan. It comprises a 6-bus system featuring 11 generators, 9 transmission lines, an installed capacity of 240 MW, and a peak load of 185 MW. The generators are distributed across two buses, namely buses 1 and 2. Essential system data necessary to conduct HL-II assessments can be found in Table 12 to Table 14.

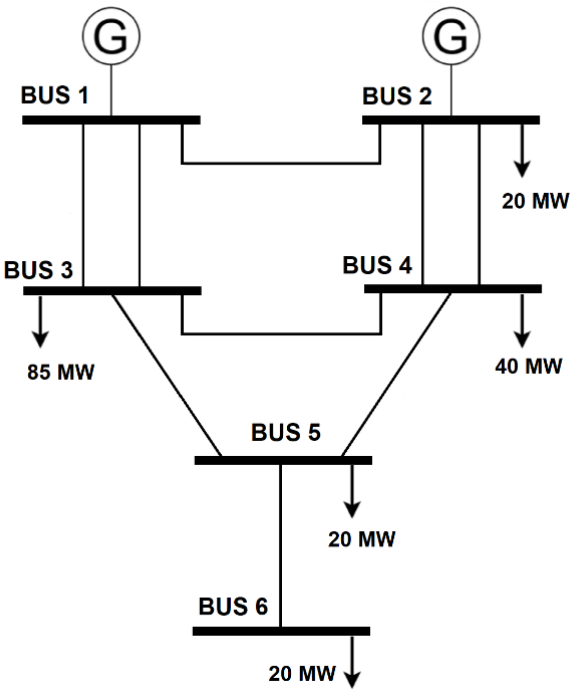

Figure 23: Roy Billinton Test System (RBTS). Source: [54].

Table 12: Generator data, RBTS test system.

Bus	Capacity [MW]	Reactive max [MW]	Reactive min [MW]	λ [1/y]	μ [1/y]
1	40.0	17.0	-15.0	6.0	194.0
1	40.0	17.0	-15.0	6.0	194.0
1	10.0	7.0	0.0	4.0	196.0
1	20.0	12.0	-7.0	5.0	195.0
2	5.0	5.0	0.0	2.0	198.0
2	5.0	5.0	0.0	2.0	198.0
2	40.0	17.0	-15.0	3.0	147.0
2	20.0	12.0	-7.0	2.4	157.6
2	20.0	12.0	-7.0	2.4	157.6
2	20.0	12.0	-7.0	2.4	157.6
2	20.0	12.0	-7.0	2.4	157.6

Table 13: Branch data, RBTS test system.

From Bus	To Bus	Resi. [pu]	Reac. [pu]	Susc. [pu]	Long term rating A	Short term rating B	Trans. Ratio	Min ang [deg]	Max ang [deg]	λ [1/y]	μ [1/y]
1	3	0.034	0.180	0.021	85	93.5	0.00	-60	60	1.5	876.0
2	4	0.114	0.600	0.070	71	78.1	0.00	-60	60	5.0	876.0
2	1	0.091	0.480	0.056	71	78.1	0.00	-60	60	4.0	876.0
3	4	0.023	0.120	0.014	71	78.1	0.00	-60	60	1.0	876.0
3	5	0.023	0.120	0.014	71	78.1	0.00	-60	60	1.0	876.0
1	3	0.034	0.180	0.021	85	93.5	0.00	-60	60	1.5	876.0
2	4	0.114	0.600	0.070	71	78.1	0.00	-60	60	5.0	876.0
4	5	0.023	0.120	0.014	71	78.1	0.00	-60	60	1.0	876.0
5	6	0.023	0.120	0.014	71	78.1	0.00	-60	60	1.0	876.0

Table 14: Bus data, RBTS test system.

Bus	Type	Load [MW]	Load [MVAR]	baseKV	Vmax [pu]	Vmin [pu]	Curtailment cost [$/MWh]
1	Slack	0.0	0.0	230	1.05	0.97	-
2	PV	20.0	4.0	230	1.05	0.97	9632.5
3	PQ	85.0	17.0	230	1.05	0.97	4376.9
4	PQ	40.0	8.0	230	1.05	0.97	8026.7
5	PQ	20.0	4.0	230	1.05	0.97	8632.3
6	PQ	20.0	4.0	230	1.05	0.97	5513.2

Appendix G

In the single-area configuration of the IEEE-RTS 79, there is an installed capacity of 3405 MW and a peak load of 2850 MW. This configuration encompasses 32 generators, with capacities ranging from 12 MW to 400 MW. Essential system data necessary to conduct HL-II assessments can be found in Table 15 to Table 17.

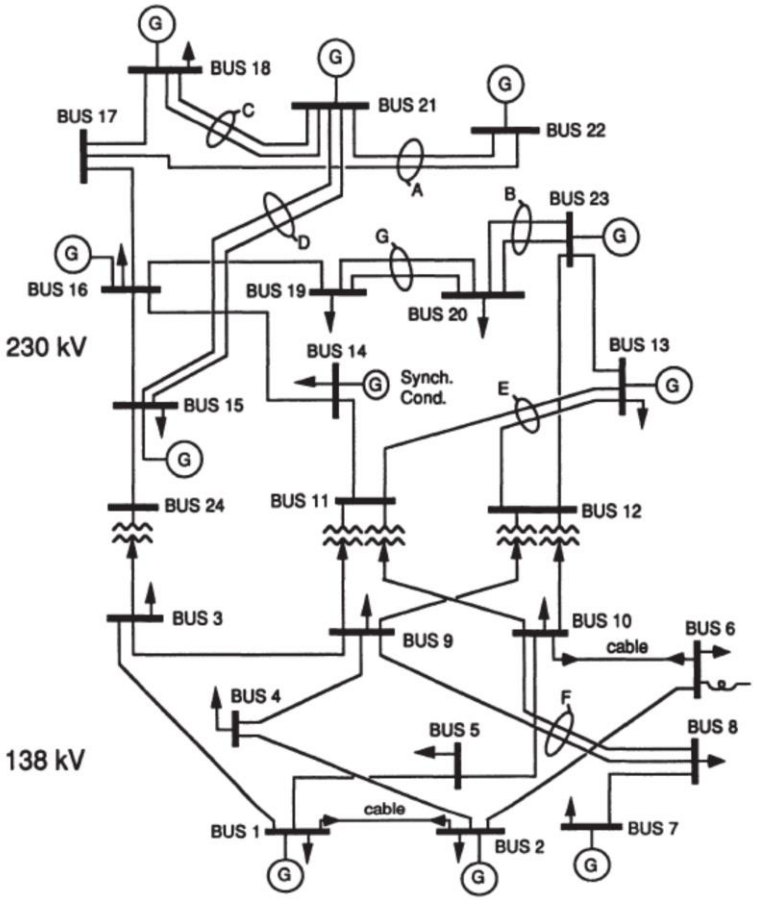

Figure 24: Original (1979) IEEE RTS. Source: [55].

Table 15: Generator data, IEEE-RTS 79 test system.

Bus	Capacity [MW]	Reactive max [MW]	Reactive min [MW]	λ [1/y]	μ [1/y]
1	20	10	0	19.5	175.2
1	20	10	0	19.5	175.2
1	76	30	-25	4.5	219.0
1	76	30	-25	4.5	219.0
2	20	10	0	19.5	175.2
2	20	10	0	19.5	175.2
2	76	30	-25	4.5	219.0
2	76	30	-25	4.5	219.0
7	100	60	0	7.3	175.2
7	100	60	0	7.3	175.2
7	100	60	0	7.3	175.2
13	197	80	0	9.2	175.2
13	197	80	0	9.2	175.2
13	197	80	0	9.2	175.2
14	0	200	-50	0.0	1.0
15	12	6	0	3.0	146.0
15	12	6	0	3.0	146.0
15	12	6	0	3.0	146.0
15	12	6	0	3.0	146.0
15	12	6	0	3.0	146.0
15	155	80	-50	9.1	219.0
16	155	80	-50	9.1	219.0
18	400	200	-50	8.0	58.4
21	400	200	-50	8.0	58.4
22	50	16	-10	4.4	438.0
22	50	16	-10	4.4	438.0
22	50	16	-10	4.4	438.0
22	50	16	-10	4.4	438.0
22	50	16	-10	4.4	438.0
22	50	16	-10	4.4	438.0
23	155	80	-50	9.1	219.0
23	155	80	-50	9.1	219.0
23	350	150	-25	7.6	87.6

Table 16: Branch data, IEEE-RTS 79 test system.

From Bus	To Bus	Resi. [pu]	Reac. [pu]	Susc. [pu]	Long term rating A	Short term rating B	Trans. Ratio	Min ang [deg]	Max ang [deg]	λ [1/y]	μ [1/y]
1	2	0.003	0.014	0.461	193	208	0.00	-60	60	0.2	546.0
1	3	0.055	0.211	0.057	193	208	0.00	-60	60	0.5	876.0
1	5	0.022	0.085	0.023	193	208	0.00	-60	60	0.3	876.0
2	4	0.033	0.127	0.034	193	208	0.00	-60	60	0.4	876.0
2	6	0.050	0.192	0.052	193	208	0.00	-60	60	0.5	876.0
3	9	0.031	0.119	0.032	193	208	0.00	-60	60	0.4	876.0
3	24	0.002	0.084	0.000	510	600	1.02	-60	60	0.0	11.4
4	9	0.027	0.104	0.028	193	208	0.00	-60	60	0.4	876.0
5	10	0.023	0.088	0.024	193	208	0.00	-60	60	0.3	876.0
6	10	0.014	0.061	2.459	193	208	0.00	-60	60	0.3	249.6
7	8	0.016	0.061	0.017	193	208	0.00	-60	60	0.3	876.0
8	9	0.043	0.165	0.045	193	208	0.00	-60	60	0.4	876.0
8	10	0.043	0.165	0.045	193	208	0.00	-60	60	0.4	876.0
9	11	0.002	0.084	0.000	510	600	1.03	-60	60	0.0	11.4
9	12	0.002	0.084	0.000	510	600	1.03	-60	60	0.0	11.4
10	11	0.002	0.084	0.000	510	600	1.02	-60	60	0.0	11.4
10	12	0.002	0.084	0.000	510	600	1.02	-60	60	0.0	11.4
11	13	0.006	0.048	0.100	600	625	0.00	-60	60	0.4	796.4
11	14	0.005	0.042	0.088	600	625	0.00	-60	60	0.4	796.4
12	13	0.006	0.048	0.100	600	625	0.00	-60	60	0.4	796.4
12	23	0.012	0.097	0.203	600	625	0.00	-60	60	0.5	796.4
13	23	0.011	0.087	0.182	600	625	0.00	-60	60	0.5	796.4
14	16	0.005	0.039	0.082	600	625	0.00	-60	60	0.4	796.4
15	16	0.002	0.017	0.036	600	625	0.00	-60	60	0.3	796.4
15	21	0.006	0.049	0.103	600	625	0.00	-60	60	0.4	796.4
15	21	0.006	0.049	0.103	600	625	0.00	-60	60	0.4	796.4
15	24	0.007	0.052	0.109	600	625	0.00	-60	60	0.4	796.4
16	17	0.003	0.026	0.055	600	625	0.00	-60	60	0.4	796.4
16	19	0.003	0.023	0.049	600	625	0.00	-60	60	0.3	796.4
17	18	0.002	0.014	0.030	600	625	0.00	-60	60	0.3	796.4
17	22	0.014	0.105	0.221	600	625	0.00	-60	60	0.5	796.4
18	21	0.003	0.026	0.055	600	625	0.00	-60	60	0.4	796.4
18	21	0.003	0.026	0.055	600	625	0.00	-60	60	0.4	796.4
19	20	0.005	0.040	0.083	600	625	0.00	-60	60	0.4	796.4
19	20	0.005	0.040	0.083	600	625	0.00	-60	60	0.4	796.4
20	23	0.003	0.022	0.046	600	625	0.00	-60	60	0.3	796.4
20	23	0.003	0.022	0.046	600	625	0.00	-60	60	0.3	796.4
21	22	0.009	0.068	0.142	600	625	0.00	-60	60	0.5	796.4

Table 17: Bus data, IEEE-RTS 79 test system.

Bus	Type	Load [MW]	Load [MVAR]	baseKV	Vmax [pu]	Vmin [pu]	Curtailment cost [$/MWh]
1	PV	108	22	138	1.05	0.95	8981.5
2	PV	97	20	138	1.05	0.95	7360.6
3	PQ	180	37	138	1.05	0.95	5899.0
4	PQ	74	15	138	1.05	0.95	9599.2
5	PQ	71	14	138	1.05	0.95	9232.3
6	PQ	136	28	138	1.05	0.95	6523.8
7	PV	125	25	138	1.05	0.95	7029.1
8	PQ	171	35	138	1.05	0.95	7774.2
9	PQ	175	36	138	1.05	0.95	3662.3
10	PQ	195	40	138	1.05	0.95	5194.0
11	PQ	0	0	230	1.05	0.95	-
12	PQ	0	0	230	1.05	0.95	-
13	Slack	265	54	230	1.05	0.95	7281.3
14	PV	194	39	230	1.05	0.95	4371.7
15	PV	317	64	230	1.05	0.95	5974.4
16	PV	100	20	230	1.05	0.95	7230.5
17	PQ	0	0	230	1.05	0.95	-
18	PV	333	68	230	1.05	0.95	5614.9
19	PQ	181	37	230	1.05	0.95	4543.0
20	PQ	128	26	230	1.05	0.95	5683.6
21	PV	0	0	230	1.05	0.95	-
22	PV	0	0	230	1.05	0.95	-
23	PV	0	0	230	1.05	0.95	-
24	PQ	0	0	230	1.05	0.95	-

Appendix H

Table 18: CSR assessment DC-Based results for 2000 replications. Base system, Case 1.

Bus	mean EENS	mean EDLC	mean SI	stderror EENS	stderror EDLC	stderror SI
-	MWh/yr	Hrs/yr	Sys-hrs	MWh/yr	Hrs/yr	Sys-hrs
1	0.000	0.000	0.000	0.000	0.000	0.000
2	0.000	0.000	0.000	0.000	0.000	0.000
3	0.000	0.000	0.000	0.000	0.000	0.000
4	0.000	0.000	0.000	0.000	0.000	0.000
5	0.086	0.003	0.002	0.063	0.002	0.001
6	0.347	0.005	0.007	0.347	0.005	0.007
7	241.706	3.167	5.089	12.829	0.166	0.270
8	0.002	0.001	0.000	0.002	0.001	0.000
9	1168.896	12.743	24.608	49.283	0.450	1.038
10	11.399	0.150	0.240	3.825	0.036	0.081
11	0.000	0.000	0.000	0.000	0.000	0.000
12	0.000	0.000	0.000	0.000	0.000	0.000
13	0.000	0.000	0.000	0.000	0.000	0.000
14	343.123	3.875	7.224	23.725	0.218	0.499
15	0.000	0.000	0.000	0.000	0.000	0.000
16	0.000	0.000	0.000	0.000	0.000	0.000
17	0.000	0.000	0.000	0.000	0.000	0.000
18	1.307	0.022	0.028	0.923	0.011	0.019
19	65.080	0.807	1.370	8.971	0.084	0.189
20	0.000	0.000	0.000	0.000	0.000	0.000
21	0.000	0.000	0.000	0.000	0.000	0.000
22	0.000	0.000	0.000	0.000	0.000	0.000
23	0.000	0.000	0.000	0.000	0.000	0.000
24	0.000	0.000	0.000	0.000	0.000	0.000
System	1831.947	15.912	38.567	79.425	0.473	1.672

Table 19: CSR assessment DC-Based results for 2000 replications. Augmented system, Case 1 with SATA 75MW/260 MWh.

Bus	mean EENS	mean EDLC	mean SI	stderror EENS	stderror EDLC	stderror SI
-	MWh/yr	Hrs/yr	Sys-hrs	MWh/yr	Hrs/yr	Sys-hrs
1	0.000	0.000	0.000	0.000	0.000	0.000
2	0.000	0.000	0.000	0.000	0.000	0.000
3	0.000	0.000	0.000	0.000	0.000	0.000
4	0.000	0.000	0.000	0.000	0.000	0.000
5	0.086	0.003	0.002	0.063	0.002	0.001
6	0.347	0.005	0.007	0.347	0.005	0.007
7	241.613	3.157	5.087	12.830	0.166	0.270
8	0.000	0.000	0.000	0.000	0.000	0.000
9	851.014	8.627	17.916	41.743	0.365	0.879
10	10.450	0.133	0.220	3.579	0.033	0.075
11	0.000	0.000	0.000	0.000	0.000	0.000
12	0.000	0.000	0.000	0.000	0.000	0.000
13	0.000	0.000	0.000	0.000	0.000	0.000
14	288.489	3.189	6.073	21.242	0.190	0.447
15	0.000	0.000	0.000	0.000	0.000	0.000
16	0.000	0.000	0.000	0.000	0.000	0.000
17	0.000	0.000	0.000	0.000	0.000	0.000
18	1.129	0.020	0.024	0.788	0.010	0.017
19	56.443	0.696	1.188	8.233	0.076	0.173
20	0.000	0.000	0.000	0.000	0.000	0.000
21	0.000	0.000	0.000	0.000	0.000	0.000
22	0.000	0.000	0.000	0.000	0.000	0.000
23	0.000	0.000	0.000	0.000	0.000	0.000
24	0.000	0.000	0.000	0.000	0.000	0.000
System	1449.571	11.788	30.517	69.903	0.396	1.472

Table 20: CSR assessment DC-Based results for 2000 replications. Augmented system, Case 1 and Case 2 with traditional solution.

Bus	mean EENS	mean EDLC	mean SI	stderror EENS	stderror EDLC	stderror SI
-	MWh/yr	Hrs/yr	Sys-hrs	MWh/yr	Hrs/yr	Sys-hrs
1	0.000	0.000	0.000	0.000	0.000	0.000
2	0.000	0.000	0.000	0.000	0.000	0.000
3	0.000	0.000	0.000	0.000	0.000	0.000
4	0.000	0.000	0.000	0.000	0.000	0.000
5	0.086	0.003	0.002	0.063	0.002	0.001
6	0.347	0.005	0.007	0.347	0.005	0.007
7	241.613	3.157	5.087	12.830	0.166	0.270
8	0.000	0.000	0.000	0.000	0.000	0.000
9	887.673	9.673	18.688	41.832	0.377	0.881
10	8.257	0.107	0.174	3.411	0.031	0.072
11	0.000	0.000	0.000	0.000	0.000	0.000
12	0.000	0.000	0.000	0.000	0.000	0.000
13	0.000	0.000	0.000	0.000	0.000	0.000
14	254.872	2.953	5.366	19.735	0.184	0.415
15	0.000	0.000	0.000	0.000	0.000	0.000
16	0.000	0.000	0.000	0.000	0.000	0.000
17	0.000	0.000	0.000	0.000	0.000	0.000
18	1.209	0.020	0.025	0.918	0.011	0.019
19	47.957	0.597	1.010	7.617	0.070	0.160
20	0.000	0.000	0.000	0.000	0.000	0.000
21	0.000	0.000	0.000	0.000	0.000	0.000
22	0.000	0.000	0.000	0.000	0.000	0.000
23	0.000	0.000	0.000	0.000	0.000	0.000
24	0.000	0.000	0.000	0.000	0.000	0.000
System	1442.014	12.834	30.358	67.363	0.405	1.418

Table 21: CSR assessment DC-Based results for 2000 replications. Base system, Case 2.

Bus	mean EENS	mean EDLC	mean SI	stderror EENS	stderror EDLC	stderror SI
-	MWh/yr	Hrs/yr	Sys-hrs	MWh/yr	Hrs/yr	Sys-hrs
1	0.000	0.000	0.000	0.000	0.000	0.000
2	0.000	0.000	0.000	0.000	0.000	0.000
3	0.000	0.000	0.000	0.000	0.000	0.000
4	0.000	0.000	0.000	0.000	0.000	0.000
5	0.086	0.003	0.002	0.063	0.002	0.001
6	0.347	0.005	0.007	0.347	0.005	0.007
7	248.843	3.517	5.239	12.915	0.174	0.272
8	0.117	0.007	0.002	0.077	0.004	0.002
9	1591.743	17.128	33.510	59.548	0.542	1.254
10	17.726	0.228	0.373	4.571	0.043	0.096
11	0.000	0.000	0.000	0.000	0.000	0.000
12	0.000	0.000	0.000	0.000	0.000	0.000
13	0.000	0.000	0.000	0.000	0.000	0.000
14	488.935	5.439	10.293	29.418	0.265	0.619
15	0.000	0.000	0.000	0.000	0.000	0.000
16	0.000	0.000	0.000	0.000	0.000	0.000
17	0.000	0.000	0.000	0.000	0.000	0.000
18	1.705	0.031	0.036	0.959	0.013	0.020
19	95.955	1.189	2.020	11.122	0.106	0.234
20	0.000	0.000	0.000	0.000	0.000	0.000
21	0.000	0.000	0.000	0.000	0.000	0.000
22	0.000	0.000	0.000	0.000	0.000	0.000
23	0.000	0.000	0.000	0.000	0.000	0.000
24	0.000	0.000	0.000	0.000	0.000	0.000
System	2445.458	20.597	51.483	96.899	0.561	2.040

Table 22: CSR assessment DC-Based results for 2000 replications. Augmented system, Case 2 with SATA 75MW/260 MWh.

Bus	mean EENS	mean EDLC	mean SI	stderror EENS	stderror EDLC	stderror SI
-	MWh/yr	Hrs/yr	Sys-hrs	MWh/yr	Hrs/yr	Sys-hrs
1	0.000	0.000	0.000	0.000	0.000	0.000
2	0.000	0.000	0.000	0.000	0.000	0.000
3	0.000	0.000	0.000	0.000	0.000	0.000
4	0.000	0.000	0.000	0.000	0.000	0.000
5	0.086	0.003	0.002	0.063	0.002	0.001
6	0.347	0.005	0.007	0.347	0.005	0.007
7	244.273	3.253	5.143	12.851	0.168	0.271
8	0.017	0.002	0.000	0.017	0.002	0.000
9	1179.621	11.828	24.834	50.747	0.441	1.068
10	16.106	0.200	0.339	4.269	0.040	0.090
11	0.000	0.000	0.000	0.000	0.000	0.000
12	0.000	0.000	0.000	0.000	0.000	0.000
13	0.000	0.000	0.000	0.000	0.000	0.000
14	414.777	4.514	8.732	26.426	0.234	0.556
15	0.000	0.000	0.000	0.000	0.000	0.000
16	0.000	0.000	0.000	0.000	0.000	0.000
17	0.000	0.000	0.000	0.000	0.000	0.000
18	1.507	0.028	0.032	0.827	0.012	0.017
19	83.786	1.028	1.764	10.197	0.096	0.215
20	0.000	0.000	0.000	0.000	0.000	0.000
21	0.000	0.000	0.000	0.000	0.000	0.000
22	0.000	0.000	0.000	0.000	0.000	0.000
23	0.000	0.000	0.000	0.000	0.000	0.000
24	0.000	0.000	0.000	0.000	0.000	0.000
System	1940.520	15.056	40.853	85.536	0.466	1.801

Table 23: CSR assessment results for augmented system, Case 1 varying SATA size.

PR \ ER	150 MWh	175 MWh	200 MWh	225 MWh	250 MWh	275 MWh	300 MWh	325 MWh	350 MWh	375 MWh	400 MWh
System EENS [MWh/yr]											
25	1625.9	1608.9	1593.7	1580.1	1569.2	1560.5	1555.0	1551.1	1548.9	1547.3	1546.0
50	1579.1	1554.1	1531.2	1510.0	1489.8	1471.4	1454.0	1437.7	1422.2	1407.8	1394.0
75	1573.4	1540.9	1510.3	1482.5	1458.6	1436.4	1415.1	1395.0	1375.7	1357.2	1339.7
100	1572.0	1538.8	1507.4	1477.9	1450.1	1423.9	1399.3	1376.8	1355.4	1334.8	1314.8
125	1571.5	1538.0	1506.5	1476.6	1448.3	1421.7	1396.4	1372.2	1351.6	1327.3	1306.1
150	1571.3	1537.8	1506.1	1476.1	1447.7	1420.9	1395.3	1371.0	1347.7	1325.4	1303.8
System EDLC [Hrs/yr]											
25	14.1	14.0	13.9	13.9	13.9	13.9	13.9	13.9	13.8	13.8	13.8
50	13.1	12.9	12.8	12.7	12.7	12.6	12.5	12.4	12.3	12.2	12.2
75	12.5	12.3	12.1	12.0	11.8	11.7	11.6	11.5	11.5	11.4	11.3
100	12.1	11.8	11.6	11.4	11.3	11.1	10.9	10.8	10.7	10.6	10.5
125	11.9	11.6	11.3	11.1	10.9	10.7	10.5	10.3	10.2	10.0	9.9
150	11.8	11.5	11.2	10.9	10.7	10.5	10.3	10.0	9.9	9.7	9.6
System SI [Sys-hrs]											
25	34.2	33.9	33.6	33.3	33.0	32.9	32.7	32.7	32.6	32.6	32.5
50	33.2	32.7	32.2	31.8	31.4	31.0	30.6	30.3	29.9	29.6	29.3
75	33.1	32.4	31.8	31.2	30.7	30.2	29.8	29.4	29.0	28.6	28.2
100	33.1	32.4	31.7	31.1	30.5	30.0	29.5	29.0	28.5	28.1	27.7
125	33.1	32.4	31.7	31.1	30.5	29.9	29.4	28.9	28.4	27.9	27.5
150	33.1	32.4	31.7	31.1	30.5	29.9	29.4	28.9	28.4	27.9	27.4
ELCC [MW]											
25	18	20	21	22	24	25	25	25	26	26	26
50	22	25	27	29	31	33	35	37	38	40	42
75	22	25	28	31	34	37	39	41	43	45	47
100	23	26	29	32	35	38	40	43	45	48	50
125	23	26	29	32	35	38	40	43	45	48	50
150	23	26	29	32	35	38	40	43	45	48	50

Table 24: CSR assessment results for augmented system, Case 2 varying SATA size.

PR \ ER	150 MWh	175 MWh	200 MWh	225 MWh	250 MWh	275 MWh	300 MWh	325 MWh	350 MWh	375 MWh	400 MWh
System EENS [MWh/yr]											
25	2171.5	2148.1	2126.9	2107.6	2092.1	2079.4	2071.5	2065.9	2062.5	2060.0	2058.2
50	2113.2	2079.5	2048.4	2019.8	1992.6	1967.4	1943.3	1920.8	1899.0	1878.7	1859.2
75	2105.8	2063.1	2022.3	1985.2	1952.7	1922.8	1894.0	1866.9	1840.7	1815.5	1790.2
100	2104.3	2060.3	2018.4	1979.4	1942.6	1907.4	1874.2	1843.7	1814.7	1786.9	1760.1
125	2103.8	2059.5	2017.4	1977.6	1940.3	1904.7	1870.7	1838.2	1807.0	1777.0	1748.3
150	2103.6	2059.2	2016.9	1977.0	1939.4	1903.5	1869.2	1836.4	1804.9	1774.5	1745.1
System EDLC [Hrs/yr]											
25	18.0	17.9	17.8	17.8	17.8	17.8	17.7	17.7	17.7	17.7	17.7
50	16.8	16.6	16.4	16.3	16.2	16.1	16.0	15.8	15.7	15.6	15.6
75	16.0	15.7	15.5	15.3	15.1	15.0	14.8	14.7	14.6	14.5	14.4
100	15.4	15.0	14.8	14.6	14.4	14.1	14.0	13.8	13.7	13.5	13.4
125	15.2	14.8	14.4	14.1	13.8	13.6	13.4	13.2	13.0	12.8	12.6
150	15.1	14.7	14.3	13.9	13.6	13.3	13.1	12.8	12.6	12.4	12.1
System SI [Sys-hrs]											
25	45.7	45.2	44.8	44.4	44.0	43.8	43.6	43.5	43.4	43.4	43.3
50	44.5	43.8	43.1	42.5	41.9	41.4	40.9	40.4	40.0	39.6	39.1
75	44.3	43.4	42.6	41.8	41.1	40.5	39.9	39.3	38.8	38.2	37.7
100	44.3	43.4	42.5	41.7	40.9	40.2	39.5	38.8	38.2	37.6	37.1
125	44.3	43.4	42.5	41.6	40.8	40.1	39.4	38.7	38.0	37.4	36.8
150	44.3	43.4	42.5	41.6	40.8	40.1	39.4	38.7	38.0	37.4	36.7

Table 25: Hourly mean EENS in MWh/hr/year for Case 1 and Case 2, SATA at bus 8.

Hour of the day	Average Load at bus 9 (MW)	Base Sys., Case 1	Augmented Sys. (SATA), Case 1	Base Sys., Case 2	Augmented Sys. (SATA), Case 2	Augmented Sys. (Trans. Asset)
-			Mean Shortfall [MWh/hr/yr]			
1	87.261	0.000	0.000	0.000	0.000	0.000
2	83.227	0.000	0.000	0.000	0.000	0.000
3	79.663	0.000	0.000	0.000	0.000	0.000
4	77.385	0.000	0.000	0.000	0.000	0.000
5	77.340	0.000	0.000	0.000	0.000	0.000
6	80.416	0.000	0.000	0.000	0.000	0.000
7	89.981	0.001	0.000	0.001	0.000	0.000
8	103.654	0.020	0.010	0.029	0.015	0.016
9	116.797	0.154	0.082	0.215	0.116	0.117
10	122.710	0.218	0.116	0.302	0.165	0.163
11	125.093	0.260	0.141	0.356	0.198	0.193
12	125.130	0.239	0.156	0.330	0.217	0.178
13	122.142	0.220	0.173	0.304	0.243	0.162
14	121.598	0.235	0.196	0.323	0.271	0.173
15	119.949	0.186	0.166	0.256	0.229	0.133
16	118.302	0.172	0.159	0.240	0.224	0.124
17	120.965	0.360	0.259	0.479	0.354	0.290
18	123.590	0.420	0.295	0.553	0.400	0.342
19	124.779	0.404	0.287	0.531	0.387	0.332
20	124.604	0.206	0.188	0.282	0.259	0.156
21	121.804	0.083	0.078	0.120	0.113	0.063
22	115.958	0.031	0.028	0.045	0.042	0.022
23	105.581	0.004	0.003	0.007	0.006	0.003
24	92.550	0.000	0.000	0.000	0.000	0.000

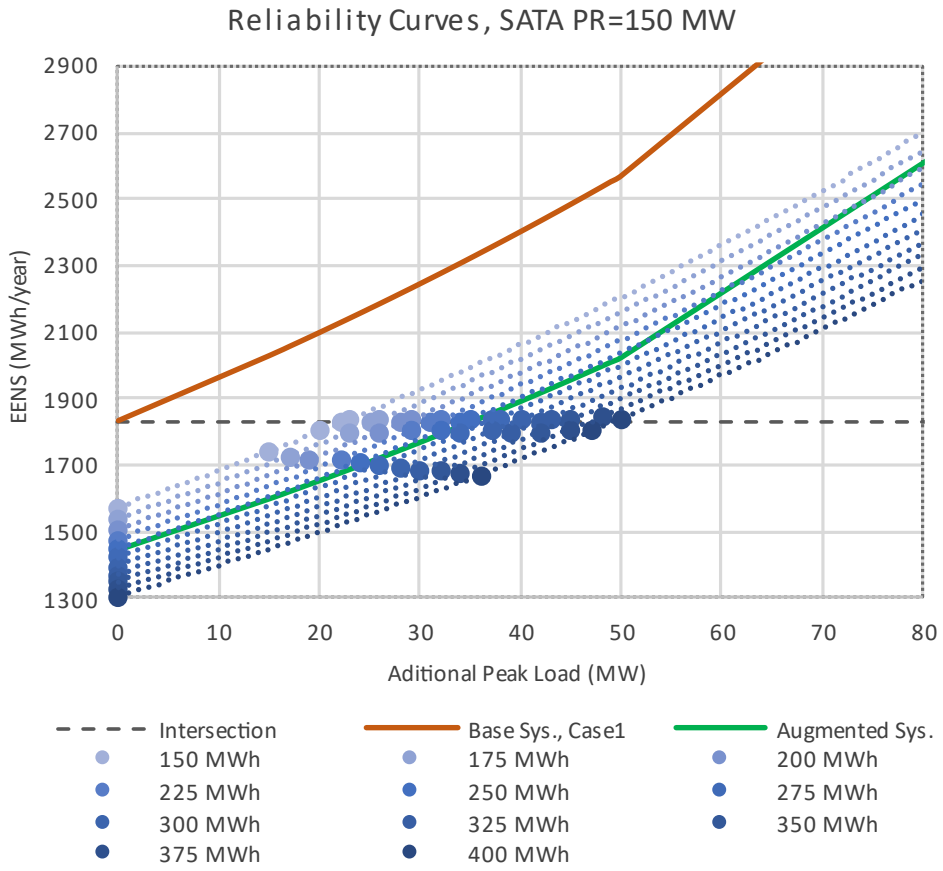

Figure 25: Reliability curves at different load levels, placed at bus 8 to increase transfer capability on three transmission lines. Augmented system, Case 1.

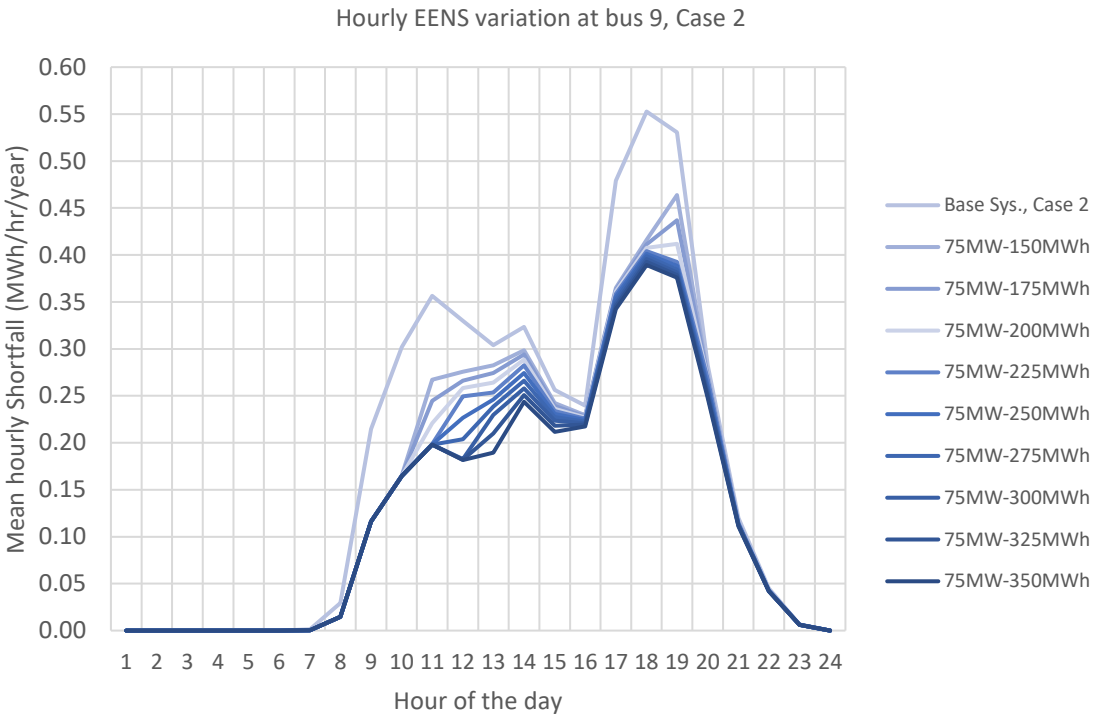

Figure 26: Hourly EENS variation at bus 9, Case 2, varying SATA's energy rating.

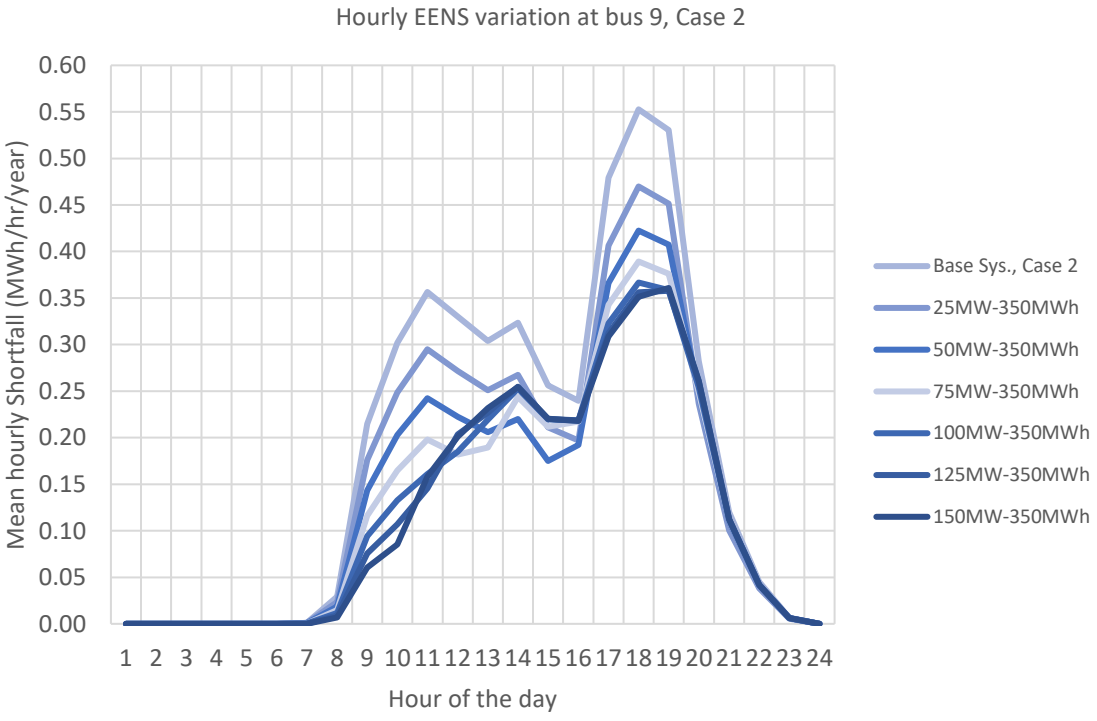

Figure 27: Hourly EENS variation at bus 9, Case 2, varying SATA's power rating.

Curriculum Vitae

Candidate's Full Name: Josif Elias Figueroa Parra

Universities Attended:

- BSc in Electrical Engineering, Power Systems Specialization. University of Santiago, Chile (2009-2015).
- Project Management Diploma. Pontifical Catholic University of Chile (2018-2018)

Publications: N/A

Conference Presentations:

- (July 2022, Denver, USA) IEEE PES Resource Adequacy Working Group. https://cmte.ieee.org/pes-rawg/meetings/. Presentation's title: "A Composite Reliability Evaluation (CSR) Tool for Transmission Planning".